DESIGN AND VALIDATION OF A WIRELESS INTERFACE FOR THE V-QUEST: A VULVAR QUANTITATIVE SENSORY TESTING DEVICE

LAYLA MITRI

A thesis submitted in partial fulfillment of the requirements for the
Master of Applied Science degree in Biomedical Engineering

Ottawa – Carleton Institute for Biomedical Engineering
Department of Mechanical Engineering
Faculty of Engineering
University of Ottawa

ABSTRACT

This thesis presents the design and validation of a wireless interface for a vulvar quantitative sensory testing device (v-QueST). The wireless interface works in tandem with an Android application which allows a patient to indicate when their pressure pain threshold has been reached via an on-screen button. Using the fully assembled prototype, the sampling frequency and response time of the wireless interface was validated. The results indicated that the sampling frequency was sufficient to meet the desired specifications, and the time delay between the tap of the on-screen button and the reading of the force measurement was negligible. However, inspection of the force time-series acquired from the v-QueST device through Bluetooth transmission revealed systematic error. Implementation of a new signal conditioner is recommended before using the v-QueST device for research or clinical applications to objectively measure vulvar pain sensitivity.

ACKNOWLEDGEMENTS

This thesis would not have been possible without the support of so many people. I would like to begin by sending my sincerest thanks to Dr. Linda McLean for her guidance throughout this entire project. She has been by mentor for many years, and I am eternally grateful for her leadership.

I would also like to thank my MFM lab colleagues, you all consistently allow me to become a better researcher. It is inspiring to have been part of a group with such smart and dedicated women. A special thanks to Ana, for helping me assemble the prototype and helping me with all the validation testing.

Thank you to Mariam, we have spent countless hours discussing so many aspects of this report, you are the greatest. Another special thank you to Jessica, Charlie, and Mariel, thank you for listening to me ramble on about all my research problems. And thank you for pretending to understand what it was about; you guys are the best.

A huge thank you to my parents and siblings, without you this would not have been possible. Thank you for always believing in my abilities, having you four by my side just makes everything a bit easier. Your unwavering faith in me is more than I could ever ask for.

And finally, “I can do all things through Him who strengthens me.” Philippians 4:13.

STATEMENT OF CONTRIBUTION

The wireless vulvar pressure measurement device for clinical use was conceived by Dr. Linda McLean.

The mechanical design of the v-QueST, including all its parts, and the signal conditioning unit with two printed circuit boards was developed by Ana Brennan. The I^2C communication of the load cell in the Arduino script for load cell readings was also developed by Ana Brennan. Ana also aided in the assembly of the protype.

The remaining portion of this thesis and the writing of this report is carried out by author of this thesis.

TABLE OF CONTENTS

LIST OF FIGURES

LIST OF TABLES

LIST OF ABBREVIATIONS

AC	Alternating current
ADC	Analog to digital converter
BLE	Bluetooth light energy
coVAS	Computerizes visual analog scale
DC	Direct current
ECG	Electrocardiogram
EMC	Electromagnetic compatibility
EMG	Electromyography
EMI	Electromagnetic interference
GUI	Graphical user interface
GVD	Generalized vulvodynia
ICC	Intraclass correlation coefficient
IDE	Integrated development environment
IMU	Inertial measurement unit
IPPS	International Pelvic Pain Society
ISM	Industrial, scientific and medical
ISSVD	International Society for the Study of Vulvovaginal Disease
ISSWSH	International Society for the Study of Women's Sexual Health
MCU	Microcontroller unit
MDC	Minimum detectable change
MFM	McLean Function Measurement
MIT AI2	Massachusetts Institute of Technology App Inventor 2

NIDAQ	National Instruments data acquisition
NRS	Numerical Rating Scale
PC	Personal computer
PCB	Printed circuit board
PLA	Polyactic acid
PPT	Pressure pain threshold
PPTol	Pressure pain tolerance
PVD	Provoked vestibulodynia
RF	Radiofrequency
RF-EMF	Radiofrequency electromagnetic field
RX	Receive
SCL	Serial clock
SDA	Serial data
sEMG	Surface electromyography
TS	Temporal summation
TX	Transmit
VAS	Visual analog scale
VGM	Vulvagesiomieter
v-QueST	Vulvar quantitative sensory testing
WPAN	Wireless personal area network

1.0 INTRODUCTION

Objective methods for testing pain perception are becoming increasingly important as our understanding of the changes that occur in pain processing with chronic pain conditions evolves [1]. Objective measurement of pain sensitivity is particularly challenging when assessing vulvar pain conditions [2]. Pressure pain sensitivity at the vulvar vestibule is commonly used in vulvodynia and is an important criteria for the diagnosis of provoked vestibulodynia (PVD), the most common type of vulvodynia [2]. Vulvodynia is a genital pain disorder described as chronic or recurrent vulvar pain experienced during sexual or non-sexual activities [3]. Vulvodynia affects a women's sexual and overall health, consequently resulting in multifactorial implications, such as psychological distress as well as negative impacts on social participation and relationships[4]. Studies have indicated that the prevalence of vulvodynia in reproductive-aged women lies between 10% to 28% [5]–[8]. Despite this high prevalence, 60% of affected women consult three or more physicians about vulvar pain before receiving a diagnosis [8], [9]. In one study, among 2269 adult women, 208 met the criteria for the diagnosis of vulvodynia, yet only three women had received a relevant diagnosis [10]. Once diagnosed, effective treatments for vulvodynia are lacking, and treatments that have shown some promise can be difficult to access due to a lack of clinical expertise and to the high costs associated with treatments not covered by provincial health insurance. Due to these barriers, less than 50% of women with vulvodynia pursue treatment for it [10].

PVD is defined by pain experienced as a result of touch or pressure provocation at the entrance of the vagina with no evidence of pathology [11]. To diagnose PVD, it is recommended that the health care provider perform a cotton swab test, whereby pressure is applied at points around the entrance of the vagina using a standard, non-lubricated, cotton swab [12]. A patient's

pain rating of greater than 3 on an 11-point Numerical Rating Scale (NRS) (from 0 to 10) at sites within the vulvar vestibule but not elsewhere confirms a PVD diagnosis [12], while provoked generalized vulvodynia (GVD) is used to describe conditions where the pain is present at sites beyond the vulvar vestibule [3]. Considered alongside patient history, the cotton swab test is the clinical standard for the diagnosis for PVD [2]. Yet the cotton swab test is not standardized; the amount of pressure applied during testing is inconsistent between healthcare providers, and may not even be consistent within healthcare providers [2].

To mitigate the limitations of the cotton swab test, Pukall et al. developed the vulvalgesiometer (VGM) [2], [13], [14]. The original VGM was a 5-set device which includes spring-loaded syringes tuned to deliver pre-determined pressure values at steps ranging from 3g to 950g [2]. The VGM has been recommended by the guidelines from the International Consultation on Sexual Medicine [15] and vulvar pressure pain thresholds (PPTs) established using the VGM demonstrate differences between women with and without PVD [14], [16]. Since the VGM requires a series of incremental pressure applications to establish a patient's PPT [2], [13], [14], the procedure with the VGM can be cumbersome, time consuming, and tiresome for women with PVD [17]. The McLean Function Measurement (MFM) lab developed an electronic version of the VGM, the vulvar quantitative sensory testing (v-QueST) device, for use in vulvodynia research. The v-QueST consists of a load cell interfaced with a spring-loaded collet which holds a cotton swab. The device is operated through a PowerLab^{TM} (ADInstruments, PowerLab 16/35, Colorado, USA) data acquisition system. It successfully eliminates the time-consuming nature of PPT determination through a VGM since only one incremental application is required to establish a patient's PPT. PPTs measured through this device have been shown to have adequate reliability for research applications, and to differ significantly between women with and without PVD [18].

Various other vulvar pressure measurement devices have been designed for research purposes [2], [13], [14], [17], [19]–[24] yet have not been used in a clinical environment, presumably because they require a customized computer program [23], [24] and/or data acquisition systems [17] or they apply PPT in a discrete manner with predetermined pressure values [2], [19], [20] which, as discussed previously, is cumbersome. A clinical vulvar pressure measurement device needs to be easy to use and is ideally wireless to provide greater freedom of motion [25] for both the health care provider and the patient.

The design of a wireless v-QueST for clinical use was refined in my undergraduate thesis [26]. It is a wireless device that operates through Bluetooth™. A wireless interface was successfully implemented into the v-QueST using an Arduino Nano and HC-06 Bluetooth module. The operator presses the cotton swab tip onto the desired test site of the patient, gradually increasing the force applied through the cotton swab until the patient reports pain at the site of the cotton swab tip (i.e. the PPT). At this point, the patient presses a handheld switch, which is wirelessly connected to the app, and the force value at the time of the button press is stored as the PPT. The app interface was optimized to include all clinically relevant information as determined through a focus group consultation. The v-QueST was able to send, via email, the date, name of the patient, location of pressure application and the patient's PPT. Inspection of the data, however, suggested that the sampling rate was too low to be clinically useful (1Hz) and that there was a large time lag (0.4s) induced by the wireless data acquisition. This time lag was deemed to be unsuitable if the device were to be used in research or clinically.

The purpose of this thesis was to improve the wireless v-QueST developed during my undergraduate thesis. The improvement of the wireless operation of the v-QueST can be done by meeting the nominal sampling frequency of 467Hz and time delay of 20ms in data transmission to

ensure that the v-QueST operates within the functional requirements of the system. The first objective was to construct a fully assembled second generation v-QueST prototype with the addition of a Bluetooth module that transfers load cell data to a wireless application. The second objective was to achieve a stable sampling rate of at least 467 Hz, taking into account the frequency at which the Arduino reads the load cell data and the speed of data transfer via Bluetooth to the application. The third objective was to validate the timing of the Bluetooth transmission of the load cell data against a load cell interfaced with a hard-wired connection to ensure that the time delay induced in the data through using the Bluetooth app was minimal, and at most 20ms.

Establishing a reliable and valid clinical pressure measurement device for measuring vulvar PPT will provide a means of standardizing the cotton swab test for PVD diagnosis and will allow for objective pain quantification that can be used to monitor changes over time or improvements associated with interventions.

2.0 LITERATURE REVIEW

2.1 Vulvar Pain

In 2015, an international consensus for vulvar pain terminology developed by the International Society for the Study of Vulvovaginal Disease (ISSVD), the International Society for the Study of Women's Sexual Health (ISSWSH), and the International Pelvic Pain Society (IPPS) classified vulvar pain as either pain caused by a specific disorder (infection, hormonal, inflammatory, etc.) or vulvodynia, chronic vulvar pain without an identifiable cause [3]. Vulvodynia was further subclassified in terms of the location of the pain, pain elicitation (generalized or provoked), and temporal pattern of pain [3]. PVD is the most common subtype of vulvodynia [2], where patients describe a burning pain at the entrance of the vagina (vulvar vestibule) caused by provocation through touch or pressure [11].

2.2 Clinical Methods of Vulvar Pressure Pain Measurement

The recommended assessment for vulvar pain diagnosis consists of three key steps: a medical interview, a pain quantification questionnaire, and a physical examination [12], [27]. During the physical examination, it is recommended the physician or healthcare provider perform an external (visual and palpation) examination of the perineum, an internal (single digit) palpation of the pelvic floor muscles (PFMs) and a sensory (pain threshold) examination [12]. The following section will discuss three methods of sensory examination for vulvar pain: the cotton swab test, the tampon test and palpation. The goal of these assessments is to determine whether touch/pressure at a particular site reproduces the patient's pain [17].

2.2.1 Cotton Swab Test

The cotton swab test is the clinical standard test for vulvodynia diagnosis and helps identify the location and intensity of pain [12]. The test can help determine the presence of mechanical allodynia (painful response to a non-painful stimulus) and hyperalgesia (lower threshold for painful response) [12], [27], [28]. During the cotton swab test, the examiner uses the tip of the cotton swab to apply pressure at various locations around the vulva [12]. A patient's pain rating of 3 or more on the 11-point NRS from 0 (no pain at all) to 10 (worst pain imaginable) [29] confirms the diagnosis of PVD [2].

The cotton swab test is a simple [2], fast, and inexpensive to perform. However, the cotton swab test is not standardized in terms of location of pressure application, sequence of pressure application at the different sites, and the amount of pressure applied between and within healthcare providers [11], [14], [29], [30]. While widely used as the clinical standard to diagnose PVD, the amount of pressure applied varies among clinicians, consequently influencing the reliability of the NRS score [29]. While useful as a screening test, it is not adequate for evaluating changes in pain sensitivity over time, for example, to monitor progress with interventions [2].

2.2.2 Tampon Test

The tampon test is used to replicate vulvar pain felt during intercourse [31]. The tampon test is self-administered [32]; the patient inserts and then removes a dry regular tampon and rates their level of pain associated with the entire process on an 11-point NRS [32]. A score above 4 on the NRS scale for pain localized to the vulvar vestibule indicates that a woman is suffering from PVD [31]–[34].

The tampon test is inexpensive, easy to perform and is performed by the patient without the help of a clinician [32]. For individuals with PVD, the tampon test replicates their pain (many patients with PVD report pain upon tampon insertion [2]), however, it has also been reported that pain levels experienced during penetrative intercourse are much higher than pain levels reported during the tampon test [31], [32]. Presumably because the tampon is smaller, softer, and more flexible than a penis [32]. Consequently, the tampon test may not be the best primary indicator of PVD [32].

2.2.3 Palpation

Palpation is the process through which an examiner, using their lubricated and gloved index finger, evaluates pain sensitivity at different areas external and internal to the vagina [35]. Palpation of healthy perineal tissues should not be painful (a pain score of higher than 3 out of 10 on the NRS is considered abnormal [9]). Palpation is also used to evaluate the tone of the PFMs. Most often this is performed through inserting a gloved digit inside the vagina to elongate the levator ani tissues; using this method, the tissues can tolerate approximately 2kg of pressure without pain, which is more force than is generally applied by the health care professional when palpating [12] [28], [29]. During digital palpation, the patient can also be asked to squeeze or contract around the examiner's index finger, a strategy that is used to evaluate muscle strength or motor control[12], yet this is beyond the scope of the current research. For the evaluation of pain sensitivity, the palpation occurs on the perineum and the main outcome is the patient reported pain on a NRS, however the palpated tissues may include the superficial layer of the PFMs if the palpation force is adequately high [12].

. Also, the application of pressure to the PFMs may trigger a PFM contraction in anticipation of the pain or through a stretch reflex , resulting in the examiner assessing the PFM tone as being high, while the patient consequently reports a higher pain score [29], [36], [37].

2.2.4 Utility of vulvar assessment techniques

Table 2.1 summarizes the advantages and disadvantages of the three types of clinical assessments used to evaluate vulvar pain. Indeed, all these tests are used in a clinical setting, while the cotton swab test is considered to be the clinical standard for evaluation of PVD, the lack of objectivity in all of these tests makes them unreliable for the assessment PVD.

Table 2.1: *Clinical assessment techniques used in the evaluation of provoked vestibulodynia: advantages and disadvantages.*

	Advantages	Disadvantages
Cotton Swab Test	Clinical standard Inexpensive Simple Identifies the precise location(s) of pain	Subjective Poorly standardized Poor interrater reliability
Tampon Test	Self-administered Inexpensive Easy to perform Standardized	May under-estimate pain during intercourse May cause pain from sources other than the vulvar vestibule Does not identify the precise location of the pain
Manual Palpation	No tools	Subjective Poorly standardized Poor interrater reliability May cause pain from other sources other than the vulvar vestibule PFM reflexes or protective guarding may influence pain rating

A better and more accurate measurement of pain perception at the vulva may be achieved through quantifiable pressure measurement techniques. Quantifiable pressure measurement devices may facilitate the diagnosis of PVD and allow for treatment monitoring of PVD [23].

However to date, the use of quantitative approaches to the measurement of pain sensitivity has been limited to research settings [2], [13], [14], [17], [20], [21], [23].

2.3 Existing Vulvar Pressure Measurement Devices

Vulvar pressure measurement devices have existed since the early 1990s [19] to quantify vulvar PPT for research purposes[2], [13], [14], [17], [19]–[24]. These devices have been designed to measure the force/pressure at which a patient first reports a sensation of pain (PPT) instead of pressure at the site of application. [23]. The PPT is often reported in grams (g) or kilograms (kg) which not a pressure unit (pressure = force/area with a unit of [N/m^2]). Because a mass reading in g or kg can be easily converted to a force (force = mass × gravity) it is more accurate to say that these devices output a force measurement; however, the term "pressure" as an output from vulvar pressure measurement devices is used throughout this thesis to be consistent with the terminology used clinically. This section contains a literature survey of vulvar pressure measurement devices, and the terminology (pressure or force application) and measurement units that are reported by the authors.

2.3.1 Pulse Generated Vulval Algesiometer

The pulse generated vulval algesiometer (Figure 2.1) was developed by Curnow et al. to eliminate the user subjectivity introduced in the cotton swab test. The device can output eight pre-set force increments from 178mN to 2046 mN. The device consists of three parts: (1) a hand-held probe with a tip force pulse generator (2) a control unit and (3) a foot switch. The hand-held probe consists of three sections: (1) a 1.5mm diameter rod which comes into contact with the patient (proximal section) (2) a 5mm diameter section which houses the thrust rod (distal section), and (3) a larger diameter section which contains a drive solenoid (end section). The proximal section

contains a removable and sterilisable stainless-steel tip fit into a drive shaft. The distal section is used as a guide for the proximal section, allowing the proximal section to move freely in the distal section. The end section houses the drive solenoid consisting of a fixed coil and a rod. The control unit is a pulse generator providing a controlled pulse of current to activate the solenoid in the end section. This consequently induces a magnetic field in the coil and pushes the rod forward over a known distance, which is determined by the amplitude of the current pulse. Pushing the rod forward causes the tip of the probe to be pressed onto the vestibule. The foot switch allows the user to select the different pre-set force increments. The pulse generated vulval algesiometer was bench tested once a day for six days and demonstrated good force reproducibility [19].

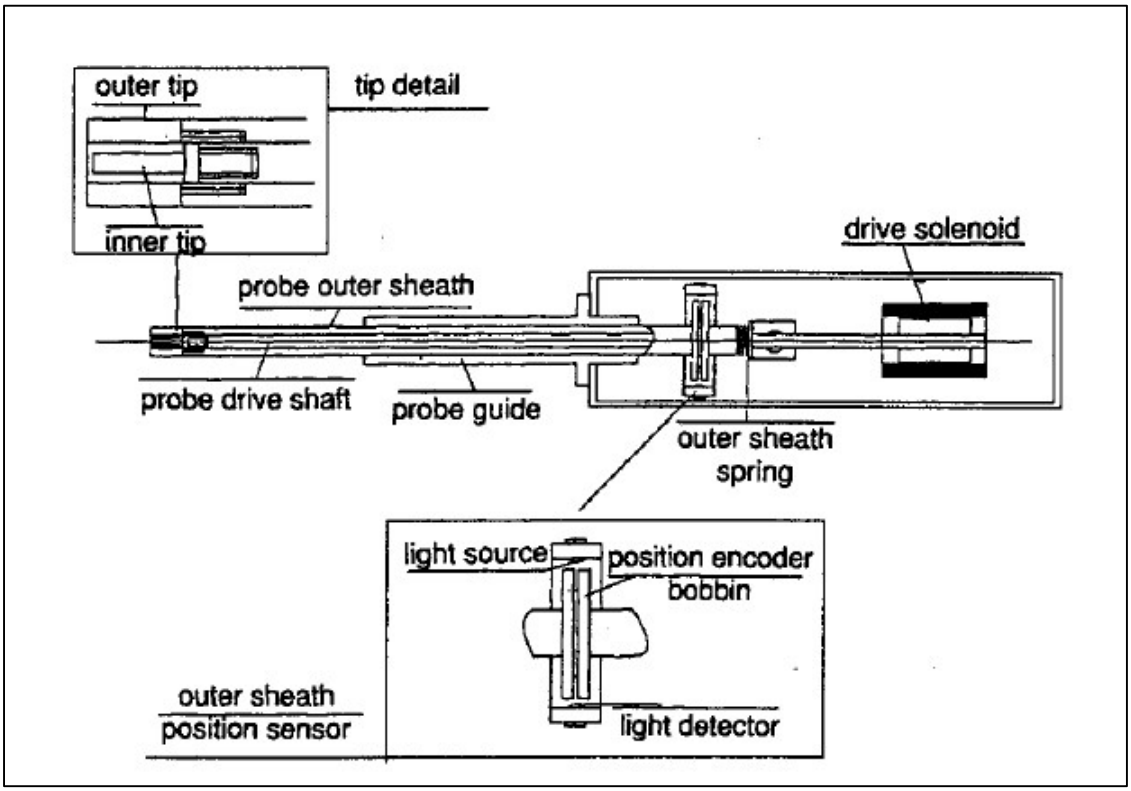

Figure 2.1: *Pulse generated vulval algesiometer* [19].

To use this device, the clinician begins at the lowest force increment and increases the force until the patient reports pain (that is, their PPT). The probe is placed on the vestibular location of interest, and, through the activation of the solenoid, it presses down onto the vestibule for a known

duration of time. Curnow's clinical study of 34 women with clinically diagnosed vestibulitis (a previous term used for PVD) and 47 women without PVD indicated that the pulse generated vulvar algesiometer could distinguish between PVD and controls – the women with PVD reported their PPT below the fourth step whereas controls did not [19]. The pulse generated vulval algesiometer was used to monitor the effect of topical ketoconazole treatment for PVD [38] and to monitor outcomes from a vulvar pain clinic in the treatment of PVD. Indeed, patients who reported improvement in their PVD symptoms also demonstrated an increase in their PPT post treatment [30].

The pulse generated vulval algesiometer has shown utility in research settings for monitoring PVD patients and distinguishing between PVD and controls [19]. However, to the author's knowledge, no reliability testing has been completed for the device (either inter-rater or inter-session) and the procedure using the device is time consuming since many pressure applications may be required to reach the patient's PPT [17]. The device was also reported by patients to be painful and distressing, especially for women with PVD who were fatigued by the end of the procedure [14]. The need to apply forces several times throughout the procedure may also influence the outcomes using this device, as a study showed that repeated palpation of the same region of the vagina results in a higher pain ratings on a visual analog scale (VAS) [11], a phenomenon referred to as temporal summation (TS) of pain [39].

2.3.2 Finger Load Cell Vaginal Algometers

Baguley et al. developed a vaginal algometer which fits onto a clinician's index finger through a thimble (Figure 2.2 (a)) and contains a measurement and display unit. A force transducer tip is integrated on one side of the thimble and protrudes in a dome shape of 12mm diameter. The force transducer measures force through strain gauges, which are arranged in a Wheatstone bridge

configuration within the measurement unit, along with a correction circuit for temperature changes. The measurement unit processes the signal from the transducer to report calibrated force in N. A peak-hold circuit is used to display the maximum force sensed by the force transducer. To use this device, a clinician inserts their finger, interfaced with the device, through the vaginal opening to the location of interest. While the clinician's finger is within the vaginal opening, and without any force application, the clinician sets the force on the display to 0N. Once the display is zeroed, the clinician applies a force to the lateral vaginal wall at a rate of 2N/s (while looking at the display unit for force feedback) and stops applying force when the patient indicates that their PPT has been reached. Baguley's device was tested at the lateral vaginal wall on 63 healthy women where it was determined that the average PPT on the right side of the vagina was 10.6N while on the left was 10.9N [22]. It is important to note that this device was used to assess pain on palpation of the lateral walls of the vagina [22], not the vulva.

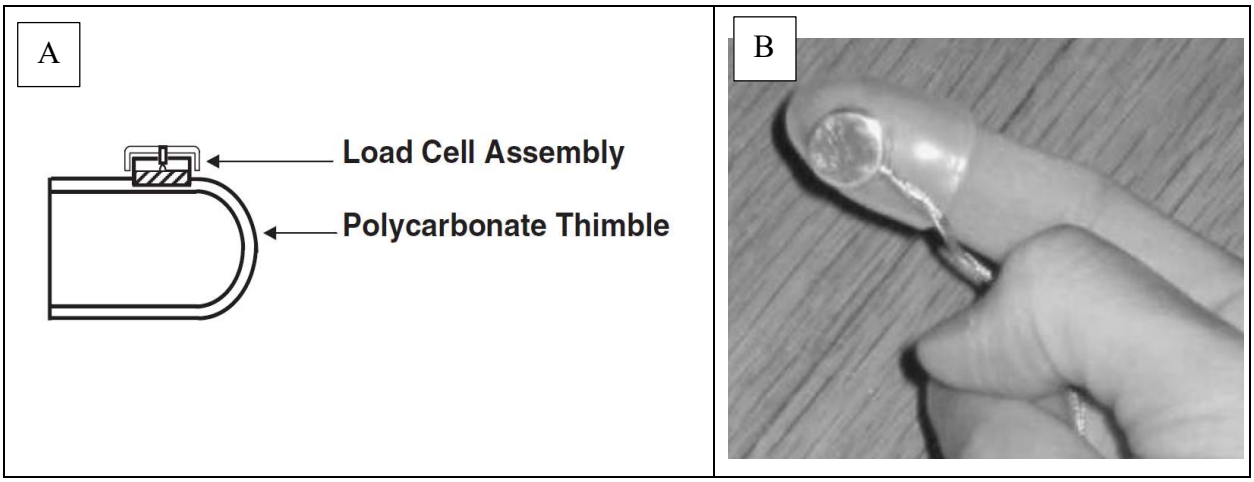

Figure 2.2: *(a) Cross section view of Baguley et al.'s finger load cell* [22] *(b) Tu et al.'s vaginal pressure algometer* [23].

Tu et al. designed a vaginal pressure algometer similar to that of Baguley's, as seen in Figure 2.2(b). It consists of a load cell (surface area of 1cm^2) mounted on a thimble. The signal from the load cell is amplified then digitized before being stored on a personal computer. A

custom-designed computer program simultaneously records the pressure reading from the load cell and a hand-held trigger is used by the participant to indicate the timing of their PPT. Both the concurrent validity and test-rest reliability (short-term and intermediate-term) for this device were evaluated by testing 19 healthy women. Concurrent validity was assessed when using the device at one test location, by correlating numerical pain rating scores to three predetermined pressure levels (1, 2, and 3 kg/cm^2). While a non-parametric test would have been more appropriate, there was a positive Pearson correlation ($r=0.61$, $p<0.05$) between the applied force and pain rated on the NRS. Intraclass correlation coefficients (ICCs) suggested that there was good to excellent short-term reliability for PPT measurements (ICC between first and second trial was 0.75, while the ICC between second and third trial was 0.64), and good reliability was found among or PPT measurements at 3 test sites (ICC ranging between 0.61-0.84) [23].

Both finger-load cell algometers have been criticized in the literature since they have not yet been used on women with vaginal pain [24]. Tu et al. noted that the PPT measurement made by their device may be influenced be the sensitivity of nearby muscles because the surface area of the finger is larger than a cotton swab [23]. Baguley et al. mentioned that there was difficulty inserting the device in some patients and a smaller device would be advantageous but not possible since the device needs to fit on the clinician's finger for guidance and control [22].

2.3.3 Spring Based Vulvalgesiometer

The Pukall VGM is arguably the most well-known vulvar PPT measurement device and is recommended in the guidelines from the International Consultation on Sexual Medicine [15]. The device design is very simple, consisting of a cotton-tipped applicator, a styrene assembly, a syringe housing, and a spring; it contains no electrical components [2], [13], [14]. The cotton-tipped applicator is placed in the syringe housing and can easily be removed and replaced between

participants, as can be seen in Figure 2.3 [2], [13], [14]. Each VGM set includes five devices [2] (originally a set of seven devices [13], [14]) with each device in the set distinguished by their spring specifications. Across the set, 25 predetermined pressure values can be applied ranging from 3g to 950g, calibrated using a digital scale [2]. To use the VGM, the clinician places the VGM over a desired location and pulls the styrene tube until a red washer reaches one of the predetermined pressure thresholds marked on the outside of the syringe housing [2]. The clinician continues to the next pressure threshold until the patient indicates their PPT has been reached [2].

Figure 2.3: *A 7 device VGM set* [14].

The VGM has demonstrated high interrater reliability (r=0.77) for PPT measurements [2], significant differences in PPT between women with PVD and controls [14], [16] and sensitivity to detect change following treatment [40]. Two other PPT measurement devices with disposable cotton-tipped applicators and spring-loaded devices have been described in the literature: Lowenstein et al.'s spring pressure device and Giesecke et al.'s vulvodolorimeter. Lowenstein's device applies pressure through a spring inside a syringe with 10 pre-determined pressure values [20]. The vulvodolorimeter consists of 2 syringes connected by a 3-way stopcock with the cotton-

tipped applicator located in the piston of one syringe [21]. As the clinician applies pressure through the applicator, air is compressed in the syringe and the unit functions like a spring [21]. To determine the PPT, the vulvodolorimeter is applied in one continuous motion until the patient indicates the first sensation of pain [21]. PPT measures using both of these devices have demonstrated differences between groups of women with PVD and controls [20], [21].

While the Pukall VGM is inexpensive, has been reported to replicate PVD pain experienced during sex [14] and was the first to incorporate the user-friendly unit of grams [13], it has been subject to criticism in the literature [17] because it is cumbersome and time-consuming to use. To avoid sensitization of the region, a long interstimulus interval (5s-10s [2]) between pressure applications is required, resulting in a time-consuming and tiresome procedure, especially for women with PVD [17]. Moreover, the discrete thresholds for pressure application mean that the PPT does not have optimal precision [17]. Finally, the PPT may be biased by user error, since the clinician must determine when the target pressure has been reached by watching the washer as it reaches the calibration mark on the outside of the syringe housing [17].

2.3.4 Vaginal Algometer

To address the existing limitations in the Pukall VGM, Cyr et al. developed the vaginal algometer. It is a load cell-based device with a removable stainless-steel tip shaped like a cotton swab as seen in Figure 2.4(a). The vaginal algometer operates in tandem with a linear potentiometer computerized visual analog scale (coVAS; range from 0 to 10) which is operated by the patient to record their pain rating, resulting in the simultaneous recording of pressure application and pain rating. Both the load cell and the coVAS are connected to a National Instruments data acquisition (NIDAQ) card that is interfaced with a computer. Bench testing of the vaginal algometer resulted excellent calibration [17]. The vaginal algometer was used to

measure both the PPT and pain pressure tolerance (PPTol), in two separate procedures. The PPTol is the maximum amount of pain tolerated by the patient. The coVAS reading indicates when the PPT and PPTol have been each reached.

To use the vaginal algometer, a piece of gauze is used to cover the stainless-steel tip to replicate the texture of a cotton swab. Pressure is then applied at the desired location while the clinician monitors the rate of pressure application, and the procedure is terminated when the patient moves the coVAS scale away from 0 (PPT) or reaches 10 (PPTol). The device was tested on women with PVD whereby PPT and PPTol measurements were evaluated for inter- and intra-session reliability as well as convergent validity against the VGM at 3 vestibular locations. Intra-session reliability was found to be excellent (ICC=0.859 to 0.988), intersession reliability was found to be good to excellent (ICC= 0.683 to 0.922) and convergent validity indicated moderate correlation between the two devices for PPT (r=0.5 to 0.614) with higher correlations between the devices for PPTol (r=0.809 to 0.842) [17].

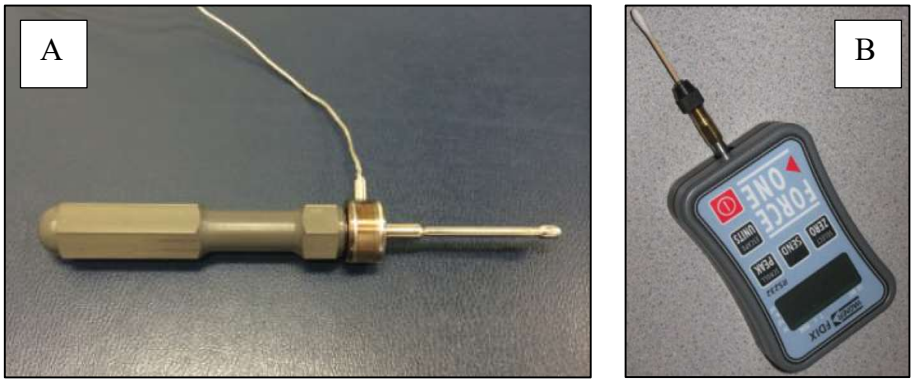

Figure 2.4: *The vaginal algometer as described by (a) Cyr et al.* [17] *and (b) Zolnoun et al.*[24]

The vaginal algometer can monitor the rate of pressure application and is the first device for which PPTol is reported [17], but it has not been analyzed in terms of inter-rater reliability. Indeed, the stated limitation of the cotton swab test is the lack of inter-rater reliability [13].

Moreover, the Cyr algometer may look intimidating to patients, and the load cell is exposed which is not ideal from an infection control perspective.

Zolnoun et al. developed a similar device to Cyr's algometer. A Wegner commercial digital algometer was interfaced with a disposable cotton swab (Figure 2.4(b)) and used for real-time data acquisition streamed to a personal computer. Using the Wegner algometer, pressure is applied at a rate of 1N/s and the patient is instructed to click a computer mouse at the first sensation of pain. Zolnoun et al. observed moderate to good inter-session reliability in women with and without PVD [24].

Zolnoun et al. have successfully developed a device that eliminates the need of predetermined pressure values [24], but Cyr et al. have criticized the device because it fails to allow the clinician to monitor the amount and rate of pressure application [17]. Similar to Cyr's device, Zolnoun's device has not been tested for inter-rater reliability.

2.3.5 MFM Lab Research v-QueST

The MFM lab has developed a research v-QueST to evaluate pain sensitivity. It can be used to measure allodynia, PPT, PPTol, and temporal summation of pain. The v-QueST assembly includes a load cell [41] (Strain Measurement Devices, Wallingford, Connecticut) in series with a spring and a housing for a collet that allows for easy cotton swab insertion and removal. The v-QueST operates at a range from 0 to 900g. When force is applied through the cotton swab tip, the force is transferred through a spring and then to a load cell through a force transfer plate. The load cell is interfaced with a 16-bit resolution analog to digital converter (ADC; National Instruments, NIDAQ USB3086, Austin, USA) which, in turn, is interfaced with a personal computer (PC) through PowerLab^{TM} (ADInstruments, PowerLab 16/35, Colorado, USA) data acquisition

software (16-bit resolution with a maximum sampling rate of 200kHz [42]). This allows the researcher to monitor the rate and amount of pressure application through a graphic interface [43] until the participant indicates their PPT has been reached.

The intra-session reliability of the v-QueST was tested on twenty-four women. Both PPT and temporal summation of pain were evaluated on two occasions within a week after their menstrual cycle. The reproducibility of the PPT was good (ICC= 0.83) while the reproducibility of TS was acceptable (ICC = 0.79) [18].

2.3.6 Conclusion

All of the devices for measuring vulvar PPT reported in the literature are wired devices being used for research purposes. Table 2.2 summarizes the important properties of each device. Other than the vulvar algesiometer [18], none of these devices has been used in a clinical setting, and implementation into a clinic would be difficult because most require a customized computer program [23], [24] or data acquisition system [17]. Also, the devices that reach the PPT in a discrete manner with predetermined pressure/force values [2], [19], [20] are unlikely to be translated to a clinical setting because of their time-consuming nature. Further, methods for proper infection control strategies have not been reported for any device.

As noted, the current v-QueST used in the MFM lab is wired directly into the ADC and interfaced with a PC through a data acquisition software. Indeed, the software and ADC are generally not available in clinical settings, and as such, the current v-QueST is not useful for clinical research nor practice [42]. Moreover, wired systems can be difficult to maneuver and this may also render the current device impractical in a clinical environment. Therefore, the ideal vulvar pressure measurement device is wireless. Wireless devices have many advantages but the

most notable advantage for this application is that it would allow the clinician and patient to manipulate the device components unencumbered by wires during the intravaginal cotton swab assessment [25]. A wireless device that digitizes data on board before communicating with a smartphone or tablet would eliminate the need for a devoted ADC and computer interface.

***Table 2.2**: Vulvar and vaginal pressure measurement devices described in the research literature.*

Device	Description	Unit	Range	Continuous or predetermined	Monitor rate of application	Method of data display	Reliability and validity
Vulval algesiometer [19]	Pulse-generated force through solenoid circuit	mN	178 to 2046	Predetermined	No	None	Bench tested (good reproducibility) Distinguishes between controls and women with PVD
Baguley's vaginal algometer [22]	Finger load cell	N	N/A*	Continuous	Yes	Display unit	Validated on healthy women Correlation of readings on lateral walls of vagina 0.72
Vaginal pressure algometer [23]	Finger load cell	kg/cm^2	0 to 3.7	Continuous	No	Customized computer program	Intravaginal validity (ICC=0.64-0.75) Test-retest validity (ICC=0.61-0.84)
Vulvalgesiometer [2]	Spring-based	g	3 to 950	Predetermined	No	None	Interrater reliability (r=0.77) Distinguishes between controls and women with PVD
Spring pressure device [20]	Spring-based	g	N/A*	Predetermined	No	None	Distinguishes between controls and women with PVD
Vulvodolorimeter [21]	Air-spring	g	0 to 1500	Continuous	No	None	Bench tested (repeatable results) Distinguishes between controls and women with PVD
Cyr's vaginal algometer [17]	Load cell	g	0 to 1000	Continuous	Yes	Data acquisition system	Bench tested (reproducibility of t=0.35, P = 0.728 and t=0.89, P= 0.382) Inter (ICC=0.683 to 0.922) and intrasession (ICC=0.859 to 0.988) reliability Convergent validity against the VGM (r=0.500 to 0.809)
Wegner algometer [24]	Commercial Wegner algometer	selectable	N/A*	Continuous	No	Customized computer program	Distinguishes between controls and women with PVD Good within-examiner correlation (r=0.76-0.84) Poor inter-examiner correlation (r=0.11-0.85)
v-QueST	Spring based load cell	g	0 to 900	Continuous	Yes	Data acquisition system	Bench tested Good reproducibility (ICC=0.79-0.83) Evaluates allodynia, PPT and temporal summation

*N/A: data were not available

2.4 Bluetooth Technology

The focus of this thesis is to prototype and validate a wireless version of the v-QueST device. As a result, it is important to briefly discuss the technical specifications of wireless technology in order that the v-QueST may be used for its intended purposes, laboratory-based research as well as research in the field (mainly physiotherapy clinics). Wireless data transmission can be achieved through telemetry or through Bluetooth™, Bluetooth is a more practical option as it requires less instrumentation to be used in the clinical setting. Indeed, most clinics employ applications that are provided through a smartphone or tablet interface [44]. Since Bluetooth™ transmission is used for wireless connection in the v-QueST, this section of the literature review focuses on options for Bluetooth technology that meet the requirements for the wireless v-QueST. Examples of wireless devices used in similar healthcare applications, the fundamentals of Bluetooth technology, Bluetooth modules which could be considered in the design of the v-QueST, and considerations of Bluetooth specifications applicable to the v-QueST are discussed.

2.4.1 Bluetooth Guidelines

Bluetooth protocols are standardized and regulated under different organizations. Wireless personal area network (WPAN) standards are controlled under the Institute of Electrical and Electronics Engineers (IEEE 802.15). The IEEE 802.15 is a working group in the IEEE standards that encompasses all WPAN operating systems. Bluetooth standards were originally maintained under IEEE 802.15 Task group I but as of 2015 the standards have been maintained by the IEEE Bluetooth Special Interest Group (SIG) [45]. In order to be used, the Bluetooth technology included in the v-QueST must comply with these protocol standards.

In terms of radio frequency electromagnetic field (RF EMF) radiation, the low-level radio frequency (RF) field used by Bluetooth does not pose any known adverse health effects [46], [47]. Most current devices (WI-FI, cellphones, radio and television broadcasts) operate in the RF-EMF environment, limiting any health threats posed by wireless medical devices [46], [47]. In the United States, wireless medical devices are controlled under FDA regulations, which highlight various wireless-related hazards [25]. To mitigate against these hazards, the FDA recommends the following

- Selection of wireless technology that minimizes electromagnetic interference (EMI) through different techniques such as frequency hopping [48].
- High wireless quality of service (a robust and continuous connection of wireless devices) [48].
- Minimization of disruption within the shared RF environment (wireless coexistence between other devices competing in the same environment) [48].
- Appropriate security management of wireless signals and data [48].
- Electromagnetic compatibility (EMC) of the wireless medical device to ensure that the RF energy emitted by the device does not cause EMI with other devices [48].
- The development and circulation of an instruction manual detailing the information on setting up and operating the device [48].
- Maintenance protocols implemented to ensure consistent, safe use of the wireless medical device [48].

2.4.2 Relevant Bluetooth Requirements for Wireless v-QueST

The wireless v-QueST device will operate using Bluetooth since it is used in most medical devices [44]. Wireless medical devices have various requirements including interoperability (communication with products from different manufacturers), low-power operation, compatibility with other radio devices, and secure transmission of data [44]. However, some of these requirements (interoperability and secure transmission of data) are not applicable for devices being used in a clinical setting for one time measurement use (i.e. these requirements are relevant for medical monitoring which requires the device to be in use for several hours at a time [44]). Of the requirements stated above, what is important for the wireless v-Quest is to ensure compatibility with other radio devices, and the requirement of moderate-power operation (low-power operation is not necessary for the wireless v-Quest, since as already stated, it is used for one-time measurements). Other important specifications include the range of the Bluetooth connection, the data sampling rate and delays in data transmission. The wireless v-QueST will require a relatively large sampling rate and, ideally, minimal transmission delays.

2.4.3 Bluetooth Classic vs. Bluetooth Light Energy

Bluetooth has undergone several iterations [49], each one adding new functionality [49]. Most notably, Bluetooth versions before 4.0 are known as Bluetooth Classic and Bluetooth versions after 4.0 are Bluetooth Low Energy (BLE) [49]. Both Bluetooth Classic and BLE offer low power features; however, BLE modules can operate for longer periods of time (months or years) using coin cell batteries without requiring replacement [50]. BLE is ideal for technology that does not require constant data streaming and is only required to operate in short spurts because the BLE protocol transfers smaller packets of data [50]. Since BLE was released in 2010, it has shown large potential for growth because BLE technology is capable of being incorporated into

any pre-existing Bluetooth infrastructure [50]. BLE uses much less power and current consumption, around half of what Bluetooth Classic uses to operate [50]. Table 2.3 compares Bluetooth Classic and BLE technical specifications.

***Table 2.3**: Technical specification comparison of Bluetooth™ classic and BLE (Bluetooth 4.0) adapted from Joh et al* [50].

	Bluetooth Classic	*BLE*
Range (m)	10*	10*
Over air data rate (Mbit/s)	1-3	1
Latency to connect (ms)	100	6
Power consumption (mA)	< 30	< 15

* Note that the range of Bluetooth can be much more [51]–[53]

The wireless v-QueST will likely be used in a clinical setting, whereby the standard size of an exam room is recommended to be 9.2m^2 [54]. Therefore, the Bluetooth range needs to be a maximum of 10m (Table 2.3). Furthermore, with regards to power consumption, BLE uses much less power and current consumption, around half of what Bluetooth Classic uses to operate [50]. Both Bluetooth Classic and BLE are capable of achieving a large sampling rate (over the air data rate Table 2.3), even at 1 Mbit/s, BLE is capable of achieving a very fast sampling frequency and a relatively small delay in data transmission.

Regarding compatibility with other radio devices, it is important to minimize EMI [25], [44]. Indeed, wireless monitors of vital signals require optimal minimization of EMI [44]. PPT assessment requires minimal EMI in case an interference requires the clinician to reassess the patient's PPT, since the assessment procedure can already be troublesome for some women [12]. Bluetooth ensures this by using a frequency hopping technique, whereby dynamic data channels are established each 1MHz (Bluetooth Classic) or 2MHz (BLE) in the 2.4 GHz band [45]. Information between Bluetooth devices is transmitted in packets and frequency hopping allows

each packet of data to hop between channels in the 2.4GHz range to limit interference from other networks within the 2.4GHz band [45]. The Bluetooth Classic hopping technique includes 79 1-MHz channels whereas Bluetooth BLE includes 40 2-MHz channels [49], [51], [55]. It has been proven that frequency hopping technique Bluetooth Classic has adopted works reliably in medical settings and has a more robust scheme due to its hopping between 79 channels opposed to 40 [44]. Considering the range of the Bluetooth connection, the data sampling rate and delays in data transmission, the wireless v-QueST could be designed with either the Bluetooth Classic or BLE, since both Bluetooth modules meet the design criteria for the system.

2.4.4 Types of Data Streaming

The goal of Bluetooth is to exchange data between two devices. Data can be exchanged using various methods and each method provides advantages and disadvantages, with trade-offs mainly being between sampling frequency and power consumption. Medical devices generally transmit digitized physiological data detected from a sensor. The data from the sensor can be sent using three methods: continuous, in intermittent bursts or using a sample and hold strategy (shown in Figure 2.5). Continuous data streaming consumes the most power; as the sensor reads the data, individual values are streamed directly to the connected device. This approach ensures that all data are sent to the connected device with minimal time delay between sample acquisition and display. Sample- and-hold techniques also ensure that all data are sent to the connected device, but in this case, the data are sent in packets. A delay between packets is used to transmit the data before sampling the new packet, whereby the first value in the packed data corresponds to the reading after the last value in the previously packed data. This approach requires less power consumption than continuous data streaming [56]. The intermittent burst technique uses the least power [57]. It samples a burst of data, then sampling pauses as the burst of data is sent, then the buffer is cleared,

resulting in an incomplete data set (shown in Figure 2.5) [56][57]. Considering a full-stream of data is needed for the wireless v-QueST in order to accurately identify the PPT, the sample-and-hold technique should be adapted for the wireless v-QueST since it also requires less power consumption than a continuous data stream.

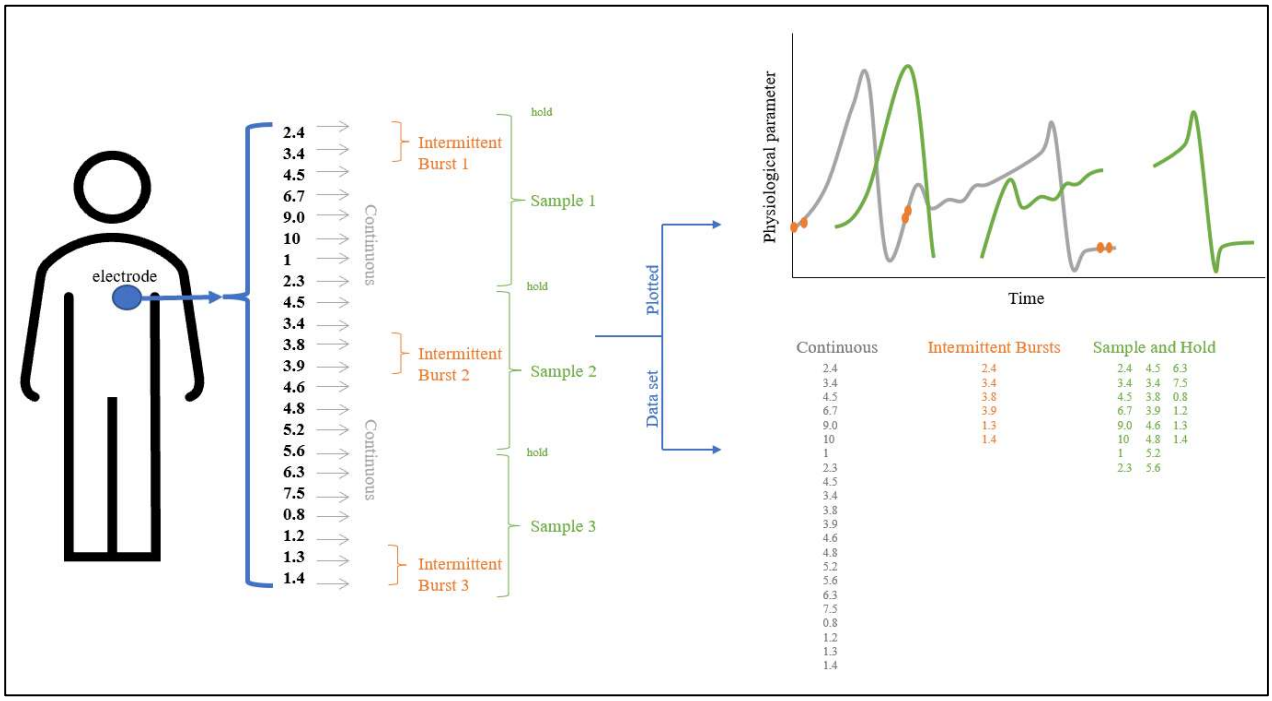

Figure 2.5: *Three sampling techniques: continuous, sample and hold, and intermittent burst. Real-time data acquisition is only maintained in continuous data streaming but sample and hold data acquisition provides a full data set which can be used post processing.*

2.4.5 Sampling Rate in Wireless Medical Devices used in Health Care Settings

Many wireless medical devices exist on market for clinical, research and personal-use applications. Relevant to the application described in this thesis, only those medical devices that require high sampling rates, specifically electrocardiogram (ECG) (nominal sampling rate >500 Hz [57]) and electromyography (EMG) (nominal sampling rate >1000Hz [58]), for which methods have been described to validate sampling rate are discussed in this section.

Researchers have developed wireless and wearable ECG sensors using AD823X microchips (heart rate monitor analog front-end microchip) [59], [60]. Bravo-Zanoguera et al. developed a portable ECG device with the AD823X microchips connected to an Arduino® Nano board interfaced to a Bluetooth HC-05 (Bluetooth classic) module (baud rate: 115200) [59]. The device can transmit data to a PC or Android smartphone via Bluetooth for visualization (a maximum sampling frequency of 909Hz but was set to sample at 500Hz) [59]. Data storage with an on-chip microSD card was validated for 36 hours at a sampling rate of 500Hz [59]. Their high sampling rate was achieved through timer interrupts (signals the processor to perform a task at specific timing intervals) [59]. Their sampling rate was validated by using the Arduino's millis() function [46], a function in Arduino which uses timer interrupts and reads the number of milliseconds passed since the Arduino board ran the program [61]. The millis() function in Bravo-Zanogera et al.'s program introduced a time flag before the sensor reading and a time flag after the sensor reading is printed to the app or microSD card [62]. The difference between these two-time flags indicates the sampling rate [59]. Using this technique, they were able to validate that their device achieved a stable sampling rate of 500Hz [59].

Bravo-Zanogera et al. further adapted various techniques for their ECG sensor, one being a phone app that produces a "live" ECG sensor display and another on-chip SD card that uses a double buffer technique, one buffer captures information from the ADC while another buffer writes the information to an SD card to be processed later [59]. While the on-chip mode of operation for their ECG sensor bypassed the need for Bluetooth transmission, their method effectively mitigated sampling delays resulting from writing ECG sensor data to an SD card [59]. This technique emulates a "sample and hold" data acquisition technique. The v-QueST will need

to adapt a similar technique to mitigate against any potential sampling delays in order to ensure accurate and reliable PPT data are acquired.

Another similar device to that of Bravo-Zanoger et al. was designed by Iskandar et al., and uses the ECG AD8232 sensor coupled with an Arduino Uno, which is, in turn, interfaced with a Bluetooth HC-05 chip accompanied by a Smartphone app [60]. The software on the Arduino Uno manages device function while the on-screen phone app receives and processes the data from the sensor [60]. While the Iskander et al. [58] app also plots the ECG data on the app in real-time. Their data transmission techniques were not discussed and no method for validation was presented.

A device by Cosmanescu et al. transmits EMG and ECG signals through an 8-bit microcontroller (Microchip PIC18LF220) interfaced with a Bluetooth module (WBTV42) that is capable of transmitting data to any Bluetooth compatible devices [58]. The sampling frequency of 2kHz was validated using an ADC channel on the microcontroller hard-wired to an oscilloscope [58]. Their wireless data transfer technique involved connecting the Bluetooth module to a remote computer, through which the remote computer initiated data transmission from the Bluetooth module and sent the data from the ADC with a byte separating every four samples [58]. The data were then parsed with a MATLAB code. This approach allowed them to confirm that they met their desired sampling rate of 2KHz [58].

A wireless surface EMG (sEMG) device by Chang et al. was also capable of achieving a 2kHz sampling rate [63]. The sEMG device uses a MSP430-F5438 microcontroller which converts the analog signal to digital through an onboard 12-bit ADC [63]. The digital EMG signal is then transferred to a Bluetooth chip which transmits the data to a remote server [63]. The TM-204B Bluetooth chip had a transmission rate of 11MB [63]. The MSP430-F5438 microcontroller uses a serial communication port set at a baud rate of 115 200 for connection with the Bluetooth module

[63]. A buffer technique was used, similar to that of Bravo-Zanogera et al., whereby some data from the ADC is placed in the Bluetooth buffer being transmitted to the remote server in order to verify sampling rate [63].

The literature reviewed in this section were used to inform the methods employed in this thesis to ensure that the v-QueST wireless device achieves a high and stable sampling rate, validated empirically.

3.0 WIRELESS V-QUEST PROTOTYPE

In this chapter, the design of the wireless v-QueST is outlined. The design of the mechanical components, software and hardware design, are explained. The functional and non-functional requirements of the wireless system are outlined. The wireless v-QueST mechanical design was retained from the wired v-QueST device designed by A. Brennan and L. McLean (WO2021072546A1 [64]), with the addition of an on-board signal conditioner. This chapter includes a detailed description of the wireless interface developed by the author, with a further detailed explanation of the wireless app, also developed by the author. Therefore, this chapter addresses the first objective of the thesis: to construct a fully assembled wireless v-QueST prototype which includes (i) a v-QueST assembly interfaced with a wireless interface which streams load cell data, and (ii) a wireless app which acquires the streamed data, processes the data, and summarizes the relevant information.

3.1 Design Requirements

The mechanical design of the wireless v-QueST was based on the original hard-wired v-QueST device used for research applications. The v-QueST device currently in use contains a spring which compresses a force transfer plate onto a load cell, with the resulting analog force being passed via hard-wire connection to an external system which provides analog amplification through a signal conditioner, analog to digital converter and then displays the data while also storing them on a personal computer (PC). The load cell in the current device is powered through an external power source.

The wireless device retains the spring and force transfer plate but is interfaced with an on-board signal conditioner, a battery, and the Bluetooth™ module. The wireless v-QueST is designed

to be small, lightweight, and easily sanitized, with all electronic components housed internally in such a way that the user cannot access them but can remove them as a unit prior to disinfecting the casing. Both devices use off-the-shelf electronic components (apart from the external system in the wired device) and allow a single patient use cotton swab to be replaced between patients.

The wired system currently in use samples force data at 2kHz. While precise specifications for the wireless v-QueST are unknown, some minimum requirements for sampling frequency and transmission delay can be deduced from the literature and from the typical operation of the device.

Nominal Sampling frequency*:* From the literature, the PPT value in women without vulvar pain is approximately 700g (approximate average of reported PPT values of healthy women [2], [13], [14], [23]) and the recommended rate of force application to determine the PPT is 694g/s (approximately 700g/s)[65]. Using a resolution of 1.5g (which is half of the first increment in Pukall's VGM [2]), a nominal sampling interval of 2.14ms would be required to achieve this resolution, which converts to 467 Hz. Therefore, 467Hz was deemed the minimal sampling rate required to produce a nominal PPT resolution of 1.5g. Indeed, most previous vulvar measurement devices determine the PPT use discrete and predetermined pressure/force values [2], [19], [20], and thus have not reported on resolution. We therefore set a functional requirement for the wireless v-QueST to sample at a minimum of 467Hz.

Transmission/sampling delay: It is optimal to have no signal delay induced by sampling methods or wireless transmission. To determine the functional requirement for acceptable delay in signal transmission by the wireless v-QueST, we considered the impact of any such delay on the patient as well as on the validity of the measurements. In terms of the impact of a transmission delay on the patient, we must consider that some women with vulvar pain are hypersensitive, reporting pain when wearing clothes [64], and at vulvar pressures in the order of 16.4g [14], while

others report their PPT to be much higher, at 165.3g [2]. Furthermore, while no differences have been investigated in women with PVD, the difference between pressure pain threshold (PPT) and pressure pain tolerance (PPTol) readings for healthy women is approximately 100g [17]. At a sampling interval of 2.14ms we would have a resolution of 1.5g (determined above); and a transmission delay of approximately 50ms would result in a difference between the actual and measured PPT of 34.5g, essentially doubling the PPT in some women, causing them more pain than is intended with the assessment, and potentially approaching their pressure pain tolerance. Thus any transmission delay must be <50ms. Another consideration in the determination of the transmission delay is the minimal detectable change (MDC) in the PPT. This has only been determined for healthy women, and is reported to be 269.6g [43]. Any transmission delay less than 90ms (i.e. half resulting in a resolution of 135g) should not impact the MDC in healthy women yet the MDC may be lower in women with vulvar pain conditions. So, for women experiencing pain, we conservatively selected 20ms as an acceptable Bluetooth transmission delay. This delay would create an error of 14g, which is lower than the lowest reported PPT value recorded from women with vulvar pain, and, if it were consistent between applications, would be unlikely to impact the validity of the device.

Based on these analyses, it was determined that the wireless v-QueST device should be applied by the clinician at a rate of 700g/s, should have a nominal sampling rate of 467Hz, a transmission delay less than 20ms.

3.1.1 Device operation and display

An MFM lab team focus group consisting of four clinicians and two researchers was conducted to identify the relevant data required for the operation of the v-QueST through the wireless app. It was determined that the application should be easy to use, provide the important

clinically relevant information on the display, and allow the user to view their rate of application while they apply force through the cotton swab tip. This resulted in the following functional and non- functional requirements

Functional requirements

- App should sample data at a minimum rate of 467Hz
- App should receive data with less than 20ms delay
- The device is easily manipulated by the user
- Live graphical display of force reading from sensor (to ensure that the rate of force application was consistent and appropriate to the application)
- On screen start button for patient to signal the clinician to begin the procedure (this ensures that the patient is ready for the test and consents to it)
- On screen button for patient to press when their PPT has been reached
- Displays the patient's PPT reading in grams
- Capacity for the user to export clinically relevant information

Non-functional requirements

- The wireless device is not intimidating to the patient
- The refresh rate of graphical force data on display screen should be at a rate that is imperceptible by the user. Visual reaction times are reported to be approximately 200ms [66], [67].
- A text file, which stores all the clinically relevant information, should be stored locally on the device and can be overwritten between uses as long as there is a reminder/warning not to overwrite data if they have not been exported

- The text file of test results should be retrievable from the device locally and sent to a clinical database via email
- A single scrollable screen app should be used to ensure that the app is easy to use
- The interface should include input text dialogues for the user to insert the name of the patient (or identification number) and the date
- The app should contain a drop-down menu for the user to select the location of pressure application (using the vulvar clock as is recorded clinically)

3.2 Mechanical Design of the v-QueST device

The wireless v-QueST has three main parts: (1) the outer casing (2) the force transfer unit and (3) the electronics unit. The outer casing is designed to house all inner components and to be easy to sanitize between patients. It contains a top cap, a casing body, and a bottom cap (Figure 3.1). The top cap and bottom cap can easily be twisted off to access the inner components and the battery compartment in the wireless prototype. Extending out of the top cap is a collet which fits a cotton swab, allowing the clinician to insert a single patient use cotton swab for each new patient without exposing the interior electronic components.

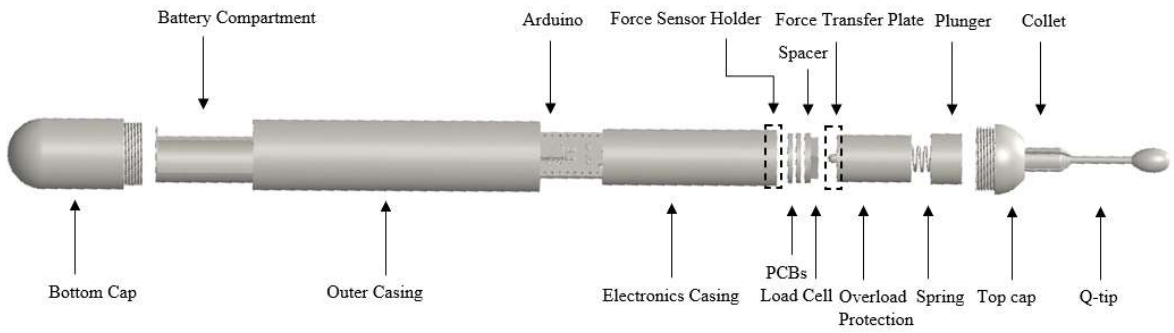

Figure 3.1: *An exploded view of the wireless v-QueST. The three sections are (1) the casing (top cap, outer casing, and bottom cap), (2) the force transfer unit (Q-tip, collet, plunger, spring, overload protection, force transfer plate, and force sensor holder) and (3) the electronics unit (load cell, spacer, printed circuit boards (PCBs), Arduino® microcontroller, Bluetooth™ module, boost converter, electronics casing, and battery compartment). Note that in this figure, a Bluetooth™ module and a boost converter are not shown but would be embedded in the electronics casing along with the Arduino® microcontroller.*

The force transfer assembly is located at the top end of the device. A cotton swab is placed in the collet which fits into a plunger. On the other side of the plunger is a spring that fits tightly into a recess within the plunger and another recess in a force transfer plate which prevents the spring from buckling. The cotton swab, collet and plunger assembly ensure that the spring (k=0.8822 N/mm [68]) is slightly preloaded (0.044 N) and thus operates within its linear range. The spring allows the clinician to apply a more gradual force against the area of interest and further provides feedback to the clinician on how much force is being appled. There is a cylindrical piece extending from the force transfer plate which fits into the SMD410 miniature load cell (Strain Measurement Devices, Wallingford, Connecticut) and transfers the force from the spring to the load cell. Extending on the other side of the force transfer plate is an overload protection. The spring and overload protection together, ensure that load cell is not overloaded. The overload protection, a long and thin tube, distributes the force away from the center of the load cell when the plunger is compressed at forces greater than 7.9N. The force transfer unit functions such that when a force is applied by the Q-tip, the plunger transfers the force to the spring, then, via the

force transfer plate, to the load cell which is located adjacent to an electronics casing and is hard-wired to it.

The electronics unit is safely embedded in the electronics casing which houses a spacer, two printed circuit boards (PCBs), the Arduino® Nano, the Bluetooth module, and a boost converter. The load cell functions as part of the electronics unit but is not embedded within the electronics casing. A force sensor holder sits on top the electronics, which encases the load cell (Figure 3.1). The load cell receives the force from the force transfer unit and transfers the analog output to a PCB. A spacer ensures that the load cell does not come in contact with a PCB as per manufacturer instructions. The four load cell wires are directly soldered into the first and second PCB, which contains the signal conditioner. The PCB then extends the four wires from the load cell to an Arduino Nano board and to a Bluetooth HC-06 module. A back case is connected to the electronics casing with SuperGlue™ adhesive; this back case houses a CR2 Energizer® lithium-ion battery (EL1CR2BP, Energizer Holdings Inc., Missouri).

The wired v-QueST contains all of the components from the casing and force transfer unit but omits all components of the electronics unit other than the load cell and corresponding force sensor holder, whereby the load cell is wired directly to an input to the PowerLab™ (ADInstruments, PowerLab 16/35, Colorado, USA) data acquisition system. In order to compensate for the lack of PowerLab system in the wireless v-QueST, unlike the wired v-QueST, within the device it contains a signal conditioner, a Bluetooth module and a battery. This consequently results in the wireless v-QueST being longer than the wired v-QueST.

The entire prototype was developed using off-the-shelf components, with casings made through 3D printing in polylactic acid (PLA). Ultimately the casing would be made of stainless steel for durability and ease of disinfection. The electronics casing and the force sensor holder are

printed in PLA as one part (as seen in Figure 3.1). The electronics unit and force transfer unit are assembled before placing them in the outer casing. Once the electronics are soldered (including battery contacts and wires to the battery casing), the spacer is carefully secured into place with SuperGlue, ensuring that no adhesive touches the load cell. The battery casing is then adhered to the back of the electronics casing, again using SuperGlue. To assemble the force transfer unit, the spring is firmly twisted to fit a recess in the force transfer plate. The force transfer plate and overload protection are printed as one part for easy assembly (Figure 3.1). The spring is then firmly twisted to fit in the plunger, and on the other side of the plunger, the collet is placed through an opening. The top cap is twisted onto the outer casing and the entire force transfer unit is placed inside. Then the electronics unit is carefully pushed through the casing, and the back casing is twisted on. Technical drawings of each part are in shown in Appendix A.1 Wireless v-QueST Technical Drawings.

3.3 Hardware

The electronics casing contains two main connections: (1) the load cell to the signal conditioner and (2) the Arduino Nano to the Bluetooth HC-06 module. The wired v-QueST uses an external ZSC31014 signal conditioner (Renesas Electronics Corporation, Tokyo, Japan) within a PowerLab data acquisition system, but to make the wireless v-QueST, a signal conditioner needed to be incorporated into the device electronics. A full circuit diagram of the hardware components can be seen in Figure 3.2.

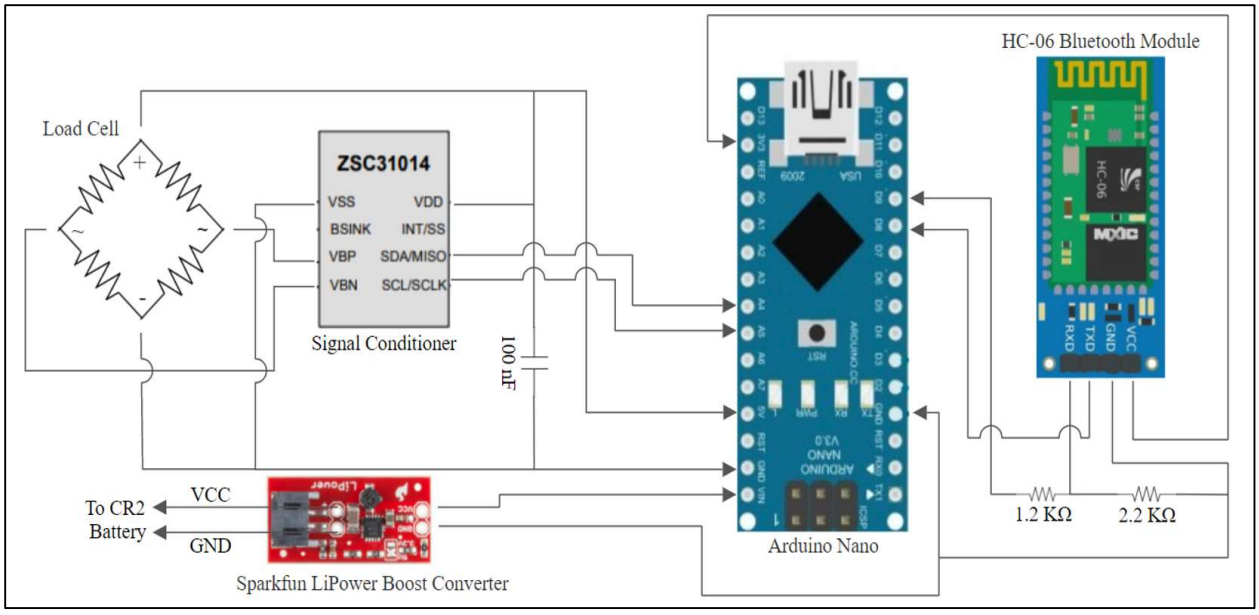

Figure 3.2: *Circuit diagram of wireless v-QueST including the SMD410 load cell, Arduino Nano, HC-06 Bluetooth™ module, Sparkfun® LiPower Boost Converter and a CR2 lithium ion battery (not shown in figure).*

3.3.1 Load cell and Signal Conditioner

The load cell in the v-QueST is a S410 miniature load cell. It is in a four-wire Wheatstone bridge configuration and has an operating range from 0 to 900g [41]. The wires extend vertically down from the load cell and were provided with extra reinforcements by the manufacturer to ensure they do not disconnect under tension. There were two PCBs designed to connect the load cell to the signal conditioner. Since one of the recurring issues in the wired v-QueST was that tension on the load cell wires would cause them to break, the upper PCB functions to relieve stress off the load cell wires. The load cell wires are only connected to the top side of the upper PCB and their corresponding connection on the bottom side of the upper PCB is relayed by a new set of wires. This ensures that the load cell wires are not stressed past the upper PCB such that the upper PCB functions to simply relay the analog information from each wire on the load cell to the lower PCB. This also allows for easier repair, in the event that the load cell breaks (which has happened in the wired v-QueST), the load cell can easily be replaced without interfering with the bottom

PCB. Between the upper PCB and the load cell is a spacer, ensuring the load cell does not sit directly on top of the PCB.

The lower PCB contains a ZSC31014 signal conditioner with amplification and analog-to-digital conversion [69]. The signal conditioner amplifies the analog signal at a pre-set programmable gain then converts the analog signal to digital through an ADC [69]. The ZSC31014 was chosen because of its operating voltage (2.7-5.5V), I^2C communication method and small size (4.9 by 6.0 by 1.5 mm) [69], [70]. The differential signals from the load cell serve as inputs to the V_{BP} and V_{BN} on the ZSC31014 and are output as amplified and digitized inputs to Arduino Nano serial data (SDA) and serial clock (SCL) [70]. The power and ground from the load cell are connected to power and ground (V_{DD} and V_{SS} [69]) of the ZSC3101. The load cell and signal conditioner are powered by the Arduino Nano with 5V excitation. Between the power and ground supplied by the Arduino is a bypass capacitor [70], as is recommended by the manufacturer. This bypass capacitor creates a short circuit to ground for alternating current (AC) signal, in such a way to remove any AC signal present in the direct current (DC) signal. The recommended excitation voltage of the ZSC31014 is 2.7V to 5.5V [69] whereas the load cell operates below its recommended excitation voltage of 10V [41], which, through communication with the manufacturer, was determined to be acceptable (A. Brennan, private communication, Mar. 2020). By operating the load cell at 5V instead of 10V, the full-scale output is decreased from 10mV to 5mV without impacting its resolution. This was verified by powering the wired v-QueST with 5V excitation, which resulted in no change in the resolution of the output signal.

The ZSC31014 signal conditioner was calibrated using the ZSC31014 calibration kit and software using 2-point calibration [70], [71], as recommended by the manufacturer [69]. The ZSC 31014 signal conditioner datasheet indicates that the nominal input span (1.00mV/V) of the load

cell results in the ADC resolution of 11.1-bits. At a nominal input span of 1.00mV/V, the ZSC31014 the amplifier gain is recommended to be set to its maximum (X192) [69]. This results in a maximum output voltage from the amplifier (0.96V) to serve as the input signal (0.96V) to the ADC, which will be on the low end of its 5 V operating range. Communication with the manufacturer determined that the ADC will then operate in the order of 0-19% of its available range (A. Brennan, private communication, May. 2020), consequently proportionally reducing the 14-bit resolution of the ADC to approximately 11.1-bits [69]. However, 11.1-bit resolution provided by the ADC will give a resolution of 0.0456% of the full-scale output, meaning that it should provide a resolution of 0.41g, which is ample for the v-QueST application.

3.3.2 Arduino and Bluetooth Wireless Interface

The conditioned load cell signal is interfaced with the Arduino Nano to be read through I^2C communication. The choice of Arduino and Bluetooth devices was heavily influenced by the size constraints of the wireless v-QueST. The wireless v-QueST was required to be easily held and manipulated in one hand, similar to a highlighter or a standard screwdriver handle.

Various microcontrollers and Bluetooth modules were explored in the design of the wireless interface. Microcontrollers were required to have two power outputs (to power both the signal conditioning unit and the Bluetooth module), to have four input signals (to accommodate the bridge configuration of the load cell) and to accommodate the small size requirements of the device. A maximum width of 20mm is necessary to ensure it fits comfortably in the user's hand, and a maximum length of 40mm is necessary to ensure the v-QueST is not too long. The Bluetooth module was required to have a high over the air data rate, and to operate using a 3.3V power supply while also meeting the small size requirements for the device. Both Bluetooth classic and BLE were explored in the design of the device, but the data rate was an important determinant since the

goal was to achieve a minimum sampling rate of 467Hz. A large influence on the decision among microcontrollers and Bluetooth modules that met the requirements was the availability of open-source material on the Internet to facilitate the design and troubleshooting of the wireless operation of the device.

The Arduino Nano was selected as the microcontroller for the wireless v-QueST. Other considerations for the microcontroller were the Wemos© D1 mini [72], Adafruit Trinket [73] and DFRobot Beetle [74]. These were not chosen due to their size (the Wemos D1 mini was too wide at 25.6mm [72]) and power output (the Adafruit Trinket and DFRobot Beetle only had one power output [73], [74]). The Arduino Nano has up to 8 analog input channels and two power outputs in a compact design (18 x 45 mm) [75]. Arduino microcontrollers have been heavily used in custom device designs in the MFM lab. While there are other microcontrollers that operate in the Arduino integrated development environment (IDE), Arduino microcontrollers have the advantage of several online resources to aid in the design process.

Both Bluetooth Classic (2Mbit/s) and BLE (1Mbit/s) have acceptable data rates for this application, since both can achieve the required minimum sampling rate of 467Hz, Bluetooth Classic was chosen because the researcher had used Bluetooth Classic in the past, and thus was familiar with it, and because there is more open-source material available for Bluetooth Classic than for Bluetooth BLE. Two Bluetooth 2.0 modules, HC-05 and HC-06, were identified as being capable of accommodating the size requirements of the device as they were both small 12mm by 37mm [76]) and Android compatible. The HC-05 operates as a master or slave while the HC-06 operates only as a slave [76]. The HC-06 module was chosen because it is simpler to program and since it will always be the slave to the Android device (master) in the v-QueST application.

The connection from the HC-06 to the Arduino is very simple. The HC-06 has an excitation voltage between 3.3-6V [76] and thus can be appropriately powered using the 3.3V output from the Arduino Nano. The transmitting (TX) and receiving (RX) ends from the HC-06 module are connected to the RX and TX pins of the Arduino (set as D8 and D9). The 5V TX pin (D9) on the Arduino requires a voltage divider to ensure that the input to the RX HC-06 module remains below the 3.3V logic level [76].

The entire system (load cell, signal conditioner, Arduino, and Bluetooth) is powered by a CR2 lithium ion 3V battery (Lithium CR2, Energizer, USA). The Arduino Nano and HC-06 Bluetooth module require high current (80mA) when initially connected and moderate current (48mA) when transmitting data [75], [76]. The CR2 lithium-ion battery is small (27 by 15.6 mm) and provides maximum continuous discharge of 1000mA with an average life of 800mAh [77]. Therefore, at a maximum discharge of 80mA, the v-QueST device can operate for 10 hours on one battery. However, during actual use the Arduino and Bluetooth do not continuously operate at their maximum current discharge, so the v-QueST device can be expected to be used for roughly 20 30-minute assessments on as single battery. The Arduino Nano requires a 5V operating voltage, so a Sparkfun® LiPower Boost Converter (Sparkfun Electronics®, Colorado) was included in the design to convert the 3V from the CR2 battery to 5V [78]. The LiPower Boost Converter has a maximum current of 600mA and undervoltage lockout, which is important because draining the CR2 battery can cause an internal short circuit which is very dangerous [78].

3.4 Software

Once the circuit was complete, it was uploaded to the Arduino. Arduino IDE was used to program the wireless interface and set-up the Bluetooth module. A SoftwareSerial library [79] was used to ensure serial communication between the Arduino and the HC-06 module by allowing

serial communication on digital pins D8 (RX) and D9 (TX) on the Arduino Nano. The wireless application was programmed on Massachusetts Institute of Technology App Inventor 2 (MIT AI2) which is Android compatible [80]. MIT AI2 is a free and open-source software that has both a designer and a blocks interface [80]. The designer graphical user interface (GUI) allows the user to drag and drop components to create the GUI of the app [80]. The blocks interface is the back end of the code, allowing the user to program specific actions and tasks for each component or screen through blocks [80]. These were used to program the back-end components of the app GUI.

3.4.1 Bluetooth Set Up

The HC-06 Bluetooth module is connected to the Arduino Nano as shown in Figure 3.2. The HC-06 Bluetooth module must be programmed and initialized. To do this, a custom Arduino script (Appendix B.1 Initial Bluetooth Setup) was created based on an adaptation of code found on an open-source blog [81]. As stated previously, the SoftwareSerial library is included in the script. Within the *void setup()* loop, two serial communications are established, one between the Arduino Nano and the computer screen (Serial) and the other between the Arduino Nano and the HC-06 module (mySerial). Within the *void loop()*, once there are bytes available to read in each serial, the readings from Serial are sent to mySerial and vice versa. The programmer can write commands into the Serial monitor and the script relays that information to the HC-06 module. When the commands are read by the HC-06 module, a reply is sent to mySerial and forwarded to the Serial monitor. The replies ensure that the commands are properly read, and that the HC-06 module is programmed correctly. Through this configuration, the HC-06 module is named (VGMBT), given a password (4102) and set at a baud rate of 115200. This is done with jumper cables before assembling the entire circuit.

3.4.2 Arduino Code

The final script uploaded to the Arduino sends load data from the load cell to the application (Appendix B.2 Wireless v-QueST). The Arduino script contains two main parts: (1) load cell data acquisition, done through a wire library, and (2) Bluetooth data transfer of the acquired load cell data, done through serial communication as described below.

Load cell data from the ZSC31014 are read by the Arduino Nano through I^2C communication (serial communication bus) by incorporating a wire library and the use of SDA and SCL pins. The I^2C slave for the ZSC31014 is given an address (28HEX (0x28)) [69] which is used to transfer data from the signal conditioner to the Arduino. The slave address of the signal conditioner sets the mode of the device as read only using the last of its 8 bits, consequently establishing the signal conditioner as the slave device in the bus. The *Wire.begin()* function initiates the wire library [82] in the *void setup()* function. In the *void loop()* function, transmission from the signal conditioner (*Wire.beginTransmission()*) begins via the slave address [83] and then the Arduino requests (*Wire.requestFrom()*) [84] and reads (*Wire.read()*) [85] the bytes from the signal conditioner's two registers (SDA and SCL). The bytes from the two registers are then concatenated by applying a bitmask, converted to a float variable, and then converted to units of force in grams (F = 900*y/16323, where 900g is the full range of the sensor, 16323 is the maximum output value in I^2C and y is the float variable).

The Bluetooth transfer of load data is accomplished through wireless communication between the HC-06 module and the Android device. In the *void setup()* function, serial communication is established between the Arduino Nano and the Bluetooth HC-06 module (mySerial) and between the Arduino Nano and the PC (Serial). The wireless connection between the HC-06 module and the Android device receives the same data as written to mySerial. The data

are sent wirelessly in the *void loop()* function, where timer0 (a precise timer built into the Arduino hardware) is used through the Arduino *micros()* function [86]. A precise timing technique, adapted from Bravo-Zanogera et al [59] is used to send data (Figure 3.3: Arduino® script of the precise timing technique, where a time flag is started before and after the data are printed into mySerial. The difference between these two-time flags is required to be greater than 1500µs (at a 666.67Hz sampling rate) for the program to print the sensor readings into mySerial. This consequently ensures that the conditioned force data from the Arduino are sent to the Bluetooth at known and stable intervals. When the sensor reading and the difference between the two-time flags (referred to as timestamps) are written into mySerial (*mySerial.Print()*) [87], there is a separator ("|") inserted for easy data parsing on the Android end. In the situation where there are data sent from the Android to the HC-06 module (indicating that the PPT has been reached), there are bytes available to receive the data in mySerial (*if (mySerial.available() > 0)*) [88]. This consequently flags the sensor reading at the time the button was pushed by adding 5000 to the reading, allowing the Android app to recognize the sensor reading indicating the PPT. The Android serial is then cleared (*mySerial.read()*) [89] to ensure that a sensor reading is not flagged again until the Android sends new data.

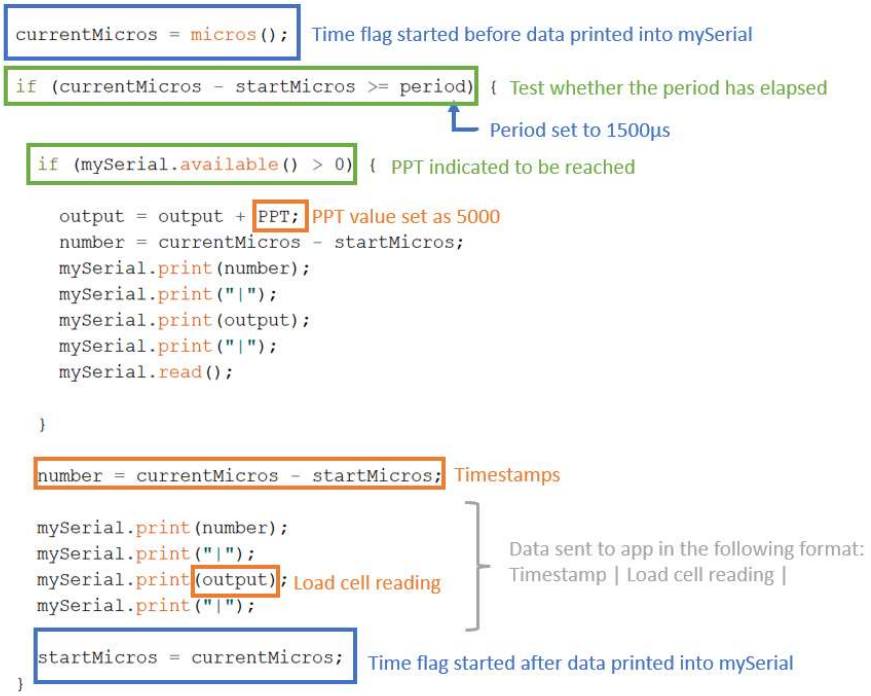

Figure 3.3: *Arduino® script of the precise timing technique.*

3.4.3 v-QueST App

The v-QueST app was designed using MIT AI2 based on input from a focus group including ten clinicians and researchers affiliated with the MFM lab. The focus group identified that a simple design was essential to user adherence and was the most important design feature. The information that the group deemed to be relevant to the application included participant name or identification (ID) number, test location, and PPT value. In addition, the group indicated that "real time" presentation of the data on a graphical interface is essential to ensure that the test was performed correctly and that the PPT identified by the software was accurate.

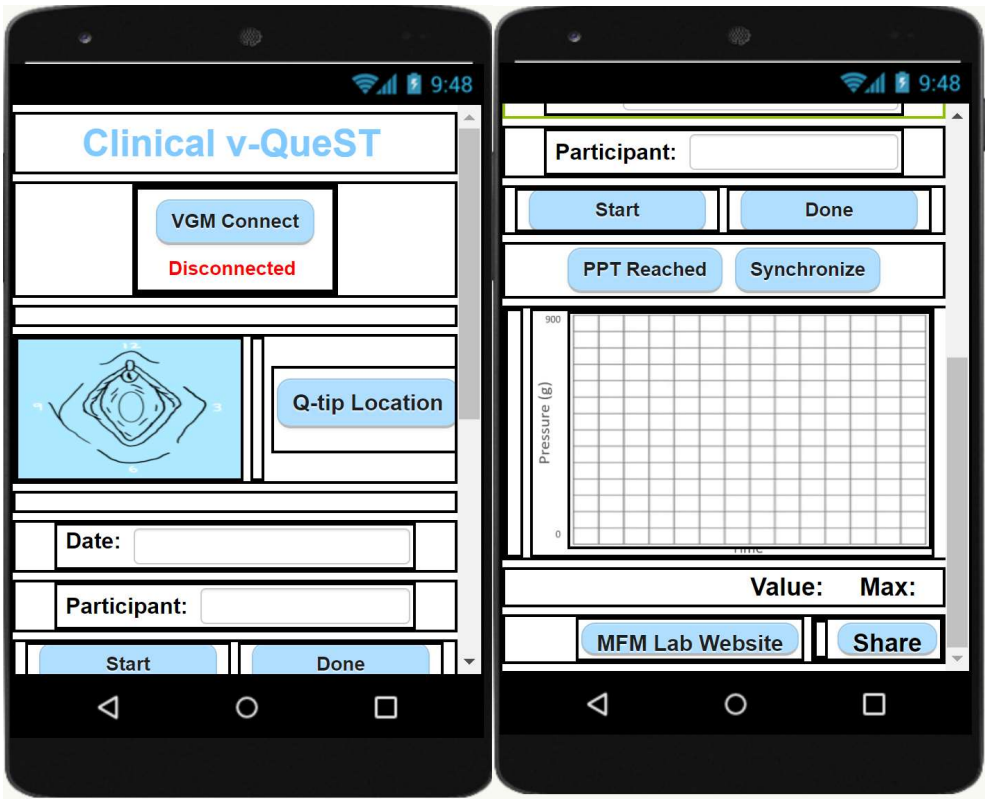

Figure 3.4: *The wireless application of the wireless v-QueST.*

Since simplicity was highlighted to be the most important aspect of the app design, the app was developed to be on one scrollable page. The scrollable page also makes the Bluetooth connection more stable because transferring the connection to different pages can lead to instability or disconnection. Moreover, all clinically relevant information is easy to enter, including testing date, participant name or ID, and test location. When the app is initialized, the Bluetooth status is shown as disconnected and the operational controls (i.e., *START*, *DONE*, *PPT Reached*, and *Synchronize*) are hidden. The internal clock within the MIT AI2 is set to remain disabled at this point. Prior to using the app, the user connects the Bluetooth HC-06 in the Android device Bluetooth settings. The full block code of the MIT AI2 app can be found in Appendix C.1 Wireless v-QueST.

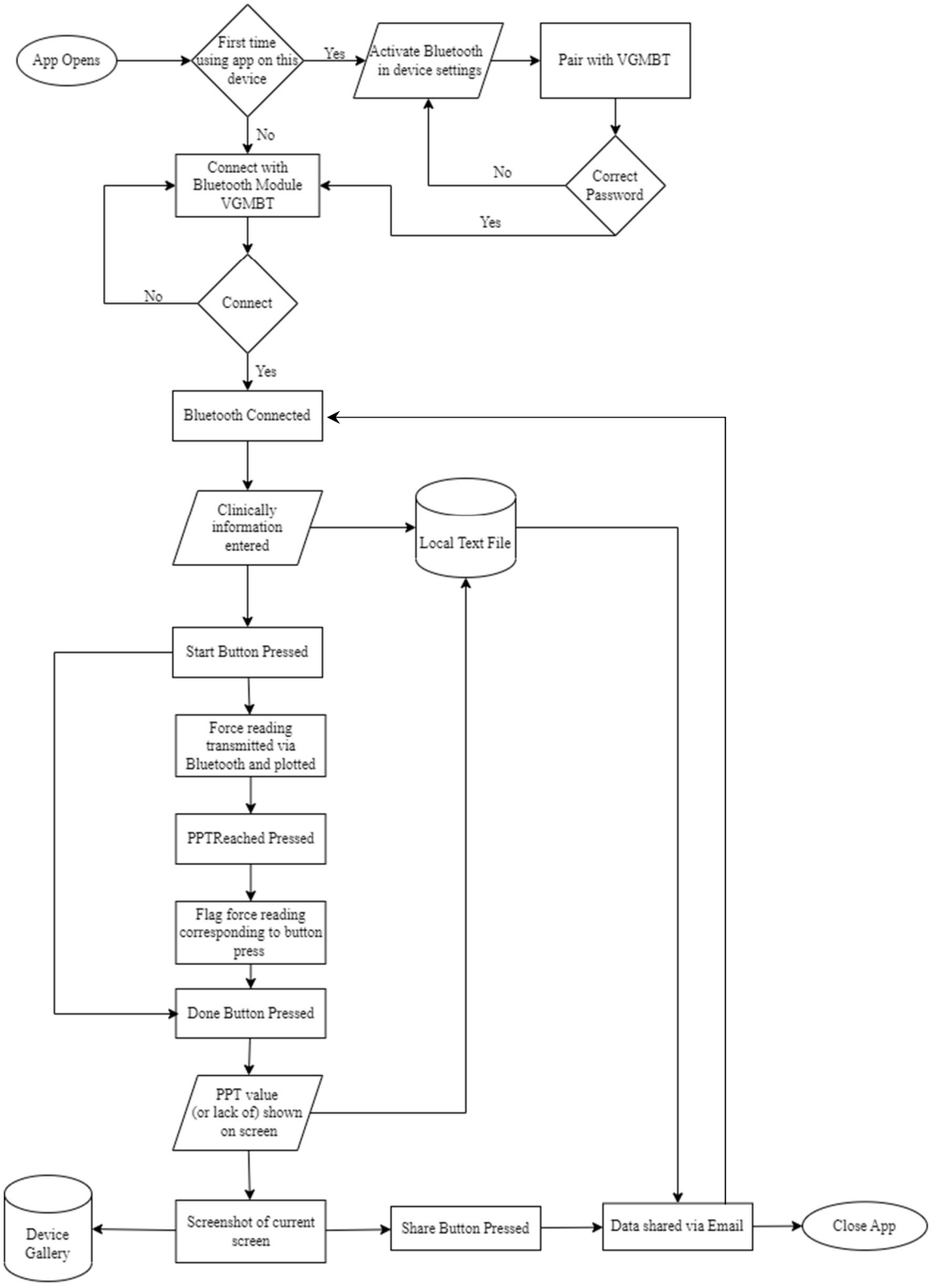

Figure 3.5: *Flowchart of App functionality*

The app has eight buttons, two input texts, one graph, two internal clocks and streams a single file. The steps required during use include:

- **VGM Connect:** When this button is pressed, a list of all Bluetooth devices connected to the Android is shown. The user selects the Bluetooth device VGMBT from the list for pairing, and the app connects to the selected Bluetooth device address and Serial Port Profile (SPP). If VGMBT is selected, a notifier pops up informing the user of a successful connection. If another Bluetooth device is selected, a notifier informs the user that they have not connected to VGMBT. If the app is unable to connect to a selected Bluetooth device, a notifier will show an error. Once connected to the correct Bluetooth (VGMBT), the Bluetooth status changes from *"disconnected"* to *"connected"* and the start button becomes visible.
- **Q-tip Location:** This button allows the user to select the test site according to a visual display of the vestibular clock. Eight options are displayed, and when the user selects the desired test location, it appears below the Q-tip Location button.
- **Date:** The date is pre-filled when the application is opened but is modifiable through input text.
- **Participant:** This is an input text. The user can enter the participant's name, or a participant or patient number if so desired to protect privacy.
- **Start:** The start button allows the user to begin streaming data from the v-QueST device to the app. When the user presses *Start*, a notifier asks the user if they are sure they want the procedure to start. Once the user agrees to start the procedure, the inputs on *Date* and *Participant* are set as read only and the *Done, PPT reached, and Synchronize* buttons become visible, the *Start* button is hidden, *List3* (the matrix that stores all load cell

measurements) is emptied, the graph is cleared, and the file (*VGM_Data*) which stores clinically relevant information, is deleted. Once the file is deleted, a new *VGM_Data* file is created with the *Date* input text, *Participant* input text and *Q-tip location* selection added to the file. *Clock1* and *Clock2* are then enabled with the timer interval in *Clock1* as 300ms. The *StartGraph* variable is set to 1, which instructs the app to plot points on the graph.

- **Clock1:** This clock timer is used to plot and store sensor reading values sent via Bluetooth. The values are only plotted and stored if the Bluetooth device connected is VGMBT and if the *StartGraph* variable is set to 1. The *Clock1* timer reads the data sent from the Bluetooth module every 300ms and concatenates the data into a temporary list of approximately 288 data entries (144 load readings with their corresponding timestamps). The temporary list is added to *List3*. The last value in the temporary list is plotted on the graph (by calling on the function *plot_on_graph*) and is displayed in the *Value text* below the graph (seen in Figure 3.4). Since the *Clock1* timer reads the Bluetooth data every 300ms, the data are updated on the graph approximately 3 times per second. The last value in the temporary list may be a timestamp or flagged as the PPT value and is edited accordingly by either subtracting 5000 (see explanation of button *PPT Reached*) from the value or retrieving the value above the last index value. Also, within this clock timer, when the *take_screenshot* variable is set to 1, a screenshot is taken of the Android screen and saved in the Android's gallery.
- **Clock2:** This clock timer will pop up a notifier if the VGMBT Bluetooth loses connection when load cell data are being sent. This clock timer has a pre-set interval of 100ms meaning that Bluetooth connection is verified approximately 10 times every second.

- **Graph:** The graph plots load cell data during collection to ensure load cell readings are increasing or decreasing as expected. The graph is plotted when the *plot_on_graph* function is called, which stores the previous load cell reading and the present load cell reading as graph variables (*X_before* and *X*) and connects them with a line. If, during the procedure, the end of the graph is reached, then the graph will clear and restart from the beginning.
- **PPT Reached:** This button allows the patient to indicate the time at which their PPT is reached. When the clinician is applying a force through the v-QueST, the patient holds the Android device and presses the *PPT reached* button when their PPT is reached. This triggers the Android to send text to the HC-06 module, consequently resulting in bytes available to receive in mySerial and flagging the load cell value corresponding to the time when the PPT Reached button was pressed. The flagged load cell value (5000 is added to the load cell reading) is then read in *Clock1,* parsed into a temporary list, and then added to *List3*.
- **Done:** The *Done* button allows the user to terminate the streaming of load cell data. Indeed, when pressed, a notifier asks the user if they are sure they want to terminate the procedure. Once the user agrees to stop the procedure, all graph variables are reset to 0 and the *StartGraph* variable is set to 0 to ensure graphing and storing data within *Clock1* is terminated. *List3* is then searched to determine if there is a flagged load cell value that indicates that the *PPT Reached* button was pressed. If there is a value found, the value is shown in the *Max text* below the graph (seen in Figure 3.4). The PPT value or the entirety of *List3* is appended to the *VGM_Data* file (described in the "File" section below), the inputs on *Date* and *Participant* are no longer read only, the *Start* button becomes visible

and the *Synchronize* and *PPT Reached* button are no longer visible. Finally, the *take_screenshot* variable is set to 1 when the *Done* button is pressed, allowing *Clock1* to trigger a screenshot. The screenshot is taken and saved in the phone gallery as a back-up in case of data transfer error or if the user forgets to send the *VGM_Data* file via the share button.

- **File:** The *VGM_Data* file is a text file stored in the SDcard inserted in the Android device, which stores all clinically relevant information. MIT AI2 can read or write to the file, but for simplicity purposes, the v-QueST app only writes to the file. The file always contains the participant's name (or ID number), date, and test location. However, depending on the procedure being run (synchronization or PPT), either the entire *List 3* array is added to the file, or only the load cell value associated with the time the *PPT Reached* button is pressed is added.
- **MFM Lab Website:** This button allows the user to access the MFM Lab Website. The user manual for the device and software will be found there in the future.
- **Share:** A button allowing the user to send the *VGM_Data* file through other applications on the Android device. Generally, the user will send the data via email and the app will set the message to be the participant's name (or ID number) and the *VGM_Data* file will be attached to the email.
- **Synchronize:** This button is used to synchronize two data sets. The v-QueST used in clinical settings will not have this button, but it will be important to have for research and validation purposes. Data are synchronized in the same way the load cell value is flagged when *PPT Reached* is pressed.

A first app iteration, shown in Figure 3.6, flagged the *PPT Reached* or *Synchronize* press at the application end. When the *PPT Reached* or *Synchronize* buttons were pressed, the app software inserted a flag ("Pressed") into *List3*. While this technique seemed to be viable, the "Pressed" trigger would be inserted into *List3* between the Bluetooth data packets (which are parsed into a temporary list). This iteration consequently resulted in the flag being inserted much later than when *PPT Reached* or *Synchronize* were pressed, inducing large and inconsistent button press delays into the data.

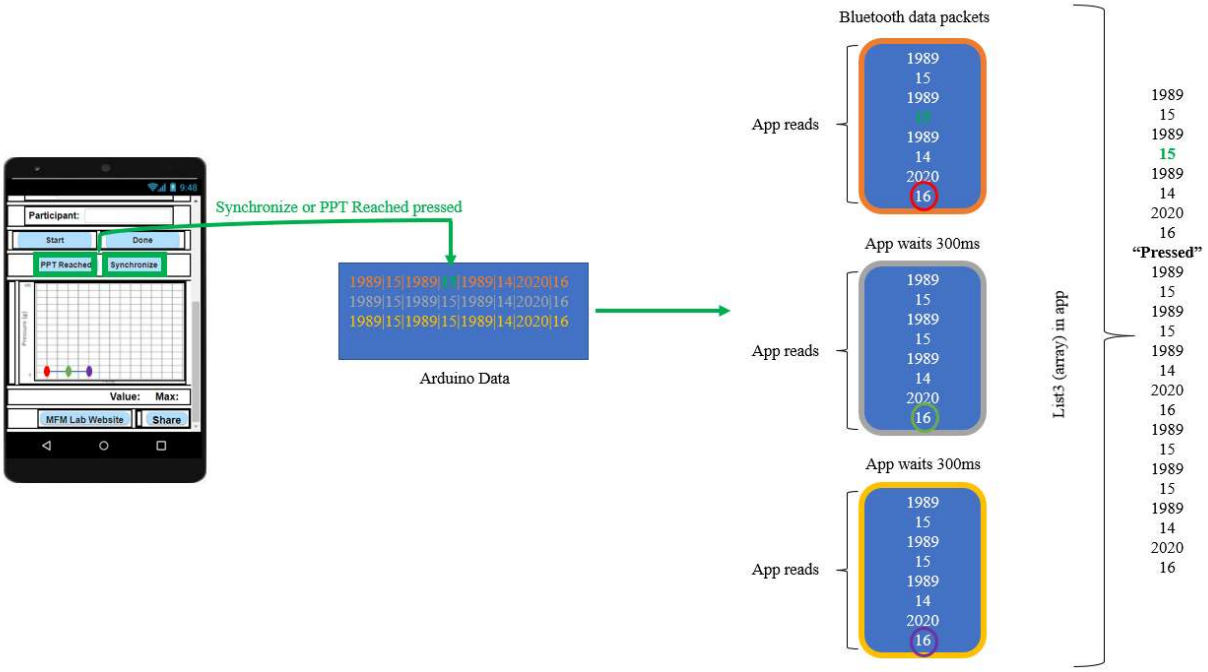

Figure 3.6*: When Synchronize or PPT Reached are pressed, a flag indicating it has been pressed is added in List3 ("Pressed"). The actual load corresponding to when either button was pressed is shown as a green number. The application adds the flag at the end of the data packet which includes the load corresponding to the button press and selects the force value at the end of that packet. This technique resulted in inaccurate flagging of a critical button press. Note that the load value at the end of each data packet is plotted on the live graph in the application.*

To bypass the limitation of the app flagging the PPT value between packets (described in Figure 3.6), it was deemed necessary to flag the PPT value at the Arduino end. As described in the *PPT Reached* and *Synchronize* button section above, when either the *PPT Reached* or the

Synchronize button is pressed (Figure 3.6), the wireless v-QueST application sends bytes to the HC-06 module (*if (mySerial.available() > 0)*). Through entering this if-statement, the load reading is incremented by 5000, a value large enough to distinguish between timestamps, and is sent in a Bluetooth data packet to the application. This technique ensures simultaneous flagging of the load value corresponding to the button press of *PPT Reached* or *Synchronize.* Indeed, both *PPT Reached* or *Synchronize* have the same functionality; however, it was chosen to have both since the *Synchronize* button included all of the load data in the text file which is exported, where as *PPT Reached* only included the PPT value. Therefore, the *Synchronize* button is just used for research purposes and will be eliminated in clinical settings.

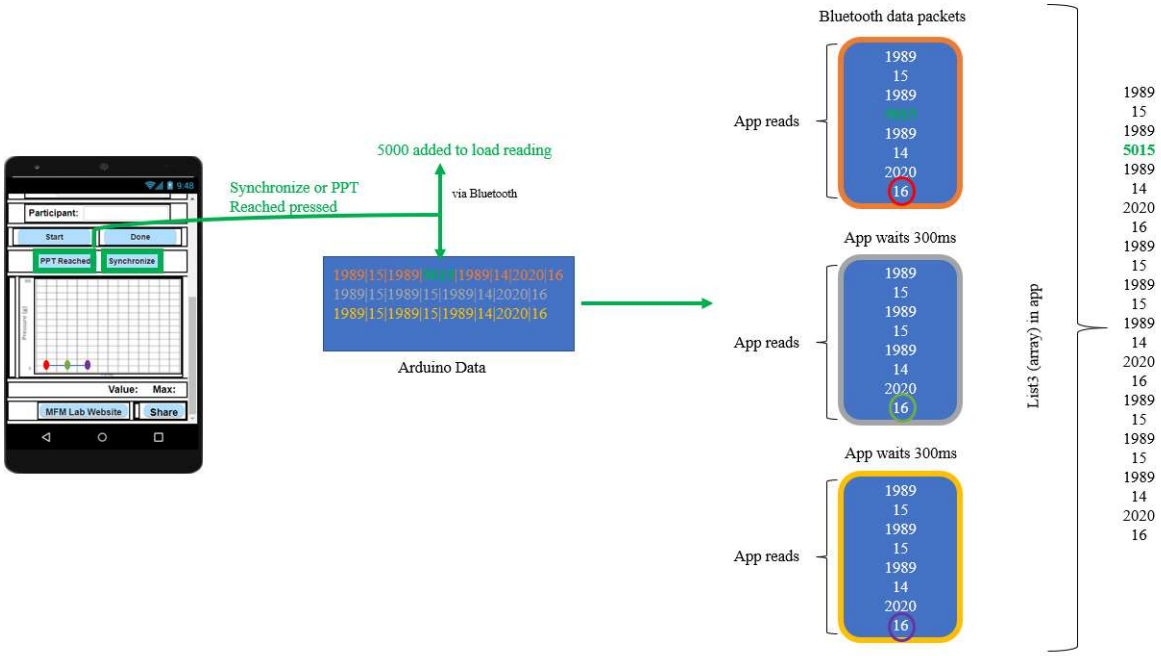

Figure 3.7: *When the Synchronize or PPT Reached button is pressed, a flag indicating it has been pressed is sent through Bluetooth™. The Bluetooth™ module receives this flag and simultaneously adds 5000 to the load reading. This load reading is sent to the application in a data packet and added to List3. This technique ensures the simultaneous flagging of the load value corresponding to a critical button press. Note that the load value at the end of each data packet is plotted on the live graph in the application.*

The application was tested on two Android devices, a Samsung Galaxy Tab E and a Samsung Galaxy S8. On each device, ten trials were conducted where force was applied to the Q-tip inserted into the v-QueST and the PPT button was pressed. The data file (containing *List3*) was sent via email. All functions worked as expected. However, when pressing the *Done* button on the Galaxy Tab E, there was a long processing time (approximately 2 minutes) to search through *List3* and find the flagged PPT value. The Samsung Galaxy S8 did not show a long processing time and searching through *List3* only took 1-3 seconds. This suggests that the older generation Galaxy Tab E (purchased in 2017) has hardware issues.

3.5 Recommended Use of Wireless v-QueST in a Clinical Setting

Evaluation of PPT using the wireless v-QueST is recommended as an aid in the diagnosis and monitoring of vulvar pain conditions. Ideally the clinician tests the v-QueST connection and their rate of application before handing the tablet or phone over to the patient. The patient is in full control of when the procedure starts and terminates, to ensure the patient consents to the procedure and is ready to begin. The outcome of the procedure can be used as a preliminary diagnosis tool, in order to assess the severity of PVD or it can be used to assess progress with treatment [15]. Use of the v-QueST in treatment planning can be greatly beneficial as the PPT would be reassessed periodically to assess if there are any changes.

3.6 Discussion

The mechanical design of the v-QueST device successfully meets all of the specified design requirements. It is small (19.7cm x 2.4 cm), compact and comfortably fits into a clinician's hand for ease of manipulation. It is wireless and safely embeds all electronic components within an electronic casing that cannot be accessed by the clinician. For infection control purposes, the

electronic components are easily removed such that the casing can be sanitized without disrupting the electronics housed within the device; and the Q-tip is discarded and replaced between participants. While the prototype made from PLA cannot be autoclaved since the temperature of an autoclave (121°C [90]) is far too close to the melting temperature of PLA (170°C [91]), the PLA casing of the device is currently disinfected by removing the electronics unit and placing the casing in Cidex™. Ideally the final product will have a metal outer casing (aluminium to keep the device light weight) but the internal electronics casing and components would still be housed in PLA or silicone, since a conductive metal could interfere with the electronic signals.

The off-the-shelf electronic components make repairs easy and successfully eliminate the need for an expensive signal conditioner or ADC, keeping the cost of the device low (the total component costs for the prototype = $413.57, with >$300 of this cost being the load cell). The electronic circuit is compact with only a few components, thus limiting sources of failure. The Android application is simple, easy to use, and maintains a wireless connection with the v-QueST such that data are streamed to the device through a custom app.

If user-group testing reveals that the device is too large to manipulate easily, there is an opportunity to reduce the length of the wireless v-QueST by 30mm by eliminating the spring without changing the load transfer to the sensor. Eliminating the spring requires consultation with clinicians because the spring was originally included to provide feedback on the amount of pressure applied. The electronic components can also be made more compact by using the Arduino Nano 33 BLE, which contains an on-board BLE chip [92]. Indeed, the use of BLE would greatly reduce the power consumption of the device but would require modifications to the app code (connecting to a BLE device requires different blocks in the MIT AI2 code). Alternatively, rechargeable CR2 lithium-ion batteries can be used instead of regular batteries to reduce operation

costs. As noted above, CR2 lithium-ion batteries allow for 10 hours of usage at maximum current discharge.

While the app worked as expected, the long processing time noted on the Galaxy Tab E device (approximately 2 minutes) is likely due to hardware issues on Galaxy Tab E device in the MFM lab. Indeed, the functionality of the app is not complicated, and the processing time on the Samsung Galaxy S8 was in the order of 1-3s. The Galaxy Tab E is an older generation device (2017). Indeed, it would be best to confirm these findings with different mobile devices of different generations as well as by different manufacturers.

3.7 Conclusion

The wireless v-QueST prototype was successfully built with an app. It is further necessary to test the wireless system to ensure the sampling rate and transmission delay fall within the specifications highlighted in this chapter. The following chapters discuss the methods and results for sampling frequency and time delay validation.

4.0 SAMPLING FREQUENCY VERIFCATION

As determined in our functional requirements (Chapter 2), the wireless v-QueST must be capable of reaching a stable sampling frequency that is a minimum of 467Hz. The software design presented in Chapter 3.4 was configured to result in a sampling frequency of 467Hz (i.e., time resolution of 2.14ms). This chapter describes the method used to validate the sampling frequency of the wireless v-QueST system. The objectives are to test the actual sampling frequency relative to the theoretical and minimum sampling frequency, and further, to test the stability of the sampling rate across different loads and over time. First, a software needed to be developed to achieve the minimum sampling frequency, then, methods were applied and tested to determine if the required sampling frequency was achieved and if it was stable over time.

4.1 Sampling Frequency Software Design

The first step in the software design was to set the baud rate on the HC-06 module. Baud rate is measured in bits/s, therefore a smaller baud rate results in a lower communication speed. The maximum baud rate that a PC can use is 115200, therefore this was the value selected since it provided a data rate of 12800bytes/s. At a baud rate of 115200, the transmission of 5 bytes (a five digit number) would only require 0.39ms, the transmission of 6 bytes (a hundred number with a hundredths decimal precision) would only require 0.46ms, and the transmission of the delimiter '|' (7bits) would require 0.06ms, therefore ASCII transmission of data was deemed acceptable for this application, as the transmission times would not result in any meaningful loss of precision in PPT outcomes.

Within the v-QueST App software, Clock 1 reads conditioned loadcell (SMD410, Strain Measurement Devices, Wallingford, Connecticut) data and timestamp values, places them in a

temporary list and plots them. The timer interval in *Clock1* was set to 1ms (1000Hz). However, when tested, it was determined that the timer interval did not provide adequate time for the block code under *Clock1* to be processed. The conditioned load cell data retrieved in *Clock1,* when set to have a 1ms time interval, had only 1 bit resolution, meaning that the data were saved as a list of binary numbers. Load readings are sent with 0.01 resolution, meaning the maximum number of digits (n=5) is 5 bytes [93], thus as the load increases, the number of digits increases, and thus so does the number of bits required to represent the number (Table 4.1) The *Clock1* interval was therefore increased until load cell readings were retrieved with adequate binary resolution (5 bytes).

Table 4.1: *Bits allocation in binary according to number of digits, adapted from Assi et al* [93].

Number of digits	Maximum number of bits
1	4
2	7
3	10
4	14
5	17

Using this approach, only one load cell measurement could be read in each *Clock1* loop. A sample and hold technique adapted from Bravo-Zanogero et al [59] was therefore developed to bypass the limitation of the clock function. This technique ensured that the sampling frequency of the data was determined through the Arduino® processor and eliminated any potential delays from Bluetooth™ transmission or the MIT AI2 App. The technique uses the *micros()* function in the Arduino software. The *micros()* function uses the 8-bit Timer0 interrupt embedded in the Arduino hardware. Two time flags are established with the *micros()* function in the Arduino script: (i) time flag before printing data into mySerial and (ii) time flag after the data are printed into mySerial.

The Arduino program cannot print into the mySerial monitor before the difference between the time flags reaches a pre-determined time interval. The time interval needed to be lower than 2000µs to account for potential delays in data processing through the Arduino IDE. The time interval was therefore set to 1500µs, allowing for a sampling frequency of approximately 667Hz. After 300ms, *Clock1* reads the Bluetooth data, which include an approximate 300 element list of timestamps with their corresponding load cell readings. This way the Bluetooth sends a complete data set after the Arduino samples data for 300ms. The sampling frequency was then validated experimentally as described below.

4.2 Methods

The sampling frequency of the wireless application was validated under three scenarios: no load (ones reading with 0.01 resolution), loaded with 33.24g (tens reading with 0.01 resolution) and loaded with 227.28g (hundreds reading with 0.01 resolution). These loads were chosen out of convenience and because of the difference in the number of digits assigned to each load. The sampling frequency was set to be 677Hz in an attempt to achieve the fastest sampling rate possible. A prototype v-QueST circuit was powered through a PC, connected to the wireless app, run using a Galaxy tab E tablet (despite its long processing times, is unlikely to have Bluetooth connection or sampling errors) and loaded under each of the three scenarios for 30 minutes. The prototype v-QueST circuit did not contain any soldering and simply connected the wires from the signal conditioner (ZSC31014, Renesas Electronics Corporation, Tokyo, Japan) to the Arduino Nano using alligator clips, with the Arduino Nano powered through the PC via a mini-B USB cable. The load cell was loaded using a simple set up developed by Ana Brennan to calibrate the ZSC31014 signal conditioner (Figure 4.1). The Arduino script was modified such that for each load, 50 samples of data were recorded every 5 minutes over a period of 30 minutes, resulting in 300

samples of conditioned load cell data for each load (Appendix B.3 Sampling Frequency Testing). The sampling was controlled through an if-loop which could only be entered when 300000000 μs (5 minutes) had been passed, which was controlled through a counter variable. The counter variable added the time interval between the two-time flags to its previous value until it reached 300000000, where it was subsequently set back to 0. Each data file from the wireless application was sent via email and included both the force (in grams) and the time intervals between samples. The data file was parsed using a custom MATLAB program, and the sampling frequency (in Hz) was determined through the inverse of the sampling interval (in μs).

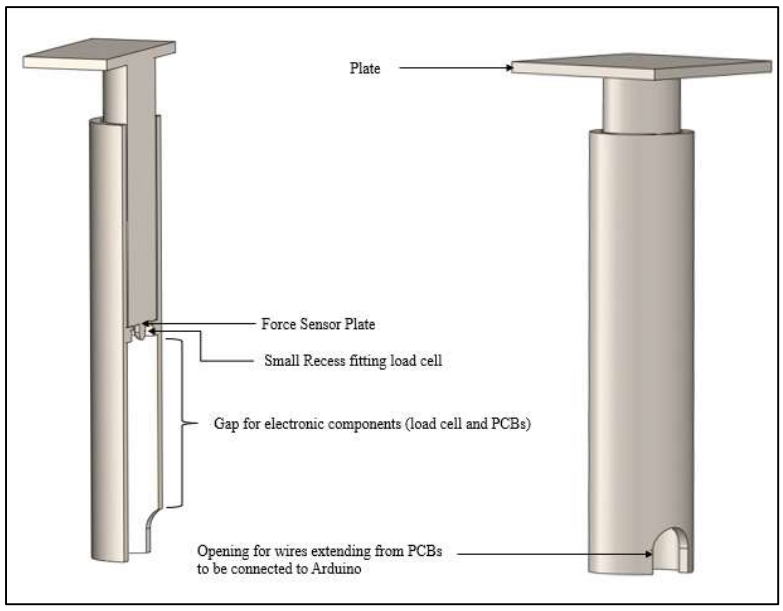

Figure 4.1: *Set up for sampling frequency testing. The load cell fits into a small recess and the printed circuit board (PCB) wires are attached to jumper cables. The PCB wires are then connected to the wireless v-QueST circuit with jumper cables (not shown in this image).*

4.3 Results

Figure 4.2a shows that the sampling frequency was lower when the load was higher, with a minimum sampling frequency of 471Hz, which was deemed acceptable as it provides a nominal resolution reading of 1.5g. However, Figure 4.2b shows that the sampling frequency can be adjusted by post-processing interpolation (using a MATLAB 2021b program and interp1

function), whereby all the samples were adjusted to the largest sampling interval (determined to be 465 Hz). The sampling frequency was not impacted by the duration of the data recording.

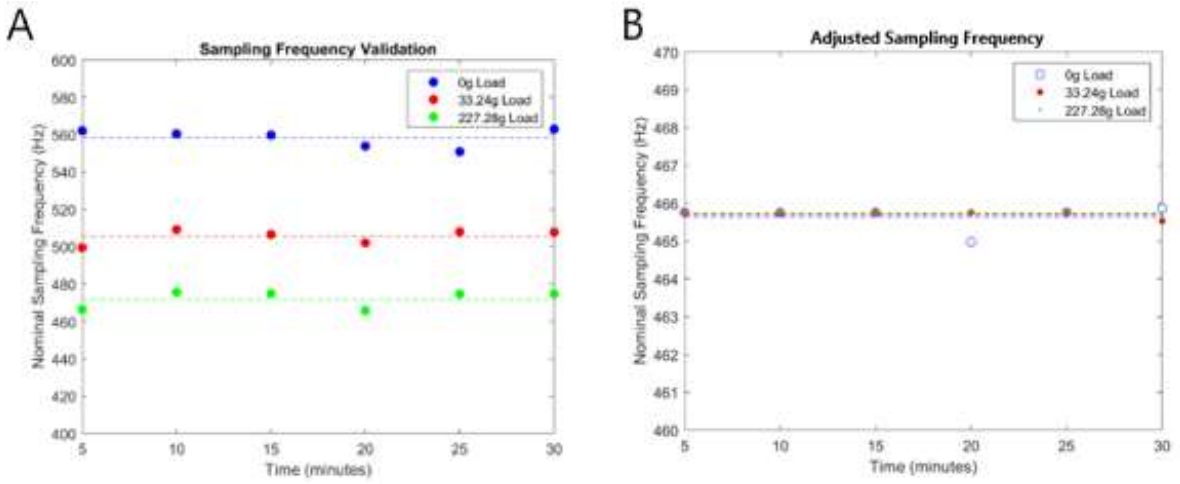

Figure 4.2: *Measured sampling frequency under three different loads. The sampling frequency was assessed for 30 minutes, with 50 samples being taken every 5 minutes. The average sampling frequency from the 50 samples is plotted for each recording window, as well as the overall average sampling frequency across all 300 samples (shown as a dotted line).(a) Raw sampling frequency under three different loads (b) Adjusted sampling frequency through post-processing interpolation using the interp1 function in MATLAB whereby the sampling frequency was set to the largest sampling interval under three different loads.*

Table 4.2 shows the sampling frequency for each load. The mean sampling rate of the wireless device/app was 512Hz and ranged between 472Hz-558Hz.

Table 4.2: *Sampling intervals observed at each of three different loads.*

Load [g]	Sampling interval [ms]					Sampling Frequency [Hz]
	Mean ±std	COV (%)	Median	Smallest interval	Largest interval	Mean
0	1.79 +/- 0.033	1.8	1.81	1.65	1.82	558.32
33.24	1.98 +/- 0.035	1.8	1.98	1.84	2.00	505.32
227.29	2.12 +/- 0.037	1.7	2.14	1.98	2.14	471.99

* Abbreviations: std = standard deviation; COV = coefficient of variation

Table 4.3: *Sampling intervals observed at each of three different loads with samples adjusted to the largest sampling interval.*

Load [g]	Sampling interval [ms]					Sampling Frequency [Hz]
	Mean ±std	COV (%)	Median	Smallest interval	Largest interval	Mean
0	2.15 +/- 0.035	1.6	2.14	1.98	2.15	465.65
33.24	2.15 +/- 0.034	1.6	2.14	1.98	2.15	465.72
227.29	2.15 +/- 0.031	1.5	2.14	1.98	2.15	465.74

* Abbreviations: std = standard deviation; COV = coefficient of variation

4.4 Discussion

The results demonstrated that the wireless app sampled at a lower frequency (roughly 512Hz) than the expected rate of 677 Hz, was impacted by the applied load, but was stable over time within the given load (low range and COV; Table 4.2). The sampling rate was substantially lower than expected. This may be attributed to the time required to pass the data via Bluetooth and processing delays within the Arduino script. As an example, a processing delay was evident in the zero-load case, where the sampling interval was 1.79ms (Table 4.2) compared to the expected sampling interval of 1.5ms.

The expected sampling of 677 Hz, maximized based on design parameters, exceeded the functional requirement minimum sampling frequency of 467Hz. It was set to be larger than 467Hz in order to account for any potential processing delays.

The sampling rate was impacted by load, whereby the sampling frequency was roughly 90Hz lower at the higher load than it was in the unloaded condition, with the sampling frequency (472 Hz) achieved at the third load was within the minimum sampling frequency of 467Hz. The sampling rate being impacted by load values may be attributed to the larger number of bits required to pass data at larger loads when compared to smaller loads. This is not surprising due to the architecture of the code to transmit data wirelessly by assessing the difference in time flags. As discussed above, each addition of a digit in resolution requires more bits to be printed by the Arduino to the HC-06 module, consequently increasing the sampling interval in the transmission of load data. Therefore, as the number of bits increases, the amount of time required for the processor to execute code (or loop in the code) consequently also increases. This consequently impacts the stability of the sampling rate during normal clinical use of the v-QueST, since in normal clinical use the load is increased until the patient reaches their pressure pain threshold, so the number of bits required to pass the data will also change, resulting in an unstable sampling rate.

When an interpolation process was implemented through post-processing, the results were promising, since through the interpolation, the sampling frequency was set to the largest sampling interval under the three different loads (determined to be 466Hz), which was very close to the specified minimum sampling frequency of 467Hz. Therefore, all three loads had the same sampling frequency of 466Hz (Table 4.3). In a research setting, this approach would be acceptable, as data can be post-processed to provide a stable and consistent sampling rate. However, in a clinical setting, the data will be presented in approximate real time, thus requires a minimum consistent sampling rate of 467Hz. In order to bypass the limitation caused by the code architecture, which results in varying the number of items executed by the processor, a timer

interrupt technique should be adopted. This involves the use of a Timer1 interrupt, as described by Bravo-Zanogero et al. [59]. The Timer1 interrupt is a 16-bit timer (maximum counter value of 65535) within Arduino which allows for a more precise timing technique (i.e., Timer0 has a maximum counter value of 255). In this case, the "compare match interrupt" (the counter value to control the rate of load data transfer, similar to the time period of 1500 μs) could be set to 4000 to provide a sampling rate of 500Hz (or a time period of 2000 μs), which is an acceptable sampling rate for this application. A timer interrupt would occur at a specific time within the processor, and thus this method would not influence the processing load. Using this approach, with the data being sent in ASCII and a delimiter attached at the end of the force reading, at a baud rate of 115200, the transmission time would be 0.2ms, which is acceptable for this application as it would not cause any meaningful change in PPT readings.

The actual sampling frequencies within the system may be faster than what is presented in Figure 4.2. The use of time flags was used to validate the sampling interval by Bravo-Zanogero et al. [57], and, while the inclusion of timestamps in the transmitted data was required to validate the sampling frequency, these values do not need to be transmitted during regular use. Indeed, once the timestamps are eliminated from the data transfer, the sampling frequency may be higher. The sampling rate can also be made faster by removing the two-decimal precision. Sending the load cell data as whole numbers will require fewer bits to transmit load values. Two decimal precision is not a functional requirement of the system.

4.5 Conclusion

The sampling frequency at all loads met the objective of having a minimum sampling frequency of 467Hz. While the sampling frequency of 472 Hz observed at the highest load (227.24

g) still met this objective, the difference in sampling frequency across different loads, caused by the architecture of the Arduino program, failed to the meet the objective of designing a system with a stable sampling rate. A post processing approach was used to achieve a stable sample interval across all loads (466Hz), which was very close to meeting the specified sampling frequency of 467Hz. However, in clinical use, the need for post-processing is not feasible. Further, given the way in which the device will be used clinically, with force monotonically increasing to a maximum, the sampling rate will vary within data files. This may be problematic when the wireless v- QueST is used in a research setting, where v-QueST data are recorded synchronously with other data, such as EMG. While the use of ASCII data transmission appears to be acceptable for this application, the implementation of timer interrupts would likely provide a faster and more stable sampling frequency and should be tested in follow-on work. The alternative approach of transmission of data in binary is also acceptable for this application and should be investigated.

5.0 LOAD AND TIME VALIDATION

Accurate load readings can be used to determine the pressure pain threshold (PPT) and therefore to assess changes in pain processing associated with PVD. Thus, the first objective of this chapter is to validate the force readings from the v-QueST system.

A time delay can be introduced in wireless data acquisition through two sources: (i) delay in the trigger button activation to flag the PPT load value and (ii) delays induced by Bluetooth™ data transmission. The *PPT Reached* button on the app is used by the patient to indicate that their PPT has been reached. The force measured through the load cell (SMD410, Strain Measurement Devices, Wallingford, Connecticut) at the time the button is activated indicates the patient's PPT, in grams. The second objective of this chapter is to investigate delays between the activation of the trigger button and the time at which the Arduino® registers this activation.

The third objective of this chapter was to validate the force transmitted and the timing of the PPT determined through the wireless interface of the v-QueST against a hard-wired system. While ideally there would be no time delay between the patient pressing the button to indicate that their PPT has been reached and the system recognizing the button press, in practice there will be some delay. There are no available data to indicate the maximum acceptable time delay between pushing the button to indicate the PPT has been reached, and the device recognizing that the button has been pressed. Therefore, we propose that a delay of less than 20ms between the button press and the indication of the PPT would be acceptable for this application. At a rate of applied force of 700g/s, this would result in up to a 14g difference in the actual PPT relative to the PPT detected by the system, which is negligible relative to the minimum detectable change in PPT (269.6g [43]).

5.1 Methods

5.1.1 Load Validation

Load validation was performed on the wireless v-QueST prototype using known calibration loads. A custom test rig was designed and printed in PLA, as demonstrated in Figure 5.1. The rig consisted of an extension plate, a holder for the v-QueST, and a base plate (detailed drawings can be found in Appendix A.4 v-QueST Custom Test Rig Technical Drawings).

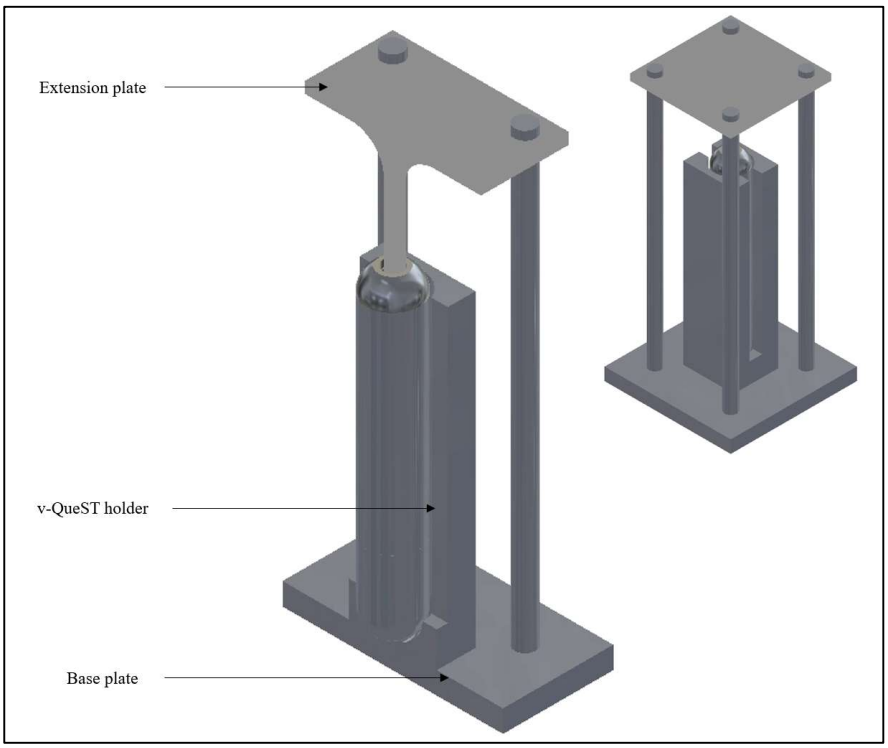

Figure 5.1: *The v-QueST custom test rig. The v-QueST is embedded in a custom holder with a base plate and four cylindrical tubes 3D printed in PLA. The tubes fit into a corresponding recess in the extension plate. When a load is placed on the extension plate, it can freely move down the cylindrical tube, mitigating any load dispersion to the base plate.*

The v-QueST holder firmly held the v-QueST in the middle of the base plate, which was securely clamped to a desk. The base plate included four cylindrical supports which extended and fit into a recess in the extension plate. By removing the collet from the v-QueST, a cylindrical tube on the extension plate fit securely into the v-QueST and the plate at the end of the extension sat

perpendicularly to the long axis of the v-QueST. The calibration loads were placed in the center of the extension plate which could freely move down the supports of the base plate, ensuring that the loads did not disperse to the baseplate.

In random order, loads between 0 to 8.5 N, incremented by 0.5N, were applied to the v-QueST via the extension plate, since the load cell is rated to hold a capacity of 9N. Each load was applied three times. Data were recorded through the wireless app, which was operated on a Samsung Galaxy Tab E, and sent in a text file. Load data were acquired (in g) at a frequency ranging from 472Hz to 558Hz as indicated in Chapter 4.0. A MATLAB R2021b program was developed to parse the v-QueST text file (Appendix D.1 v-QueST Parse) and the mean load value was determined for each load, converted to Newtons. The mass of the extension plate (31.43g) was removed from the calibration values. The relationship between the expected and recorded load was examined.

5.1.2 Time Delay Introduced by Activation of the Trigger Button

The timing of the PPT was flagged via Bluetooth as described in Chapter 3 sections 3.3.2 and 3.3.3. To validate this approach, a custom Arduino program (Appendix B.4 Trigger Button Activation Testing) and MIT AI2 app (Appendix C.2 Trigger Button Activation Testing) were designed to interface with the HC-06 Bluetooth module powered through a laptop. The app allowed the user to connect to the HC-06 Bluetooth module which was interfaced with the Arduino Nano. There were two serial monitors in the custom Arduino script (1) the Bluetooth serial monitor between the microcontroller and the Bluetooth module (referred to as *mySerial* below) and (2) the serial monitor between the Arduino and the PC (referred to as *Serial* below). The *void loop()* function in the Arduino script includes an *if-statement* that is entered when there are bytes available to receive in mySerial (*if (mySerial.available() > 0)*). The custom MIT AI2 application will only send bytes

when the trigger button ("Press Me" in Figure 5.2) is pressed. In order to determine if there is a significant delay between the time the activation trigger is pressed and the time at which the Arduino registers this activation, the *micros()* function establishes three-time flags: (1) before entering the if-statement (*currentMicros_1*) (2) after entering the if-statement (*currentMicros_2*) and (3) after exiting the if-statement (*startMicros*). Therefore, the difference between *currentMicros* and *startMicros* is taken when entering and not entering the if-statement. Through comparing these differences, the Arduino script determines the time taken for the wireless interface to register a button press.

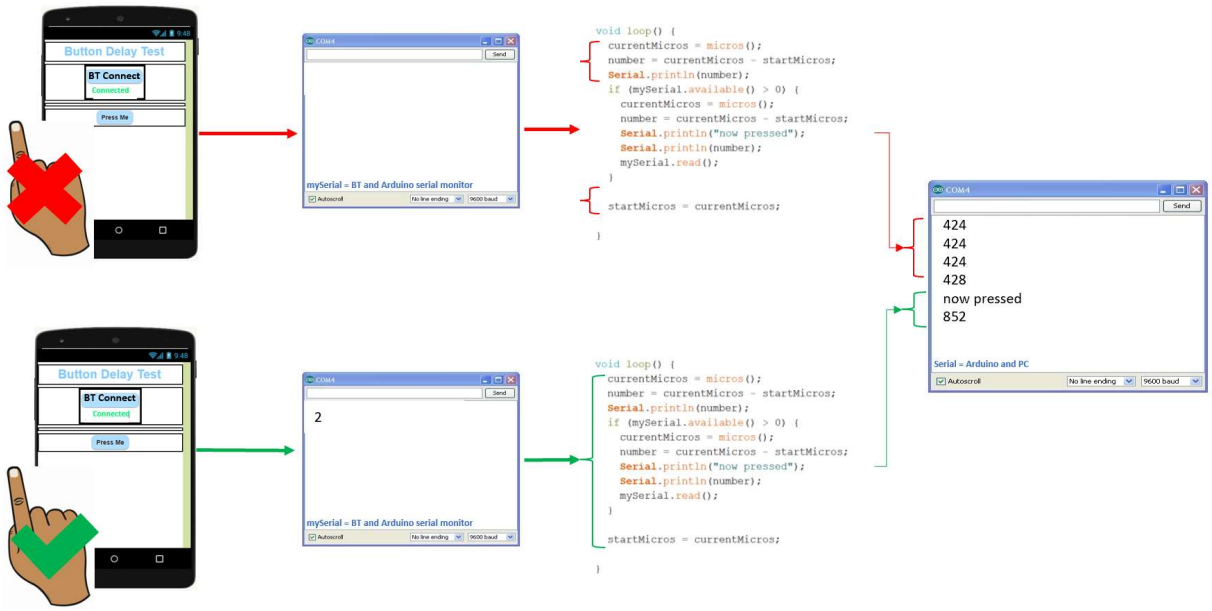

Figure 5.2: *The custom MIT AI2 application with the Arduino® script used to detect trigger button activation time. The trigger button in this image is the "Press Me" button shown in the application. In the case where the button is not pressed, mySerial remains empty and the Arduino® script omits the if-statement and outputs the time taken to run through the void loop() into the Serial monitor. In the case where the button is pressed, mySerial is not empty and the Arduino® script enters the if-statement. The time taken to enter the if-statement, or the time taken for the wireless interface to register a button press, is output into the Serial monitor.*

Using this system, a research assistant activated the trigger button through thirty repetitions while the researcher operated the app on a Galaxy Tab E Android device. The time delay between activating the button, determined through the Arduino data stream, and the time the button press

was registered on the wireless interface was determined for each trial. The data stream on the Serial monitor was copied in Excel and the "ctrl f" feature on Excel allowed the researcher to find the time at which "now pressed" was printed into the Serial monitor. The difference between the number below "now pressed" (difference between *currentMicros_2* and *startMicros*) and the number above "now pressed" (difference between *currentMicros_1* and *startMicros*) was recorded as the time a button press was registered on the wireless interface (shown in Figure 5.1). The mean (±standard deviation) time delay between the button activation and the app registration that the button was activated was determined.

5.1.3 Time Delay Introduced through Bluetooth Transmission

Validation of the Bluetooth transmission of load data through the wireless interface was accomplished using the fully assembled wireless v-QueST prototype and a second, calibrated, hard-wired load cell (EBB-5, EBB Series, Transducer Techniques, Temecula, USA) connected to an external ADC (PowerLab^{TM}) and PC. The validation of the timing and amplitude of the load data transmitted wirelessly first required load validation for the load cell within the v-QueST.

Validation of the timing of load data as detected by the v-QueST and recorded through the mobile app was performed using the hard-wired load cell (considered the criterion standard), connected in parallel with the v-QueST. The hard-wired load cell had a linear operating range of 1.5N-25N and was interfaced with a PowerLab data acquisition system (ADInstruments, PowerLab 16/35, Colorado, USA) using a 16-bit analog to digital conversion board (National Instruments, NIDAQ USB3086, Austin, USA). Once the v-QueST was properly calibrated, the wired load cell was secured to a desk, as presented in Figure 5.3. A synchronization channel was generated through a digital marker (stylus tip button) on an Arduino board that was concurrently hard-wired into a channel on the PowerLab system. The technician pressed the synchronize button

on the app with the stylus tip while simultaneously triggering a step response (0, 5) in the corresponding PowerLab channel (Figure 5.4). The *Synchronize* button on the app was programmed to flag the v-QueST load value when the button was pressed and when the stylus touched the screen. Based on the findings of Chapter 4.3, the data sets were not synchronized until the load displayed on the v-QueST app exceeded 100g in order to have a consistent sampling rate. This also consequently ensured the load applied to the wired load cell was within its linear operating range (1.5N-30N). The stylus tip button was powered through a Lenovo laptop computer.

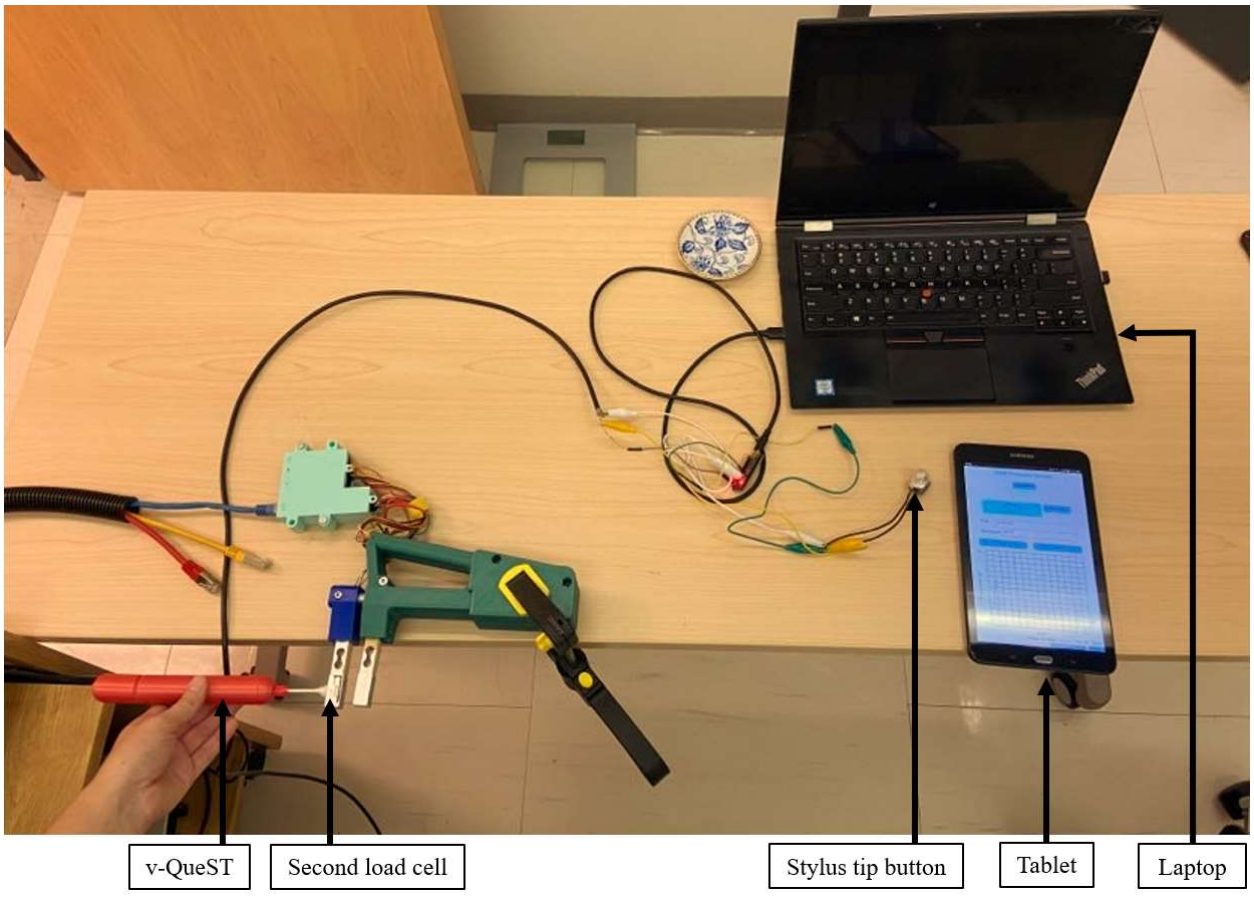

Figure 5.3: *Set-up for validation of the time delay for the wireless interface of the v-QueST. The v-QueST is pressed against a second hard-wired load cell which is interfaced with a PowerLab™ data acquisition system. The load data from the v-QueST is displayed and saved on the Galaxy Tab E tablet. The stylus tip button is powered through a Lenovo laptop and connected to the PowerLab™ system.*

Seventy-four trials were completed; in each trial the stylus was pressed onto the *Synchronize* button on the app and then the technician pressed the v-QueST (connected through the wireless application) against the wired load cell connected to the PowerLab data acquisition system. The trials were further separated into fast rate of force application and slow rate of force application, with rates of application significantly faster or slower than the recommended rate of 700g/s in order to assess the impact force rate application could have on Bluetooth data transmission. Thirty-four trials were applied with a fast rate of force application (roughly 61.16 N/s or 6236 g/s) and forty-one trials were applied with a slow rate of force application (roughly 1.02 N/s or 102 g/s). More trials were taken for the slow rate of force application to account for potential outliers due to mechanical failures within the v-QueST (ie. the fast rate of force application trials was performed first and when performing the slow rate of force application trials, the repetitive force applied within the parts of the v-QueST caused shifting within the interior components of the v-QueST). Data from wired load cell were sampled at 1000Hz while data from the v-QueST were sampled at 472Hz (nominally as determined in Chapter 4.3). The data from the

app (the timestamp and the load measured) were written to a text file.

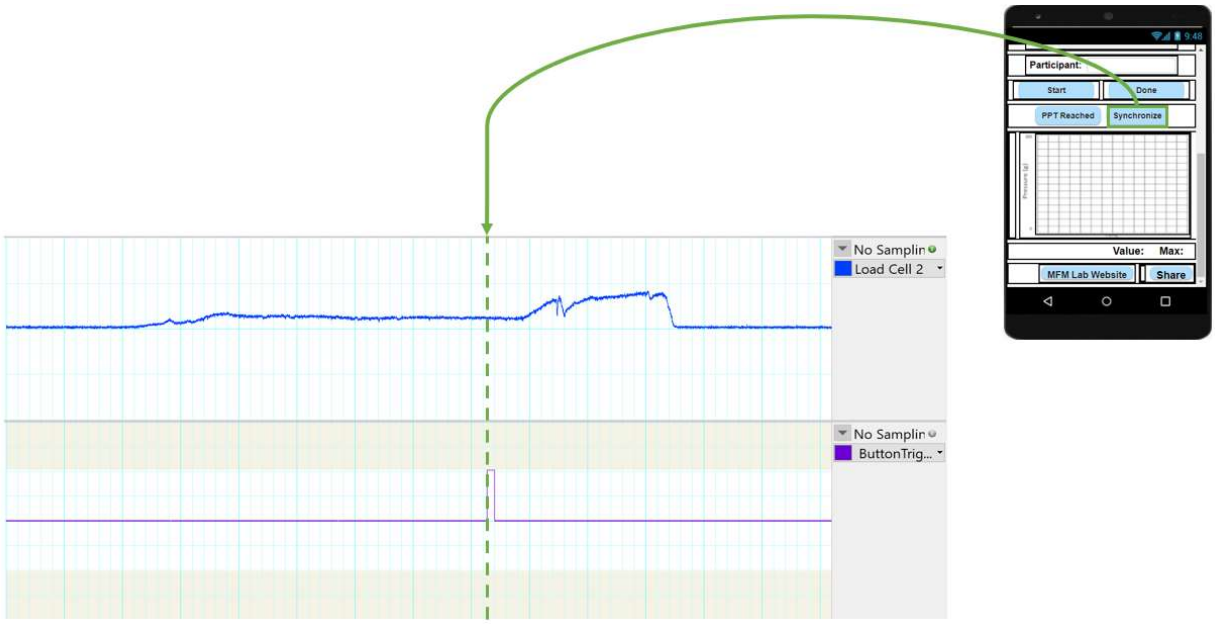

Figure 5.4: *The top channel is load data (in Newtons) acquired from the load cell interfaced with the PowerLab™ system, while the bottom channel shows the voltage recorded when the stylus tip triggered the button. When the stylus tip button is used to press the Synchronize button on the application, the corresponding PowerLab™ channel (channel 2) registers a step response (0,5).*

While this method was validated for the *Synchronize* button, it is noteworthy that the *PPT Pressed* button flags the load reading the same way as the *Synchronize* button. Therefore, validating the time delay when pressing the Synchronize button also validates the method in which the patient indicates their PPT has been reached.

Once the v-QueST data were parsed (Appendix D.1 v-QueST Parse), a MATLAB R2021b program (Appendix D.2 Time Delay Analysis) first applied a low pass filter to the hard-wired load cell data (second order dual pass Butterworth Filter with frequency cut-off 10Hz) and determined the time at which the filtered hard-wired load data first crossed each threshold (4, 5, and 6N) relative to the synchronization mark (i.e. when channel 2 registered a step response). Then the parsed and organized v-QueST data were read from an Excel file, calibrated, and interpolated by a factor of 2 (the *interp* function in MATLAB [94]). The *interp* function performs the ideal

bandlimited interpolation by using the two nearest nonzero samples through a linear phase finite input response [95]. The v-QueST data were not filtered since the use of the v-QueST in a clinical setting software filtering would not be advisable due to the processing time and power it would require, as well as delays that might be introduced in PPT timing as well as the display. Three load thresholds were selected because they were within the linear range of the wired load cell while also being within the clinically meaningful operating range of the v-QueST device, for each load threshold (4,5, and 6N), the time that the threshold was crossed in forces acquired through the hard-wired load cell was compared to the time the same threshold was crossed in the data acquired through the v-QueST device and app.

Linear regression analyses were used to evaluate the validity of the timing data from the v-QueST relative to the hard-wired load cell interfaced with the PowerLab system. Bland Altman analyses were performed to identify the mean time difference (±standard deviation) and the variance in the time difference when each system first registered the load as exceeding each threshold (4, 5, and 6 N). An α=0.01 was used as the threshold for statistical significance for all tests.

5.2 Results

5.2.1 Load Validation

Figure 5.5 shows that there was a strong linear relationship between the forces measured by the v-QueST and the wired load cell.

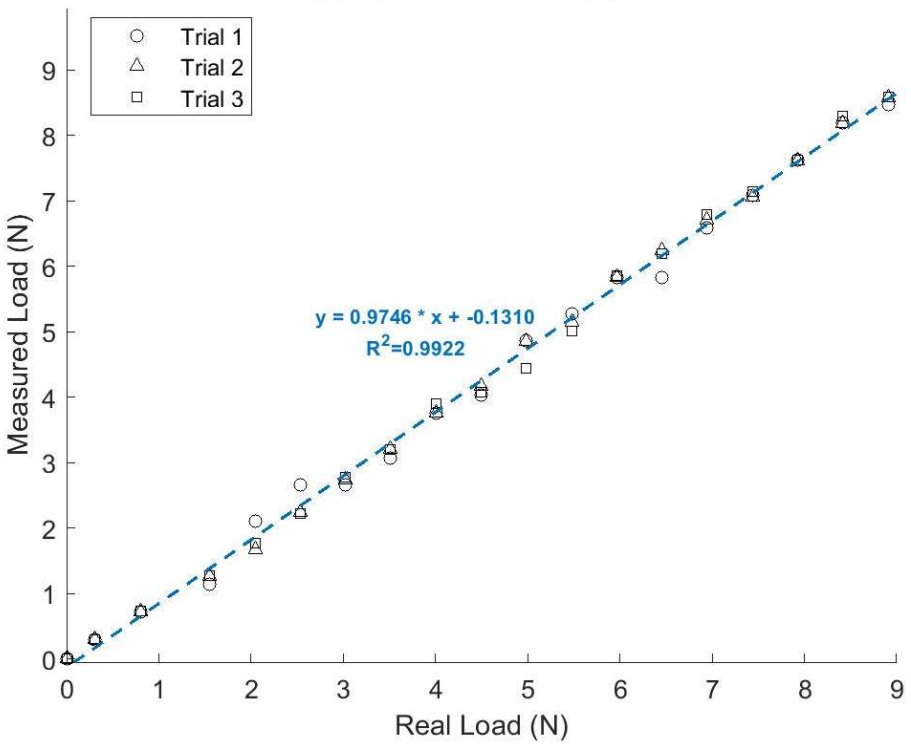

Figure 5.5*: Load validation for v-QueST load cell. Load measurement was validated using calibration weights at 0.5N increments applied three times each in random order.*

5.2.2 Time Delay Introduced by Activation of the Trigger Button

The difference between the Arduino and the PC time flags printed to the Serial monitor are shown in Figure 5.6. From thirty button presses, the average difference was determined to be 420.53 ± 25 µs.

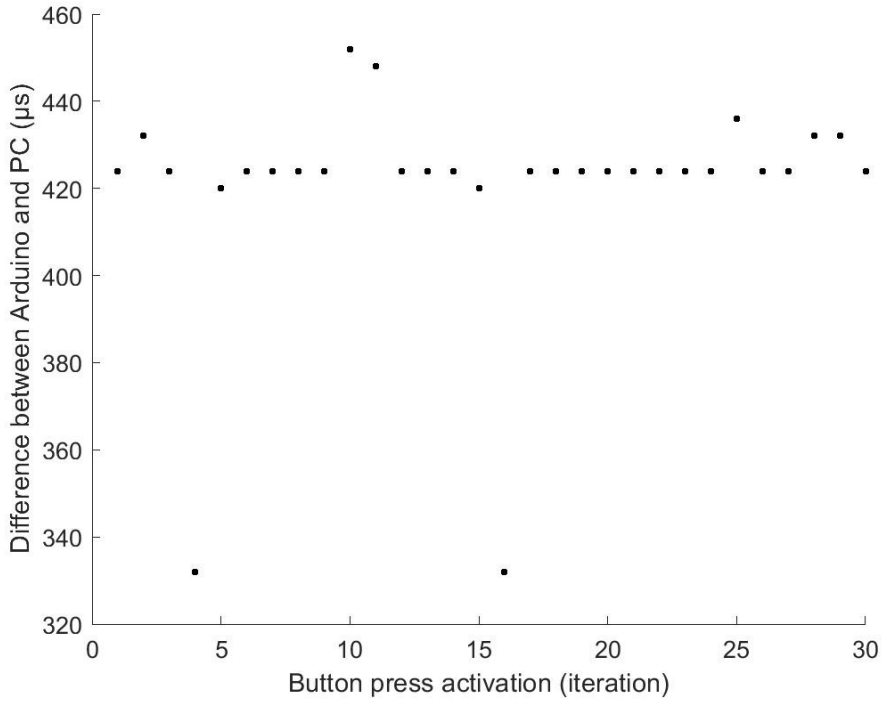

Figure 5.6: *Thirty trials of the time delay introduced by activation of the trigger button by assessing the difference between the Arduino and the PC time flags printed into the serial monitor.*

5.2.3 Time Delay Introduced through Bluetooth Transmission

Five trials under the high rate of force application condition and ten trials under the slow rate of force application condition were excluded for the following reasons:

- Synchronize button error: The synchronization function was not triggered in either the v-QueST data or the PowerLab channel. A total of two fast application trials and five slow application trials were discarded based on this reason.
- Bluetooth application error: One fast trial was discarded because the delay between the v-QueST and the wired load cell data was extremely large (0.25ms), likely caused by a transient Bluetooth disconnection.
- Mechanical error in the v-QueST: The forces were not aligned between the v-QueST and the wired load cell in two data sets. Further inspection revealed that the movement of the

plunger in the mechanical assembly of the v-QueST was impeded by friction in the 3D printed casing (Figure 5.7). A total of two fast application trials and five slow application trials were discarded.

- Failure to reach the threshold force: Two fast trials never reached the 6N load threshold. The times that the force reached the 4N and 5N thresholds were retained in the analysis.

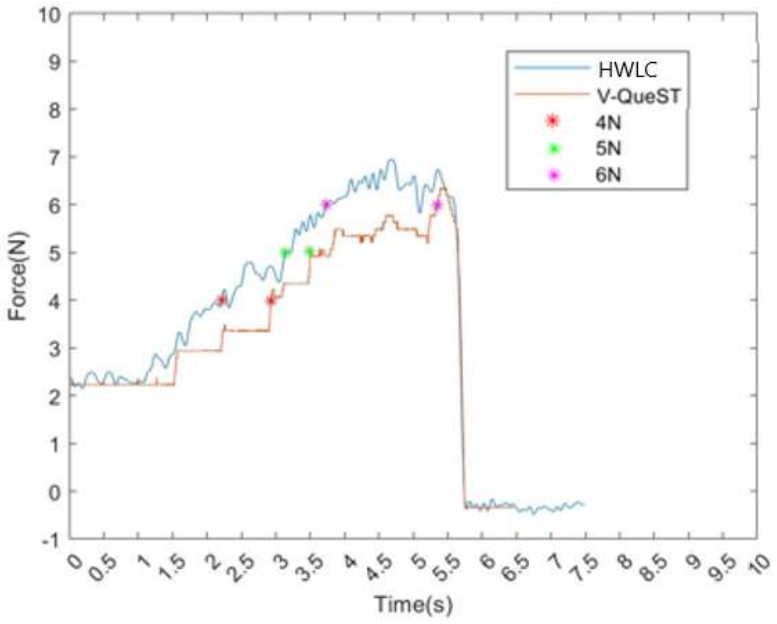

Figure 5.7: *Force data from the hard-wired load cell (HWLC) and v-QueST load data. The v-QueST signal shows stepwise increases in force, which appeared to be related to impeded plunger movement within the v-QueST assembly due to rough ridges in the 3-D print.*

The rate of force application was determined to be 61.16 ± 44.44 N/s (6236.58 ± 4531.62 g/s) for the "fast" trials. In terms of the time that each system first registered forces above each threshold (i.e., 4N, 5N, 6N), for the fast rate of force application (Table 5.1), linear regression models demonstrated slopes (β_1) that were approximately 1, no significant intercepts (β_0) and an excellent model fit (Adj R^2). These findings suggest that there is a strong linear relationship between the two systems with no significant offset and little unexplained variance. The Bland-Altman analysis identified significant mean differences in the time that each loading threshold was crossed.

Table 5.1: *Linear regression and Bland-Altman parameters comparing the time each system registered force threshold crossings at thresholds of 4, 5 and 6N.*

		Linear Regression Analysis							Bland-Altman analysis				
Type	Force (N)	β_1 (95% CI)	p	SE	β_0 [ms] (95% CI)	p	SE [ms]	AdjR^2	MD [ms]	p	SD [ms]	LLOA [ms]	ULOA [ms]
Fast	4	0.9986 (0.9797, 1.0175)	<0.01	0.0092	-9.0 (-33.7, 15.7)	0.46	12.0	0.9976	-10.7	<0.01	29.4	-68.4	47.1
	5	1.0027 (0.9848, 1.0205)	<0.01	0.0087	-16.5 (-40.2, 7.2)	0.16	11.5	0.9979	-13.3	<0.01	28.0	-68.2	41.5
	6	1.0013 (0.9819, 1.0206)	<0.01	0.0094	-15.2 (-41.8, 11.4)	0.25	12.9	0.9978	-13.6	<0.01	30.2	-72.9	45.6
Slow	4	1.1256 (0.9952, 1.2559)	<0.01	0.0637	30.8 (-276.3, 337.8)	0.84	150.1	0.9121	316.6	<0.01	227.8	-130.0	631.0
	5	1.0097 (0.8576, 1.1619)	<0.01	0.0744	159.4 (-354.8, 673.6)	0.53	251.4	0.8593	191.5	<0.01	297.1	-390.9	773.9
	6	0.9268 (0.7934, 1.0602)	<0.01	0.2735	457.5 (-101.8, 1016.8)	0.11	273.5	0.8701	156.6	<0.01	300.8	-433.0	746.2

Abbreviations: $\beta_{1=}$ slope; $\beta_{0=}$ intercept; SE= standard error; AdjR^2= adjusted R^2; MD= mean difference; SD= standard deviation; LLOA= lower limit of agreement, ULOA= upper limit of agreement.

The rate of force application was determined to be 1.02 ± 0.41N/s (104.01 ± 41.81 g/s) for the "slow" trials. For slow rate force application (Table 5.1), linear regression models again demonstrated significant slopes (β_1) close to 1. These findings suggest that there is a strong linear relationship between the two systems with no significant offset. The fit of the linear models to the data was excellent (0.8593 < adjusted R^2 < 0.9121) thus there is little unexplained variance. The Bland-Altman analysis identified significant mean differences in the timing between the two systems when each threshold was crossed, with larger ranges in mean difference observed in the slow trials than observed in the fast trials.

Observation of the synchronized data sets showed that the data were aligned yet that there were delays induced through sampling errors. Figures 5.11 shows an example of the time delay between the synchronized v-QueST and hard-wired load cell systems when a fast rate of force application was used, while Figures 5.12-5.14 show examples of the time delay between the synchronized systems when slow rates of force application were used.

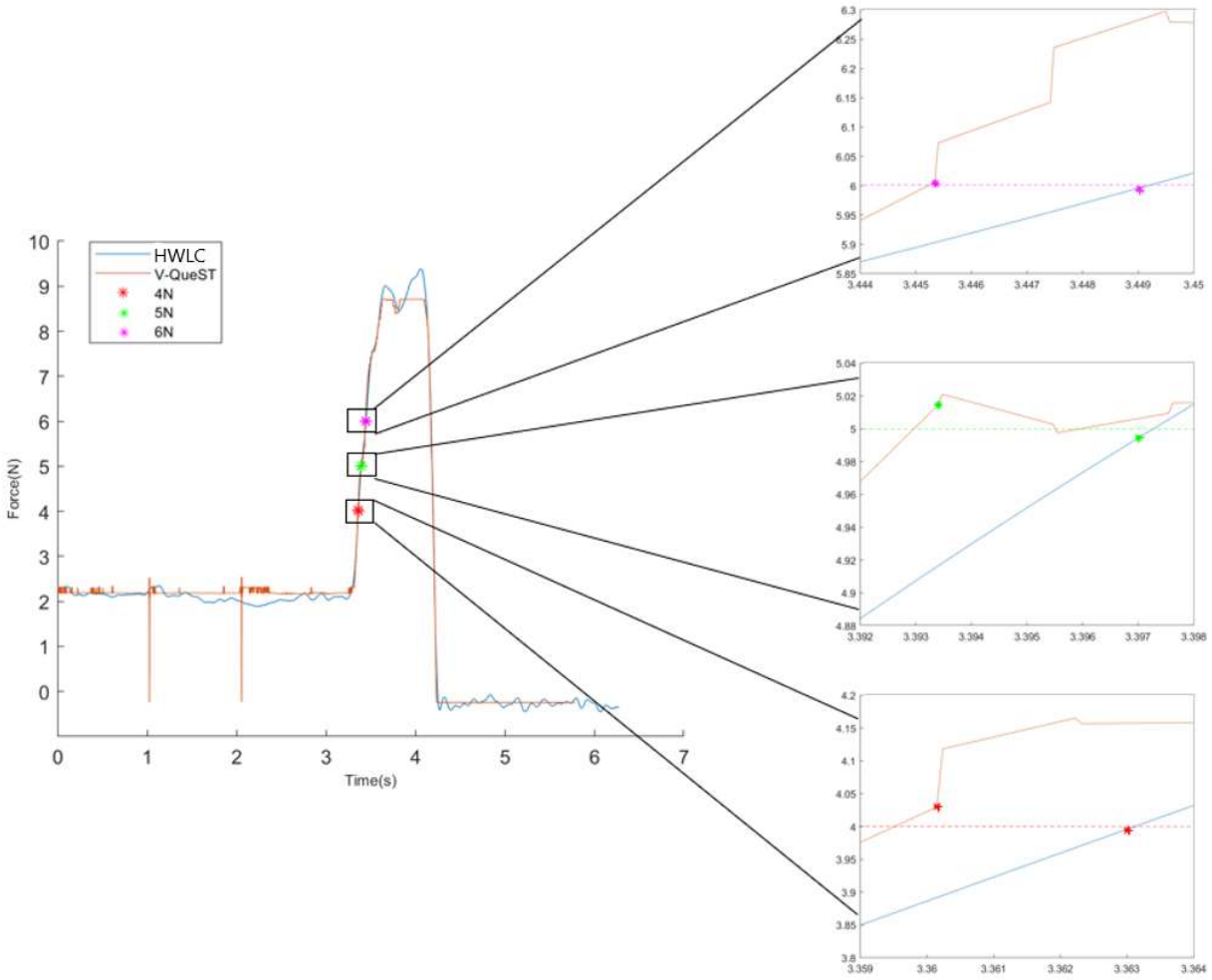

Figure 5.8: *Fast rate of force application where the force data acquisition were synchronized between the v-QueST app and the hard-wired load cell (HWLC). A negligible delay was observed at the 4N (-3ms), 5N (13ms) and 6N (-4ms) threshold.*

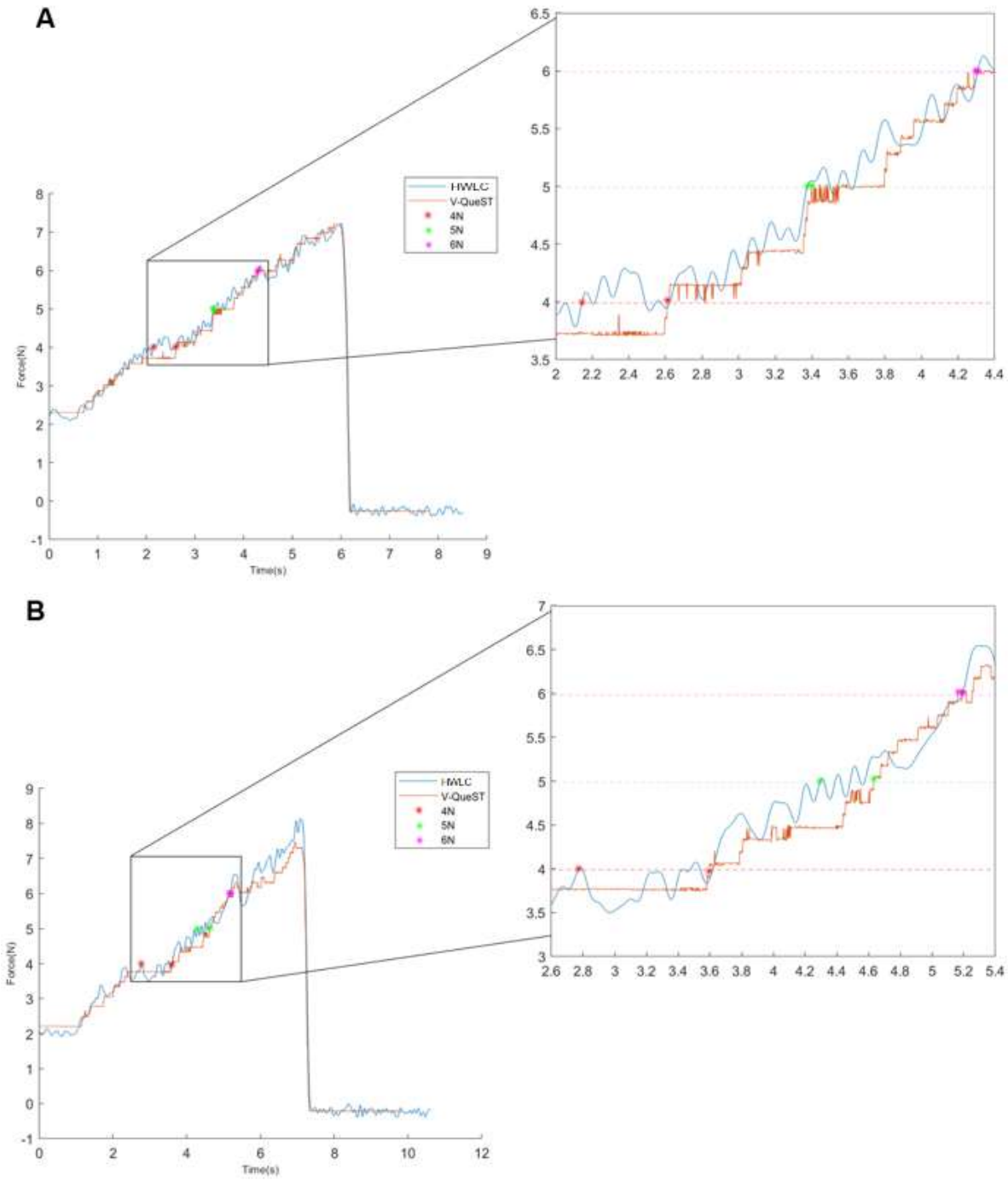

Figure 5.9: *Slow rate of force application where the force data acquisition was synchronized between the v-QueST app and the hard-wired load cell (HWLC). (A) Data from the two systems are aligned with a negligible time delay observed when the force crossed the 5N (23 ms) and 6N (-13 ms) thresholds, however a substantial time delay is observed where the force crossed the 4N threshold (466ms) (B) Data from the two systems are aligned with a delay in the time at which the force crossed the 6N (-29 ms) threshold, but substantial delays are seen in the time the systems recorded the force as having crossed the 4N (820ms)and 5N (338ms) thresholds.*

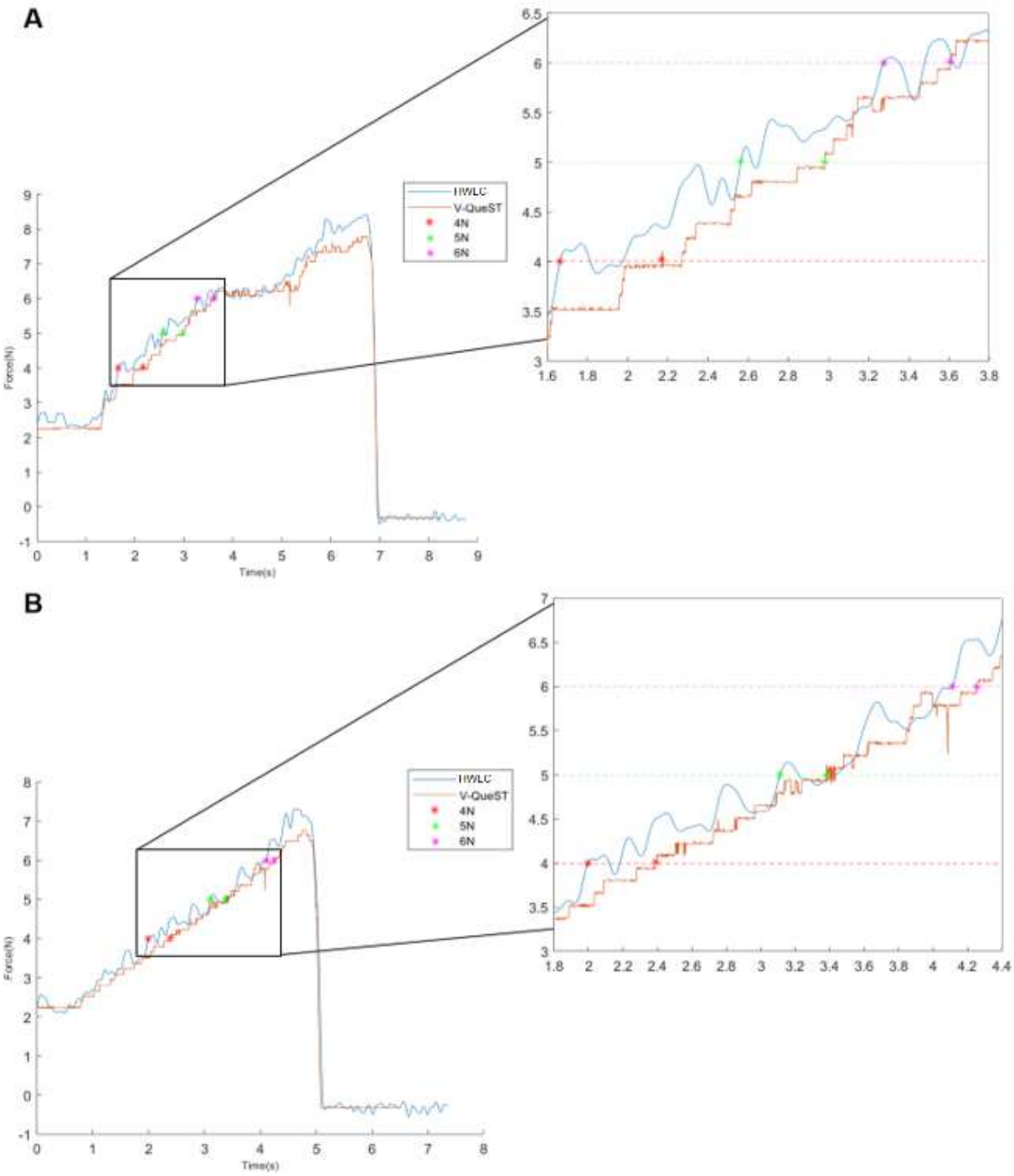

Figure 5.10: *The v-QueST and the hard-wired load cell (HWLC) were aligned during a slow rate of force application, however a substantial delay (above 200ms) was observed between the two systems in terms of when the force exceeded each of the three thresholds (4N, 5N, 6N).*

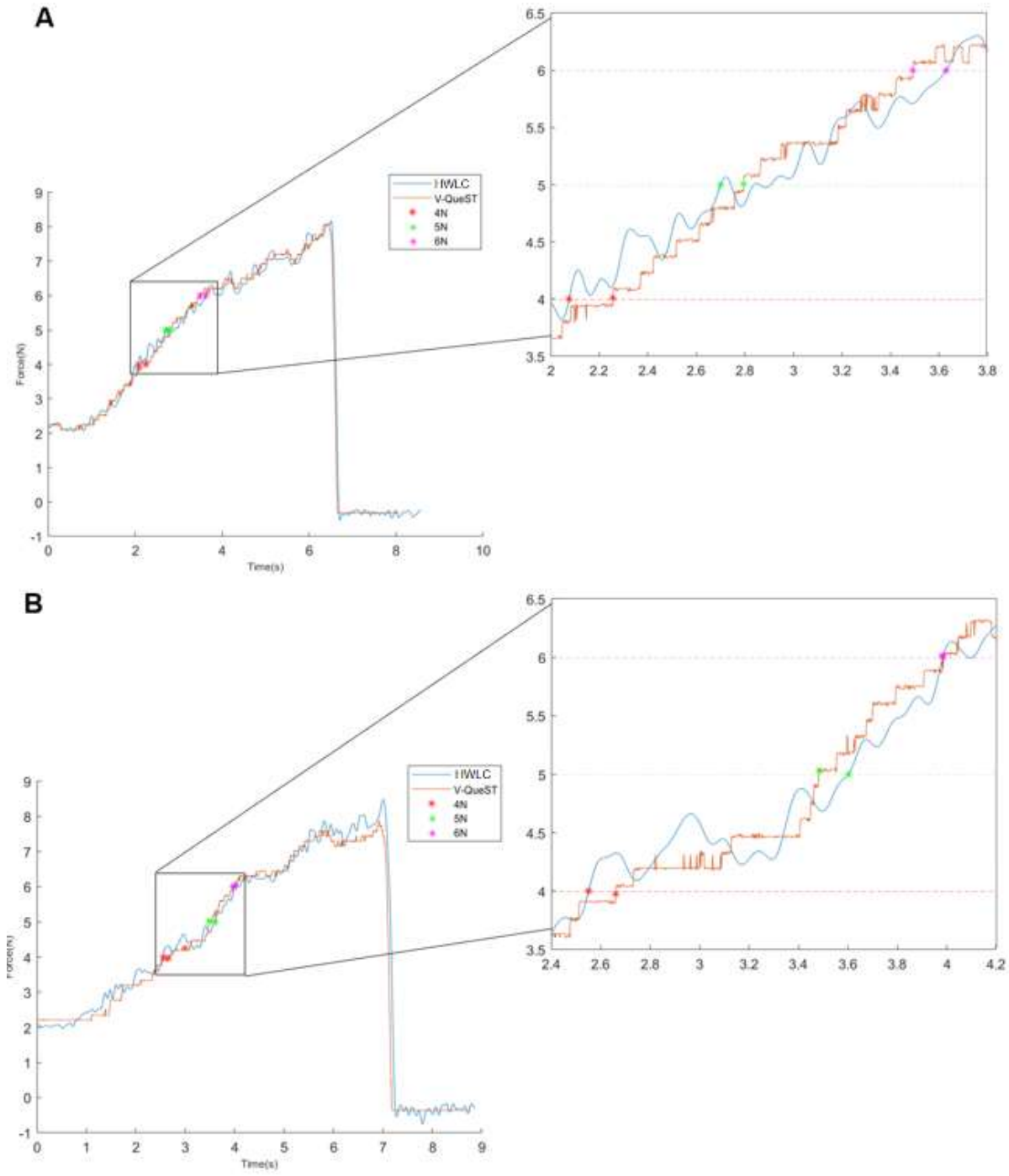

Figure 5.11: *Slow rate of force application where the force data acquisition was synchronized between the v-QueST app and the hard-wired load cell (HWLC); the time delay is below 200ms across all three thresholds. (A) A time delay is observed when the force crossed the 4N threshold (181ms), the 5N threshold (95ms) and the 6N threshold (-137ms) (B) A time delay is observed when the force crossed the 4N threshold (85ms), the 5N threshold (-138ms) and the 6N threshold (-17ms).*

5.3 Discussion

The mean time taken for a button press to register on the wireless interface was below 0.5ms and thus is very small relative the specified acceptable delay of 20ms. The time delay is also small relative to the sampling interval (a frequency of 472Hz has a sampling interval of 2.1ms). Trigger button activation time therefore does appear to introduce any meaningful delay into the detection of the PPT. For example, at a nominal loading rate of 700g/s, a delay of 0.42ms would result in a difference in the PPT of 1.4g, which is much smaller than the minimal detectable change expected between testing sessions [43] and the smallest PPT reported by women with PVD (16.4g) [14].

Figure 5.6 also shows little variance between the thirty iterations of a button press to register on the wireless interface. The large variance seen in some iterations is likely due to processing speed differences within the Arduino Nano.

The delay determined through this method is likely larger than the actual delay observed, as the retrieval of the time flags, subtraction of the time flags and printing of the numbers into the Serial monitor, require processing time that is not taken into account in this current method.

The findings from the load calibration suggest that the v-QueST system calibration through the ZSC31014 calibration kit was excellent. The small offset (0.146N) was removed prior to computing the threshold crossing time. To ensure that the wired load cell was operating within its linear range, for the time delay analysis, the *Synchronize* button was only pressed once the wired load cell reached its linear region, i.e., the force applied was greater than 1.5N. This also ensured that the v-QueST load was above 100g, resulting in a consistent sampling frequency of 472Hz based on the results of Chapter 4.0.

When the force was applied through the v-QueST at the faster rate, the time that the force exceeded the threshold occurred earlier in the v-QueST data than in the hard-wired load cell data stream acquired through the PowerLab™ system (Table 5.1). This is likely due to parsing errors on the v-QueST; when data are parsed in *Clock 1* and placed into the temporary list. A plausible reason for this is that the load was applied at such a fast rate that the load data were sometimes sent incompletely. For instance, the load could measure 504.14g but this value could be processed as two separate readings in the app, 50g and 1.14g, which is likely attributable to a bit error (a character is added between the two readings) resulting in a parsing error at the app end (seen as dips prior to force increase in Figure 5.8). There was also likely a small delay between the time that the stylus tip button touched the screen of the tablet and the time that the button press triggered the step response in the PowerLab channel which can be evident based on the timing data extracted from the fast force application trials (ie. the v-QueST reached the threshold prior to the hard-wired load cell). However, the largest mean difference was -13.6ms, which is smaller than the acceptable delay of 20ms. At a nominal application rate of 1.5g every 2.14ms, a delay of 13.6ms would result in a difference in the PPT of 9.52 g, which is smaller than the 16.4g PPT for women with PVD [14] and much smaller than the MDC between test sessions in healthy women.

The fast rate of force application resulted in large variance in the difference in the timing between the two systems, whereby the limits of agreement (approximately 100ms) were much larger than the mean difference (-10.7ms, -13.3ms and -13.6ms) (Table 5.1). However, in most trials, the signal acquired from the v-QueST crossed the threshold before that recorded from the hard-wired load cell. This variance is illustrated in Figure 5.8, where both signals are aligned but there is a difference in time delay across all three thresholds. The large limits of agreement could lead to a maximum delay of -73ms, which, at a rate of application of 1.5g every 2.14ms, means

the PPT difference would be 51.1g, which, while smaller than 296.6g (the minimal detectable PPT change between sessions [43]), may be problematic when evaluating the PPT of women with PVD,and may induce unwanted pain since the v-QueST device would continue to be pressed by the user until the device recognizes that the button was pressed. This may be particularly problematic for women with PVD who report very small PPTs [14].

When the force was applied more slowly, the mean difference in the time at which each system recorded forces as exceeding the three threshold values was smaller as the force increased, however, as the force threshold increased, the standard deviation of the mean difference increased (Table 5.1) meaning there was more variance in the extent of synchronization between the two systems. The variance in the time delay at each force (4N 5N and 6 N) is evident in Figure 5.9 (A), Figure 5.9 (B), Figure 5.10 (A) and Figure 5.10 (B). The large variance in time delay (>700ms) would result in significant changes in PPT at a rate of application of 1.5g every 2.14ms and is therefore unacceptable.

A systematic error was observed in the acquired data which appears to have impacted synchronization at both fast and slow force application conditions, as seen in the limits of agreement in Table 5.1. The much higher time delay observed when transmitting the PPT value observed when the force was applied at a slow rate (rate=102g/s; delay = 316ms) compared to a faster rate (rate= 6236g/s; delay = 10.7ms) did not have an equally large impact on the recorded PPT. Indeed, the error in the PPT value recorded during the slow rate of force application was actually smaller (32g) than that recorded during the fast rate of force application (62g).

The load resolution observed was approximately 0.4g, which matches the resolution from the ADC (discussed in Chapter 3.3.1) and can be seen in Figures 5.8-5.10. This confirms that there is a systematic error that has a larger effect on the trials where the force was applied at a slow

rate (as shown in Figure 5.10 and Figure 5.11) compared to those where force was applied at a faster rate (Figure 5.8). As indicated in Chapter 3.3.1, the ZSC31014 (Renesas Electronics Corporation, Tokyo, Japan) signal conditioner within the v-QueST operates at an excitation voltage of 5V, consequently resulting in the load cell being powered below its recommended voltage of 10V (discussed in Chapter 3.3.1). The nominal input ranges from the load cell (1.00mV/V) to the ZSC31014 resulted in the maximum analog gain set to X192 and the resolution from the ADC became 11.1 bits compared to its intended 14 bits. Indeed, the ADC was also operating at the low end of its range.

While the experiment performed here was developed under the assumption that the electronic components within the wireless v-QueST were valid, this does not appear to be the case. At this point, to properly assess the true validity of the wireless v-QueST system against a wired system, it is important to observe the ADC signal using an oscilloscope in order to determine the actual error. The system may require more amplification of the load cell output or higher resolution on the ADC. The ZSSC3240 (Renesas Electronics Corporation, Tokyo, Japan) 24-bit signal conditioner could be a viable option because of its higher gain and resolution settings [96].

We chose to evaluate the time delay between the v-QueST and a criterion standard (wired load cell) using threshold crossings to emulate how the system would be used in clinical or research studies. An alternative approach would be to evaluate delays in timing at the onset of force application or at the point where the force returns to zero. However, the synchronous force readings between the v-QueST and the wired load cell occurred only until the peak force was reached (i.e. the v-QueST and wired load cell are no longer touching after the peak force and the rate of force decline as each system to returned to zero was not controlled); therefore, analyzing the time delay associated with the forces reaching zero load would not have been valid. Analyzing the time delay

at the onset of force application would not have reflected how the system is used clinically. Women with PVD generally have a PPT of approximately 100g [2], [13], [17], and at a rate of pressure application of 0.7g/s, they would require approximately 143ms to reach a 100g of force. In addition, the wired load cell was not linear below 1.5N.

Mechanical issues may have influenced the findings of this study. During testing, it was noted that the collet moved towards the top cap and out of the plunger. When force was applied through the collet, this motion caused the plunger to move first and then later compress the spring, which may have induced a time delay in the v-QueST data. As a temporary solution, a piece of tape was placed where the collet met the plunger to secure its location in order to ensure proper force transfer between the collet and the plunger. It is recommended in future iterations of the design that SuperGlue^{TM} be used to fix the bottom of the collet to the plunger to eliminate this problem.

It was also noted that, due to the repetitive forces applied to the load cell, the entire electronics unit shifted downward within the electronics casing. Consequently, the cylindrical component of the force transfer plate could no longer fit in the load cell, resulting in no force being transferred to the load cell. The electronics casing was cut shorter (using a blade), and the entire unit was pushed through so the load cell could properly sit in the force sensor holder. It is recommended in future design iterations to shorten the length for the electronics unit holder by approximately 0.5cm to correct this problem and to ensure proper force transfer to the load cell.

5.4 Conclusion

The findings from the load calibration suggest that the v-QueST system load readings are excellent.

The delay introduced between the activation of the trigger button and the time at which the Arduino registers this activation was determined to be negligible. However, the observed delay is likely much smaller than what was reported due to processing times required to run through the code.

The validation of the time delay Bluetooth transmission of load data through the wireless interface was shown to be inconclusive as the systematic error introduced by the ADC signal conditioner led to unacceptable time delays. It is necessary to eliminate this error in order to properly assess any time delay that is introduced through Bluetooth data transmission.

6.0 CONCLUSIONS AND RECOMMENDATIONS

6.1 Discussion

The three main objectives of this thesis were to construct a fully assembled wireless v-QueST prototype which transfers load cell data to a wireless application via Blueooth, to achieve and validate a stable sampling rate over 467Hz, and to validate the timimg of Bluetooth data transmission against a hard-wired load cell connection.

A wireless interface between an on-board ADC, an Arduino Nano and an HC-06 Bluetooth module was succesfully implemented. An Android application was designed, which allows the clinician to monitor the rate of data application and export, via email, the clinically relevant information. Both the live display of data and use of an app make the wireless v-QueST easily implementable in a clinical setting. The wireless v-QueST allows for live data display, while further allowing a clinician to have unimpeded range of motion and easy manipulation of the device.

After designing and building the wireless prototype, the two main experiments included in this thesis were the validation of the sampling frequency and the evaluation of time delays induced through the use of the Bluetooth wireless system. The sampling frequency validation demonstrated that the sampling frequency was adequate, but that the sampling frequency was lower at higher loads when a larger number of significant digits needed to be transferred. This limitation was attributed to the architecture of the Arduino program. Other authors have reported fluctuating Bluetooth™ sampling rates [97]–[101], most notably when an ECG sensor was designed to sample at 500Hz and demonstrated variability of up to 80Hz [97]. The findings of this study were

comparable, whereby the sampling rate of the v-QueST system varied upto 90Hz at a similar sampling rate.

The activation delay seen with the use of the trigger button resulted in a very small delay (0.42ms) that should have no appreciable effect on the use of the device as planned. Bluetooth transmission delay has been noted in literature [102]–[105] and has been observed to be affected by the size of the file being sent [103]. However, the delays reported in the literature are smaller than what was observed in this study. One study noted an approximate 1ms delay to transmit 60 bytes [104] while another reported a 1.12ms delay to transfer 70 bytes [105]; in the current study, the data sent from the Android app in the v-QueST to the Bluetooth interfaced with an Arduino™ was one bit of data and resulted in a 0.42ms delay. While this magnitude of delay is acceptable for the clinical application of the v-QueST, the time required for the system to run through each line of the code appears to have impacted the results.

There was minimal time delay associated with the Bluetooth transmission of load data. However, the time delays associated with threshold detection did not meet the specified acceptable delay (20ms). A systematic error appears to be a major cause of the errors in timing. This systematic error is likely caused by the combination of components included in the device. In the current prototype, the ZSC31014 signal conditioner (amplifier and ADC) is powered by its recommended 5V of excitation, but the load cell within the wireless v-QueST is consequently powered at only half of its recommended 10V excitation. The amplification gain (X192) results in the load output remaining below 1V. At voltages ≤ 1V, the ADC is only using approximately 20% of its available range (5V). The overall effect was a reduction of the 14bit resolution of the ADC to 11.1bits, which appears to have contributed to the systematic error observed. There is also a

potential that the systematic error is, at least in part, due to the operation of the load cell at half of its excitation voltage. This requires further investigation.

6.2 Contributions

Detailed in this thesis are the rationale for and the design of both the app and the wireless interface for a wireless v-QueST device, paying particular attention to achieving a stable and high (467Hz) sampling rate, and a capacity to accurately detect a threshold based on user input. The device described in this thesis did not meet the functional requirements outlined for the device.

The signal transmission rate failed to allow for a refresh rate on the graphing feature of the app, as the graph refreshed at only 300ms intervals and was therefore not useful in monitoring the rate of force application as intended. The refresh rate can be modified to be less than visual reaction times in order to allow the user to accurately monitor their force application rate.

Methods to validate the wireless interface in terms of amplitude and timing were developed and contribute to the advancement of wireless medical technologies as these methods can be adapted to validate other sensor-based wireless interfaces. Further, the effect of increasing the number digits (ie. increasing number of bits) on wireless sampling rate, as well as the impact of inadequate ADC resolution on the assessment of Bluetooth delay are presented. To the best of the author's knowledge, the wireless v-QueST is the first wireless vulvar pressure measurement device developed for research or clinical use.

6.3 Limitations

The wireless v-QueST is only Android compatible, due to the use of the HC-05 module. In terms of the design of the wireless v-QueST, the biggest limitation is the power supply to the load cell, which is limited to 5V, half of the recommended excitation voltage. Indeed, powering the

load cell at half of its excitation voltage could have impacted the finding that there was substantive error in threshold detection. Validation of the sampling frequency of the wireless v-QueST was also completed using only three discrete loads, chosen out of convenience due to work from home environment imposed by the COVID-19 pandemic. While the sampling frequency could have been tested with a wider variety of loads that correspond to the number of bits required for transmission, the findings appear to be adequately robust to confirm that the number of bits passed does have an influence on the sampling rate.

The timing validation for the wireless interface was completed using the same Android device – which may have biased the results because the device's wireless performance could affect the outcome of the results. Furthermore, the timing validation was only performed within the range of 1.5N to 8N because the hard-wired load cell used as the criterion standard has a linear operating range above 1.5N. As such, the timing validation results are only generalizable for forces within the range tested, and not the full range of the load cell from the wireless v-QueST device.

Lastly, the detection of a systematic error limits the interpretability of the timing validation for force threshold data. This is largely applicable to the slow rate of force application results where the systematic error had a larger effect; therefore, resulting in a larger time delay than the fast rate of force application. More so, choosing to assess the delay at an extremely fast and slow rate does not adequately represent the recommended use of the system at 700g/s. While this choice was made to have a range of force application rates to determine their impact on the time delay, it remains a limitation.

6.4 Next Steps

Based on the findings in this thesis, several steps are recommended before the wireless v-QueST device should be used in clinical or research settings.

6.4.1 Improve the Graphing Feature on the App

Since the graphing feature on the app refreshes only every 300ms, which is larger than human visual reaction times (200ms [66], [67]), it is necessary to decrease the plotting interval to at least 200ms. This can be implemented by changing the *Clock1* timer settings, to read the data sent from the Bluetooth module every 100ms. Ideally the timer setting would be set to 100ms in order to be less than or equal to human visual reaction times; however, if that is not possible (due to the limitations of the clock interval discussed in Chapter 4.1), 200ms interval might suffice. The adequacy of the refresh rate will need to be tested in future iterations.

6.4.2 Improve the Sampling Frequency of the Wireless Data Transmission

Since the sampling frequency is impacted by the addition of digits, it is necessary to implement a technique which ensures a stable sampling frequency. The transmission of data at the baud rate of 115200 was deemed to be adequate for this application, however the method of using a loop with time flags appears to have caused instability in the sampling frequency. As the number of bytes increased in the load reading, so did the amount of time required to transmit these bytes. Consequently, the time to run through the loop also increases. A stable sampling frequency of 500Hz can likely be achieved by implementing a Timer1 interrupt and servicing the interrupt to transmit the load reading at a compare-match value of 4000.

6.4.3 Improve the Load Measurement System to Eliminate Systematic Error

While the design of the load measurement system was beyond the scope of this thesis, it influenced the findings. The first problem that needs to be addressed in the next iteratio of the prototype is the systematic error. An unassembled version of the wireless v-QueST should be evaluated such that the load cell can be powered with 10V excitation while the signal conditioner remains powerd with 5V excitation. By applying an incremental load to wireless v-QueST and streaming continuous data, the research team can determine, the extent to which the the low excitation voltage of the load cell influences the force readings. If the systematic error is eliminated with this testing, a new load cell should be sourced or designed such that it requires 5V excitation [106]. If the systemtic error is not eliminated once the load cell is powered at 10V, it will be necessary to analyze the signal of the ADC powered at 5V and 10V through an oscilloscope. Since the ADC in the ZSC31014 voltage range is fixed, and the amplification is already at its maximum, if the resolution of the ADC is not adequate after the load cell is powered at 10V, the next step would be to implement a new signal conditioner that can provide greater amplification, such as the 24-bit ZSSC3240. The ZSSC3240 signal conditioner might be a good choice because of its higher gain capacities and programmable resolution settings, therefore with a gain of X540, the ADC can adequately provide a maximum of 23-bit resolution. Indeed, once a new signal conditioner is implemented, the study presented in in Chapter 5.2.1 should be repeated to verify that the Bluetooth transimission resuts in negligible time delay.

6.4.4 Validate the Timing of the PPT at Loads Lower than 1.5N

Due to limitations in access to a load cell with linear characteristics at low loads (<1.5N), the wireless v-QueST system was only validated for loads above 1.5N. However, women with

PVD often have a PPTs that are lower than 1.5N [2], [13], [17]. It is recommended assess if a Bluetooth transmission time delay is seen within this lower force range (0N-1.5N).

6.4.5 Validate the Timing of the PPT at a rate of application of 700g/s

The recommended rate of force application for PPT readings is approximately 700g/s [65]. However, it was chosen to assess the timing at a larger range of rate applications to determine the impact of force rate application on the time delay. Therefore, it is recommended to assess if a Bluetooth transmission time delay is seen at the recommended rate of force application.

6.4.6 Validate the Timing of the Wireless v-QueST on various Android devices against a Wired Version of the Same Device

There is an opportunity to more accurately assess the Bluetooth transmission of the load data by pressing the wired v-QueST against the wireless v-QueST. Using these two systems simultaneously could provide a more accurate analysis of timing delays between a wired and wireless system, since both v-QueSTs use the same load cell (i.e. the same operating range). While this was not possible in the context of the COVID pandemic due to supply chain issues, such an analysis may provide more meaningful results.

There is further an opportunity to assess the wireless v-QueST against the wired version with various Android device. This ensures if the Android device's wireless performance could affect the outcome of the results.

6.4.7 Evaluation of Measurement Properties

Once a new signal conditioner is tested and validated, and the wireless v-QueST has been tested in its lower range of force values, it is recommended that the wireless v-QueST be tested for both inter rater and intra rater reliability and convergent validity against the current wired version of the v-QueST device.

6.4.8 User Group Feedback

It is important that the design of the wireless v-QueST meets both clinical and research needs. As such, it is recommended that the wireless v-QueST (along with the app) be introduced to local clinicians and tested by them in a clinical setting. During these sessions, it can be determined if the spring within the v-QueST should be eliminated or if it is useful in terms of rate of pressure application. The feedback from these sessions would result in iterative improvements in the wireless v-QueST design.

6.5 Conclusion

The wireless v-QueST presented in this thesis is the first Bluetooth device of its kind and was designed to be used in clinical gynaecology and physiotherapy settings. The wireless interface and all electronics of the v-QueST device are safely embedded in an electronics casing and are battery powered for safety and for ease of use. The electronics casing cannot be accessed by the user but the battery can easily be changed by twisting off a bottom cap. The wireless v-QueST is inexpensive and it does not require connection to a data acquisition system or a customized computer program. It is designed to be easy to use while displaying information deemed by the user group to be clinically relevant. The patient indicates when their PPT has been reached by pressing a button on the screen of the application. This eliminates time delays associated with the

clinician having to process the patient's verbal cue that the PPT is reached and then reacting to that cue.

The load measurements obtained by the wireless v-QueST are valid. The trigger button activation delay and the time delay of Bluetooth transmission of load data under fast force application appear to be negligible with respect to the specified acceptable delay, but the time delay attributed to the Bluetooth transmission of load data under slow force application was found to be much larger than the specified acceptable delay. Yet a large component of the delay observed between the force streamed from the v-QueST and that recorded using a wired load cell appears to be based on the low force resolution of the wireless v-QueST, which appears to have a larger impact when the force is applied slowly then when it is applied quickly. Overall, the findings of this thesis support the development of the wireless v-QueST for both research and clinical use. The wireless v-QueST has the capacity to become the gold standard for quantifiable and reliable pain measurement in vulvodynia.

REFERENCES

[1] X. Xu and Y. Huang, "Objective pain assessment: A key for the management of chronic pain," *F1000Research*, vol. 9, 2020, doi: 10.12688/F1000RESEARCH.20441.1.

[2] C. F. Pukall, R. A. Young, M. J. Roberts, K. S. Sutton, and K. B. Smith, "The vulvalgesiometer as a device to measure genital pressure-pain threshold," *Physiol. Meas.*, vol. 28, no. 12, pp. 1543–1550, 2007, doi: 10.1088/0967-3334/28/12/008.

[3] J. Bornstein *et al.*, "2015 ISSVD, ISSWSH and IPPS consensus terminology and classification of persistent vulvar pain and vulvodynia," *Obstet. Gynecol.*, vol. 127, no. 4, pp. 745–751, 2016, doi: 10.1097/AOG.0000000000001359.

[4] C. F. Pukall *et al.*, "Vulvodynia: Definition, Prevalence, Impact, and Pathophysiological Factors," *J. Sex. Med.*, vol. 13, no. 3, pp. 291–304, 2016, doi: 10.1016/j.jsxm.2015.12.021.

[5] L. D. Arnold, G. A. Bachmann, R. Rosen, and G. G. Rhoads, "Assessment of vulvodynia symptoms in a sample of US women: a prevalence survey with a nested case control study," *Am. J. Obstet. Gynecol.*, vol. 196, no. 2, pp. 128.e1-128.e6, 2007, doi: 10.1016/j.ajog.2006.07.047.

[6] B. D. Reed, H. K. Haefner, A. Sen, and D. W. Gorenflo, "Vulvodynia incidence and remission rates among adult women: A 2-year follow-up study," *Obstet. Gynecol.*, vol. 112, no. 2, pp. 231–237, 2008, doi: 10.1097/AOG.0b013e318180965b.

[7] B. D. Reed, S. Crawford, M. Couper, C. Cave, and H. K. Haefner, "Pain at the vulvar vestibule: A web-based survey," *J. Low. Genit. Tract Dis.*, vol. 8, no. 1, pp. 48–57, 2004, doi: 10.1097/00128360-200401000-00011.

[8] B. L. Harlow and E. G. Stewart, “A population-based assessment of chronic unexplained vulvar pain: have we underestimated the prevalence of vulvodynia?,” *J. Am. Med. Womens. Assoc.*, vol. 58, no. 2, pp. 82–88, 2003.

[9] L. D. Arnold, G. A. Bachmann, R. Rosen, S. Kelly, and G. G. Rhoads, “Vulvodynia: Characteristics and associations with comorbidities and quality of life,” *Obstet. Gynecol.*, vol. 107, no. 3, pp. 617–624, Mar. 2006, doi: 10.1097/01.AOG.0000199951.26822.27.

[10] Barbara D. Reed *et al.*, “Prevalence and demographic characteristics of vulvodynia in a population-based sample,” *Am. J. Obstet. Gynecol.*, vol. 206, no. 2, pp. 170.e1-170.e9, 2012, doi: 10.1016/j.ajog.2011.08.012.Prevalence.

[11] S. Bergeron, Y. M. Binik, S. Khalifé, K. Pagidas, and H. I. Glazer, “Vulvar vestibulitis syndrome: Reliability of diagnosis and evaluation of current diagnostic criteria,” *Obstet. Gynecol.*, vol. 98, no. 1, pp. 45–51, 2001, doi: 10.1016/S0029-7844(01)01389-8.

[12] J. Sorensen, K. Bautsita, G. Lamvu, and J. Feranec, “Evaluation and Treatment of Female Sexual Pain: A Clinical Review,” *Cureus*, vol. 10, no. 3, 2018, doi: 10.7759/cureus.2379.

[13] C. F. Pukall, Y. M. Binik, S. Khalifé, R. Amsel, and F. V. Abbott, “Vestibular tactile and pain thresholds in women with vulvar vestibulitis syndrome,” *Pain*, vol. 96, no. 1–2, pp. 163–175, 2002, doi: 10.1016/S0304-3959(01)00442-0.

[14] C. F. Pukall, Y. M. Binik, and S. Khalifé, “A New Instrument for Pain Assessment in Vulvar Vestibulitis Syndrome,” *J. Sex Marital Ther.*, vol. 30, no. 2, pp. 69–78, 2004, doi: 10.1080/00926230490275065.

[15] J. J. D. M. Van Lankveld *et al.*, “Women’s Sexual Pain Disorders,” *J. Sex. Med.*, vol. 7, no.

1, pp. 615–631, Jan. 2010, doi: 10.1111/J.1743-6109.2009.01631.X.

[16] K. B. Smith, C. F. Pukall, and S. M. Chamberlain, “Sexual and Relationship Satisfaction and Vestibular Pain Sensitivity among Women with Provoked Vestibulodynia,” *J. Sex. Med.*, vol. 10, no. 8, pp. 2009–2023, Aug. 2013, doi: 10.1111/JSM.12213.

[17] M. P. Cyr, D. Bourbonnais, A. Pinard, O. Dubois, and M. Morin, “Reliability and convergent validity of the algometer for vestibular pain assessment in women with provoked vestibulodynia,” *Pain Med. (United States)*, vol. 17, no. 7, pp. 1220–1228, 2016, doi: 10.1093/pm/pnv069.

[18] F. I. Antonio, M. P. Rodrigues, C. F. Pukall, and F. Tremblay, “Pressure pain threshold and temporal summation of the vulvar vestibule: reliability of a new approach using an electronic vulvalgesiometer.,” 2020.

[19] J. S. H. Curnow, L. Barron, G. Morrison, and P. Sergeant, “Vulval algesiometer,” *Med. Biol. Eng. Comput.*, vol. 34, no. 3, pp. 266–269, 1996, doi: 10.1007/BF02520086.

[20] L. Lowenstein *et al.*, “Vulvar vestibulitis severity - Assessment by sensory and pain testing modalities,” *Pain*, vol. 107, no. 1–2, pp. 47–53, 2004, doi: 10.1016/j.pain.2003.09.012.

[21] J. Giesecke, B. D. Reed, H. K. Haefner, T. Giesecke, D. J. Clauw, and R. H. Gracely, “Quantitative sensory testing in vulvodynia patients and increased peripheral pressure pain sensitivity,” *Obstet. Gynecol.*, vol. 104, no. 1, pp. 126–133, 2004, doi: 10.1097/01.AOG.0000129238.49397.4e.

[22] S. D. K. Baguley, J. S. H. Curnow, G. D. Morrison, and L. F. Barron, “Vaginal algometer: Development and application of a device to monitor vaginal wall pressure pain threshold,”

Physiol. Meas., vol. 24, no. 4, pp. 833–836, 2003, doi: 10.1088/0967-3334/24/4/302.

[23] F. F. Tu, C. M. Fitzgerald, T. Kuiken, T. Farrell, and R. Norman Harden, "Vaginal pressure-pain thresholds: Initial validation and reliability assessment in healthy women," *Clin. J. Pain*, vol. 24, no. 1, pp. 45–50, 2008, doi: 10.1097/AJP.0b013e318156db13.

[24] D. Zolnoun, E. Bair, G. Essick, R. Gracely, V. Goyal, and W. Maixner, "Reliability and reproducibility of novel methodology for assessment of pressure pain sensitivity in pelvis," *J. Pain*, vol. 13, no. 9, pp. 910–920, 2012, doi: 10.1016/j.jpain.2012.06.006.

[25] "Wireless Medical Devices | FDA." https://www.fda.gov/medical-devices/digital-health-center-excellence/wireless-medical-devices (accessed Jan. 06, 2022).

[26] L. Mitri, "Design and Validation of a Wireless Interface for a Vulvar Quantitative Sensory Testing (v-QueST) Device," 2020.

[27] A. Oshinowo, A. Ionescu, T. E. Anim, and G. Lamvu, "Dyspareunia and Vulvodynia," *Pelvic Pain Manag.*, pp. 44–57, 2016, doi: 10.1093/med/9780199393039.003.0006.

[28] A. T. Goldstein, C. F. Pukall, C. Brown, S. Bergeron, A. Stein, and S. Kellogg-Spadt, "Vulvodynia: Assessment and Treatment," *J. Sex. Med.*, vol. 13, no. 4, pp. 572–590, Apr. 2016, doi: 10.1016/j.jsxm.2016.01.020.

[29] N. O. Rosen, S. Bergeron, and C. F. Pukall, "Recommendations for the Study of Vulvar Pain in Women, Part 1: Review of Assessment Tools," *J. Sex. Med.*, vol. 17, no. 2, pp. 180–194, Feb. 2020, doi: 10.1016/J.JSXM.2019.10.023.

[30] L. J. Eva, W. M. N. Reid, A. B. MacLean, and G. D. Morrison, "Assessment of response to treatment in vulvar vestibulitis syndrome by means of the vulvar algesiometer," *Am. J.*

Obstet. Gynecol., vol. 181, no. 1, pp. 99–102, 1999, doi: 10.1016/S0002-9378(99)70442-4.

[31] D. C. Foster *et al.*, "The tampon test for vulvodynia treatment outcomes research: Reliability, construct validity, and responsiveness," *Obstet. Gynecol.*, vol. 113, no. 4, pp. 825–832, 2009, doi: 10.1097/AOG.0b013e31819bda7c.

[32] M. B. Kaarbø, K. G. Danielsen, G. K. Haugstad, A. L. O. Helgesen, and S. Wojniusz, "The Tampon Test as a Primary Outcome Measure in Provoked Vestibulodynia: A Mixed Methods Study," *J. Sex. Med.*, vol. 18, no. 6, pp. 1083–1091, Jun. 2021, doi: 10.1016/J.JSXM.2021.03.010.

[33] L. E. Hullender Rubin, S. D. Mist, R. N. Schnyer, M. T. Chao, and C. M. Leclair, "Acupuncture Augmentation of Lidocaine for Provoked, Localized Vulvodynia: A Feasibility and Acceptability Study," *J. Low. Genit. Tract Dis.*, vol. 23, no. 4, pp. 279–286, Oct. 2019, doi: 10.1097/LGT.0000000000000489.

[34] N. A. Phillips *et al.*, "Presenting symptoms among premenopausal and postmenopausal women with vulvodynia: A case series," *Menopause*, vol. 22, no. 12, pp. 1296–1300, 2015, doi: 10.1097/GME.0000000000000526.

[35] A. Gyang, M. Hartman, and G. Lamvu, "Musculoskeletal Causes of Chronic Pelvic Pain," *Obstet. Gynecol.*, vol. 121, no. 3, pp. 117–123, 2016, doi: 10.1093/med/9780199393039.003.0013.

[36] S. Thibault-Gagnon and M. Morin, "Active and Passive Components of Pelvic Floor Muscle Tone in Women with Provoked Vestibulodynia: A Perspective Based on a Review of the Literature," *J. Sex. Med.*, vol. 12, no. 11, pp. 2178–2189, Jan. 2015, doi: 10.1111/JSM.13028.

[37] K. Bø and H. B. Finckenhagen, “Vaginal palpation of pelvic floor muscle strength: Inter-test reproducibility and comparison between palpation and vaginal squeeze pressure,” *Acta Obstet. Gynecol. Scand.*, vol. 80, no. 10, p. 883, 2001, doi: 10.1034/J.1600-0412.2001.801003.X.

[38] G. D. Morrison, S. J. Adams, J. S. Curnow, R. J. Parsons, P. Sargeant, and T. A. A. Frost, “A preliminary study of topical ketoconazole in vulvar vestibulitis syndrome,” *J. Dermatolog. Treat.*, vol. 7, no. 4, pp. 219–221, 1996, doi: 10.3109/09546639609089552.

[39] C. Horn-Hofmann, M. Kunz, M. Madden, E. L. Schnabel, and S. Lautenbacher, “Interactive effects of conditioned pain modulation and temporal summation of pain-the role of stimulus modality,” *Pain*, vol. 159, no. 12, pp. 2641–2648, 2018, doi: 10.1097/J.PAIN.0000000000001376.

[40] I. Danielsson, T. Torstensson, G. Brodda-Jansen, and N. Bohm-Starke, “EMG biofeedback versus topical lidocaine gel: a randomized study for the treatment of women with vulvar vestibulitis,” *Acta Obstet. Gynecol. Scand.*, vol. 85, no. 11, pp. 1360–1367, Nov. 2006, doi: 10.1080/00016340600883401.

[41] “S410 Low Profile Load Cell - Strain Measurement Devices.” https://www.smdsensors.com/products/type/s410-low-profile-load-cell/ (accessed Feb. 04, 2022).

[42] ADInstruments, “Basics of Data Acquisition.” .

[43] F. I. Antonio, M. P. Rodrigues, L. Mitri, and A. Brennan, “Assessing pelvic floor muscle activation responses to pressure at the vulvar vestibule: a novel approach using an electronic vulvalgesiometer. | Request PDF,” 2020.

[44] A. H. Omre, “Bluetooth Low Energy: Wireless Connectivity for Medical Monitoring,” *J. Diabetes Sci. Technol.*, vol. 4, no. 2, pp. 457–463, 2010, [Online]. Available: www.journalofdst.org.

[45] V. K. Garg, “CHAPTER 19 Wireless Personal Area Network—Bluetooth,” in *Wireless communications and networking*, Elsevier Morgan Kaufmann, 2007, pp. 682–703.

[46] “RF Safety FAQ | Federal Communications Commission.” https://www.fcc.gov/engineering-technology/electromagnetic-compatibility-division/radio-frequency-safety/faq/rf-safety (accessed Jan. 13, 2022).

[47] “Radiation: Electromagnetic fields.” https://www.who.int/news-room/questions-and-answers/item/radiation-electromagnetic-fields (accessed Jan. 13, 2022).

[48] “Radio Frequency Wireless Technology in Medical Devices Guidance for Industry and Food and Drug Administration Staff,” Accessed: Jan. 07, 2022. [Online]. Available: http://www.regulations.gov.

[49] “Bluetooth Technology Overview | Bluetooth® Technology Website.” https://www.bluetooth.com/learn-about-bluetooth/tech-overview/ (accessed Jan. 13, 2022).

[50] H. Joh and I. Ryoo, “A hybrid Wi-Fi P2P with bluetooth low energy for optimizing smart device’s communication property,” *Peer-to-Peer Netw. Appl.*, vol. 8, no. 4, pp. 567–577, Jul. 2015, doi: 10.1007/S12083-014-0276-0/FIGURES/12.

[51] C. Church, S. Lehmann, and D. Young, “BR / EDR Connection Handover Profile.” 2020.

[52] Bluetooth Special Interest Group (SIG), “Master Table of Contents & Compliance Requirements BLUETOOTH SPECIFICATION Version 4.0.” p. 85, 2010.

[53] Bluetooth Special Interest Group (SIG), “Bluetooth Core Specification Version 5.0,” *Bluetooth Core Specification Version 4.2*, no. December. p. 2684, 2016, [Online]. Available: https://www.bluetooth.org/en-us/specification/adopted-specifications.

[54] University of New Mexico, “Clinic Standards,” Albuquerque, Jun. 2007.

[55] N. Gupta, *Inside Bluetooth Low Energy*, 2nd ed. Artech House, 2016.

[56] E. Balestrieri, L. De Vito, F. Lamonaca, F. Picariello, S. Rapuano, and I. Tudosa, “Research challenges in Measurement for Internet of Things systems,” *Ad Hoc Networks*, vol. 7, no. 4, pp. 4–14, 2018, [Online]. Available: www.imeko.org.

[57] F. Wolling, S. Heimes, and K. Van Laerhoven, “Unity in Diversity: Sampling Strategies in Wearable Photoplethysmography,” *IEEE Pervasive Comput.*, vol. 18, no. 3, pp. 63–69, Jul. 2019, doi: 10.1109/MPRV.2019.2926613.

[58] A. Cosmanescu, B. Miller, T. Magno, A. Ahmed, and I. Kremenic, “Design and implementation of a wireless (Bluetooth®) four channel bio-instrumentation amplifier and digital data acquisition device with user-selectable gain, frequency, and driven reference,” *Annu. Int. Conf. IEEE Eng. Med. Biol. - Proc.*, pp. 2053–2056, 2006, doi: 10.1109/IEMBS.2006.260527.

[59] M. Bravo-Zanoguera, D. Cuevas-González, M. A. Reyna, J. P. García-Vázquez, and R. L. Avitia, “Fabricating a Portable ECG Device Using AD823X Analog Front-End Microchips and Open-Source Development Validation,” *Sensors*, vol. 20, no. 20, p. 5962, Oct. 2020, doi: 10.3390/s20205962.

[60] W. J. Iskandar, I. Roihan, and R. A. Koestoer, “Blue electrocardiogram (ECG): ECG with

bluetooth feature integrated with smartphone," *AIP Conf. Proc.*, vol. 2344, no. 1, p. 050003, Mar. 2021, doi: 10.1063/5.0047431.

[61] "TimerInterrupt - Arduino Reference." https://www.arduino.cc/reference/en/libraries/timerinterrupt/ (accessed Apr. 17, 2022).

[62] "millis() - Arduino Reference." https://www.arduino.cc/reference/en/language/functions/time/millis/ (accessed Apr. 17, 2022).

[63] K. M. Chang, S. H. Liu, and X. H. Wu, "A Wireless sEMG Recording System and Its Application to Muscle Fatigue Detection," *Sensors 2012, Vol. 12, Pages 489-499*, vol. 12, no. 1, pp. 489–499, Jan. 2012, doi: 10.3390/S120100489.

[64] "WO2021072546A1 - Force measurement device - Google Patents." https://patents.google.com/patent/WO2021072546A1/en?inventor=Ana+Bryn+BRENNAN (accessed Apr. 28, 2022).

[65] A. M. Kinser, W. A. Sands, and M. H. Stone, "Reliability and validity of a pressure algometer," *J. Strength Cond. Res.*, vol. 23, no. 1, pp. 312–314, Jan. 2009, doi: 10.1519/JSC.0B013E31818F051C.

[66] P. D. Thompson *et al.*, "Voluntary stimulus-sensitive jerks and jumps mimicking myoclonus or pathological startle syndromes," *Mov. Disord.*, vol. 7, no. 3, pp. 257–262, 1992, doi: 10.1002/MDS.870070312.

[67] B. J. Kemp, "Reaction time of young and elderly subjects in relation to perceptual deprivation and signal-on versus signal-off conditions," *Dev. Psychol.*, vol. 8, no. 2, pp.

268–272, Feb. 1973, doi: 10.1037/H0034147.

[68] “Compression Spring PC034-360-13000-MW-1190-C-N-IN - The Spring Store.” https://www.thespringstore.com/pc034-360-13000-mw-1190-c-n-in.html (accessed Feb. 04, 2022).

[69] “ZSC31014 - Resistive Sensor Signal Conditioner with Digital Output | Renesas.” https://www.renesas.com/us/en/products/sensor-products/sensor-signal-conditioners-ssc-afe/zsc31014-resistive-sensor-signal-conditioner-digital-output (accessed Feb. 04, 2022).

[70] A. B. Brennan, “Design of an Electromechanical Force Probe,” 2020.

[71] “ZSC31014KIT - Evaluation Kit for ZSC31014 | Renesas.” https://www.renesas.com/us/en/products/sensor-products/sensor-signal-conditioners-ssc-afe/zsc31014kit-evaluation-kit-zsc31014 (accessed Feb. 04, 2022).

[72] “LOLIN D1 mini — WEMOS documentation.” https://www.wemos.cc/en/latest/d1/d1_mini.html (accessed May 01, 2022).

[73] “Adafruit Trinket - Mini Microcontroller - 3.3V Logic [MicroUSB] : ID 1500 : $6.95 : Adafruit Industries, Unique & fun DIY electronics and kits.” https://www.adafruit.com/product/1500 (accessed May 01, 2022).

[74] “Beetle Board - Compatible with Arduino Leonardo - ATmega32U4 - DFRobot.” https://www.dfrobot.com/product-1075.html (accessed May 01, 2022).

[75] “Arduino Nano — Arduino Online Shop.” https://store-usa.arduino.cc/products/arduino-nano?selectedStore=us (accessed Feb. 04, 2022).

[76] “DSD TECH Official Website: DSD TECH HC-06 Bluetooth 2.0 SPP Wireless BT DIP

Module for Arduino UNO R3 Nano MEGA Raspberry Pi." http://www.dsdtech-global.com/2017/07/dsd-tech-hc-06-bluetooth-20-spp.html (accessed Feb. 04, 2022).

[77] "CR2 Battery." https://www.energizer.com/specialty-batteries/energizer-cr2-battery (accessed Feb. 04, 2022).

[78] "LiPower - Boost Converter - PRT-10255 - SparkFun Electronics." https://www.sparkfun.com/products/10255 (accessed Feb. 04, 2022).

[79] "Arduino - SoftwareSerial." https://www.arduino.cc/en/Reference/softwareSerial (accessed Feb. 04, 2022).

[80] "About Us." https://appinventor.mit.edu/about-us (accessed Feb. 04, 2022).

[81] "Arduino and HC-06 (ZS-040) | Martyn Currey." http://www.martyncurrey.com/arduino-and-hc-06-zs-040/ (accessed Feb. 04, 2022).

[82] "Arduino - WireBegin." https://www.arduino.cc/en/Reference/WireBegin (accessed Feb. 04, 2022).

[83] "Arduino - WireBeginTransmission." https://www.arduino.cc/en/Reference/WireBeginTransmission (accessed Feb. 04, 2022).

[84] "Arduino - WireRequestFrom." https://www.arduino.cc/en/Reference/WireRequestFrom (accessed Feb. 04, 2022).

[85] "Arduino - WireRead." https://www.arduino.cc/en/Reference/WireRead (accessed Feb. 04, 2022).

[86] "micros() - Arduino Reference." https://www.arduino.cc/reference/en/language/functions/time/micros/ (accessed Feb. 04,

2022).

[87] “Serial.print() - Arduino Reference.” https://www.arduino.cc/reference/en/language/functions/communication/serial/print/ (accessed Feb. 04, 2022).

[88] “Serial.available() - Arduino Reference.” https://www.arduino.cc/reference/en/language/functions/communication/serial/available/ (accessed Feb. 04, 2022).

[89] “Serial.read() - Arduino Reference.” https://www.arduino.cc/reference/en/language/functions/communication/serial/read/ (accessed Feb. 04, 2022).

[90] “Autoclave Temperature in Class N and Class B Autoclaves | Felixtrument.” https://felixtrument.ca/autoclave-temperature/ (accessed Feb. 04, 2022).

[91] S. N. Vouyiouka and C. D. Papaspyrides, “Mechanistic Aspects of Solid-State Polycondensation,” *Polym. Sci. A Compr. Ref. 10 Vol. Set*, vol. 4, pp. 857–874, Jan. 2012, doi: 10.1016/B978-0-444-53349-4.00126-6.

[92] “Arduino Nano 33 BLE — Arduino Online Shop.” https://store-usa.arduino.cc/products/arduino-nano-33-ble (accessed Feb. 04, 2022).

[93] M. El Assi, A. Ghaddar, S. Tawbi, and G. Fadi, “RESOURCE-EFFICIENT FLOATING-POINT DATA COMPRESSION USING MAS IN WSN,” *Int. J. Ad hoc*, vol. 4, no. 5, 2013, doi: 10.5121/ijasuc.2013.4502.

[94] “Interpolation — increase sample rate by integer factor - MATLAB interp.”

https://www.mathworks.com/help/signal/ref/interp.html (accessed May 24, 2022).

[95] "Interpolation FIR filter design - MATLAB intfilt." https://www.mathworks.com/help/signal/ref/intfilt.html (accessed May 24, 2022).

[96] "ZSSC3240 - High-End 24-Bit Sensor Signal Conditioner with Analog and Digital Output | Renesas." https://www.renesas.com/us/en/products/sensor-products/sensor-signal-conditioners-ssc-afe/zssc3240-high-end-24-bit-sensor-signal-conditioner-analog-and-digital-output (accessed Feb. 04, 2022).

[97] J. Lonnblad, J. G. Castano, M. Ekstrom, M. Linden, and Y. Backlund, "Optimization of wireless Bluetooth/spl trade/ sensor systems," *26th Annu. Int. Conf. IEEE Eng. Med. Biol. Soc.*, vol. 3, pp. 2133–2136, doi: 10.1109/IEMBS.2004.1403625.

[98] "Research on a reference signal optimisation algorithm for indoor Bluetooth positioning - Dialnet." https://dialnet.unirioja.es/servlet/articulo?codigo=8224430 (accessed May 01, 2022).

[99] E. Sharifi, "Analysis of Vehicle Detection Rate for Bluetooth Traffic Sensors: A Case Study in Maryland and Delaware," 2011, Accessed: May 01, 2022. [Online]. Available: https://www.researchgate.net/publication/268128878.

[100] H. L. Mjøsund, E. Boyle, R. Mygind Mieritz, T. Skallgård, and P. Kent, "Clinically acceptable agreement between the ViMove wireless motion sensor system and the Vicon motion capture system when measuring lumbar region inclination motion in the sagittal and coronal planes," doi: 10.1186/s12891-017-1489-1.

[101] Y. Zhang *et al.*, "Electronic Skin Wearable Sensors for Detecting Lumbar-Pelvic

Movements," doi: 10.3390/s20051510.

[102] R. Rondon, A. Mahmood, S. Grimaldi, and M. Gidlund, "Understanding the Performance of Bluetooth Mesh: Reliability, Delay, and Scalability Analysis," *IEEE Internet Things J.*, vol. 7, no. 3, pp. 2089–2101, Mar. 2020, doi: 10.1109/JIOT.2019.2960248.

[103] R. A. Rashid and R. Yusoff, "Bluetooth performance analysis in personal area network (PAN)," *2006 Int. RF Microw. Conf. Proc.*, pp. 393–397, 2006, doi: 10.1109/RFM.2006.331112.

[104] M. J. Morón, R. Luque, E. Casilari, and A. Diaz-Estrella, "An analytical study of the delay in bluetooth networks using the personal area network profile," *IEEE Commun. Lett.*, vol. 11, no. 11, pp. 845–847, Nov. 2007, doi: 10.1109/LCOMM.2007.071117.

[105] J.-R. Luque, M.-J. Morón, and E. Casilari, "A characterization of the performance of Bluetooth 2.x + EDR technology in noisy environments," *Wirel. Networks*, doi: 10.1007/s11276-015-0888-1.

[106] "S420 Circuit Board Mounted Load Cell," Accessed: May 14, 2022. [Online]. Available: www.smdsensors.com.

APPENDICES

Appendix A: Technical Drawings and Specifications

A.1 Wireless v-QueST Technical Drawings

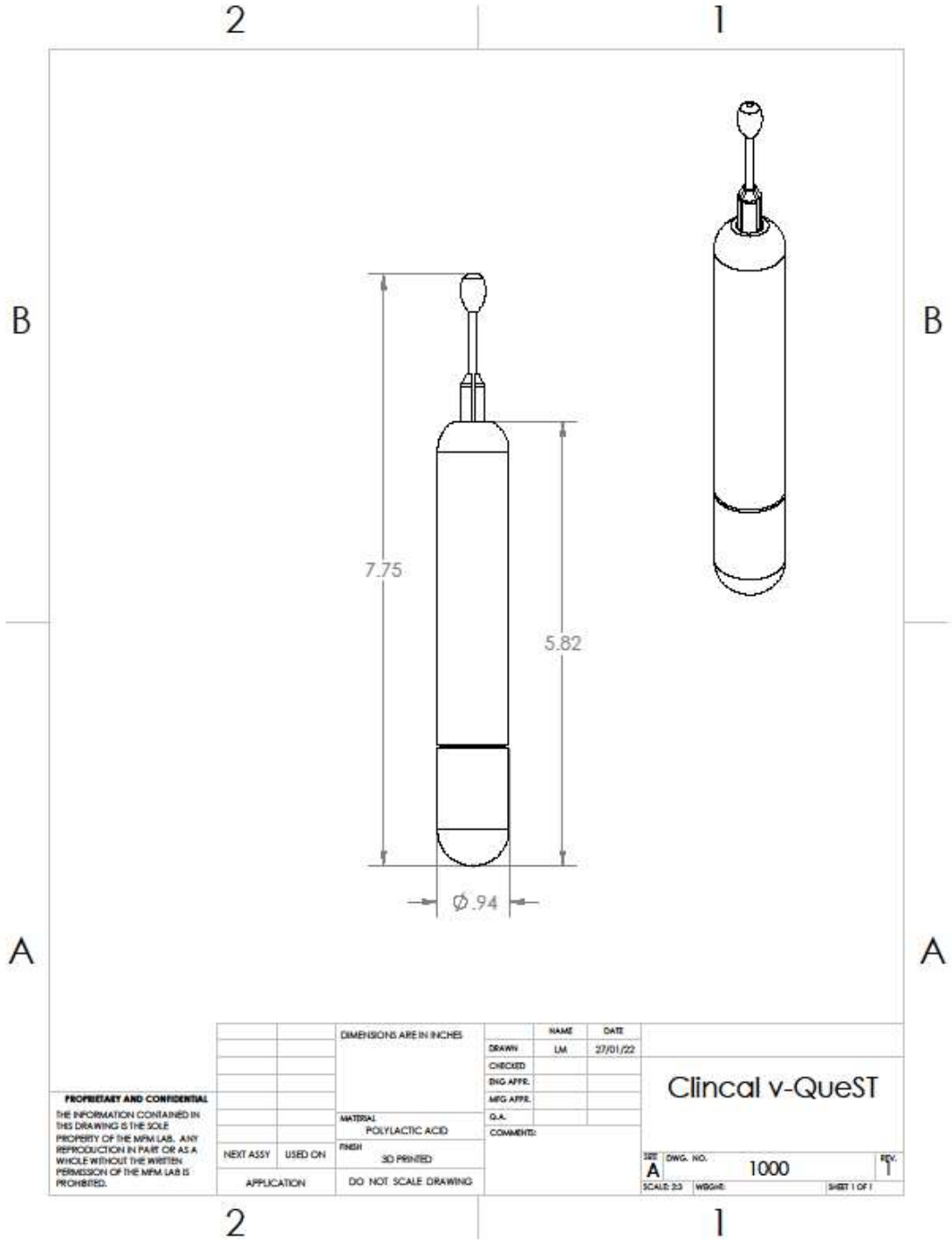

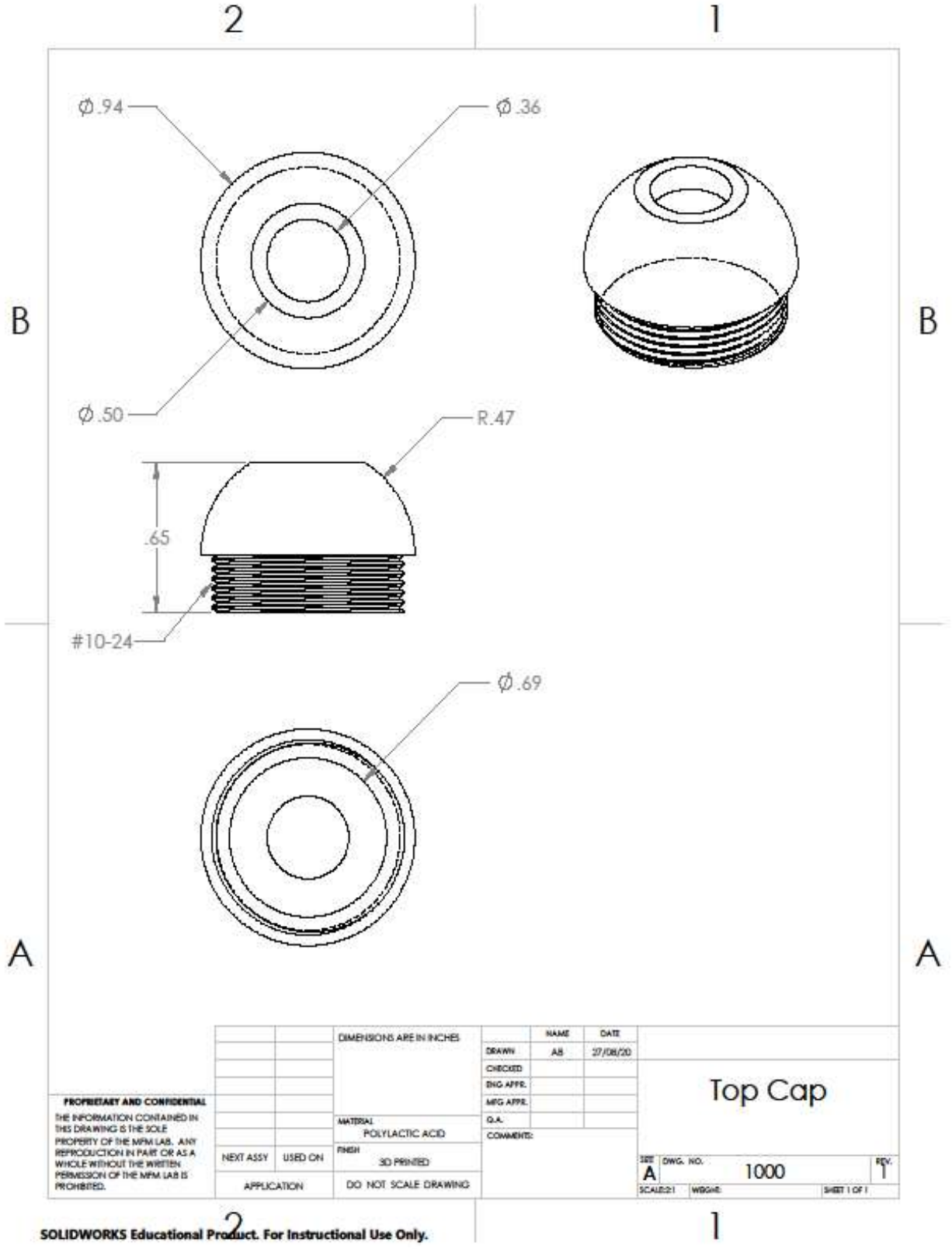
2
1
B
B
A
A
Ø .94
Ø .36
Ø .50
R.47
.65
#10-24
Ø .69
DIMENSIONS ARE IN INCHES
NAME
DATE
DRAWN
AB
27/08/20
CHECKED
ENG APPR.
MFG APPR.
Q.A.
COMMENTS:
MATERIAL
POLYLACTIC ACID
FINISH
3D PRINTED
NEXT ASSY
USED ON
APPLICATION
DO NOT SCALE DRAWING
PROPRIETARY AND CONFIDENTIAL
THE INFORMATION CONTAINED IN THIS DRAWING IS THE SOLE PROPERTY OF THE MPM LAB. ANY REPRODUCTION IN PART OR AS A WHOLE WITHOUT THE WRITTEN PERMISSION OF THE MPM LAB IS PROHIBITED.
Top Cap
SIZE
A
DWG. NO.
1000
REV.
1
SCALE:2:1
WEIGHT:
SHEET 1 OF 1
SOLIDWORKS Educational Product. For Instructional Use Only.

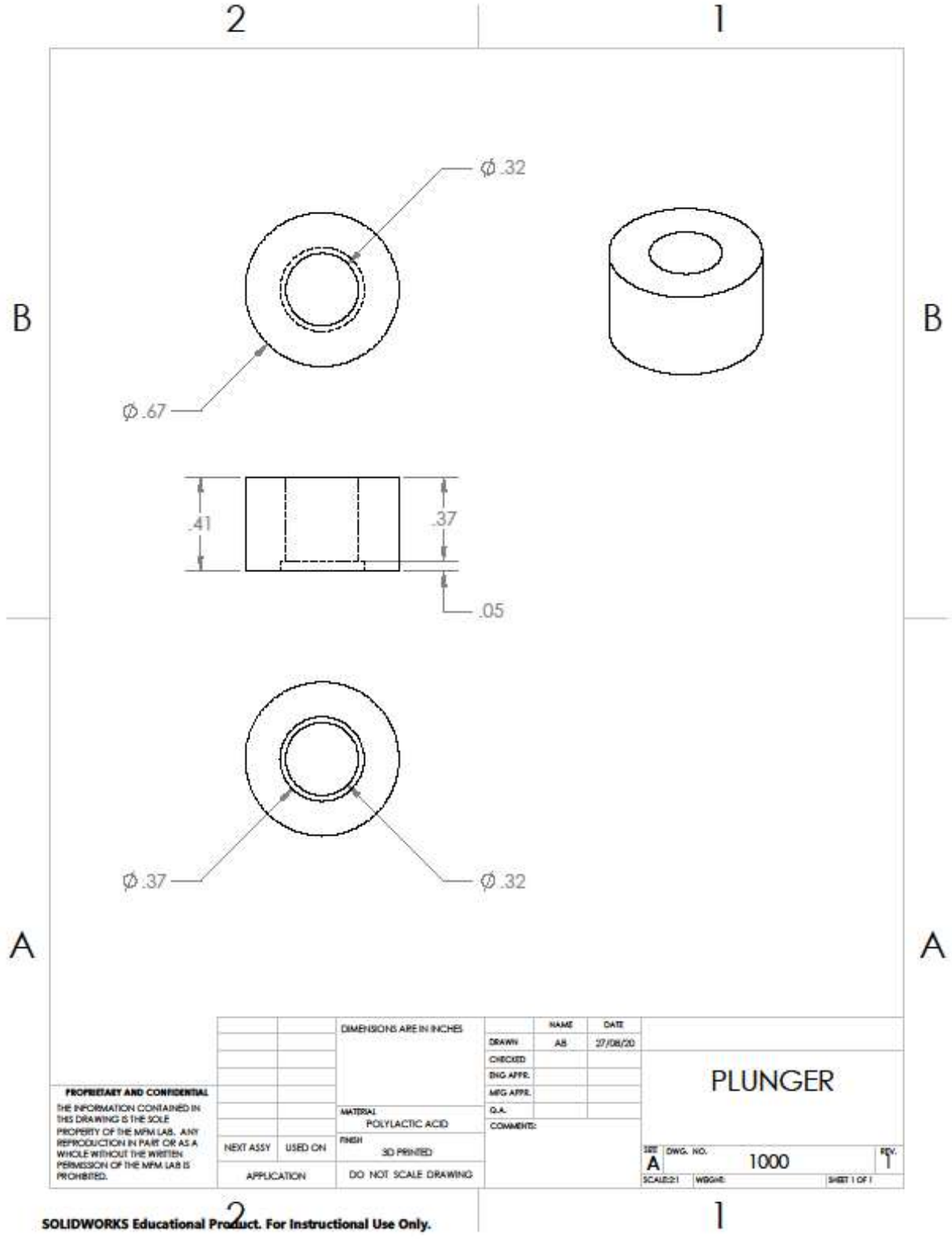
2
1
B
B
A
A
Ø .32
Ø .67
.41
.37
.05
Ø .37
Ø .32
DIMENSIONS ARE IN INCHES
NAME
DATE
DRAWN
AB
27/08/20
CHECKED
ENG APPR.
MFG APPR.
Q.A.
COMMENTS:
MATERIAL
POLYLACTIC ACID
FINISH
3D PRINTED
NEXT ASSY
USED ON
APPLICATION
DO NOT SCALE DRAWING
PROPRIETARY AND CONFIDENTIAL
THE INFORMATION CONTAINED IN THIS DRAWING IS THE SOLE PROPERTY OF THE MPM LAB. ANY REPRODUCTION IN PART OR AS A WHOLE WITHOUT THE WRITTEN PERMISSION OF THE MPM LAB IS PROHIBITED.
PLUNGER
SIZE
A
DWG. NO.
1000
REV.
1
SCALE:2:1
WEIGHT:
SHEET 1 OF 1
SOLIDWORKS Educational Product. For Instructional Use Only.

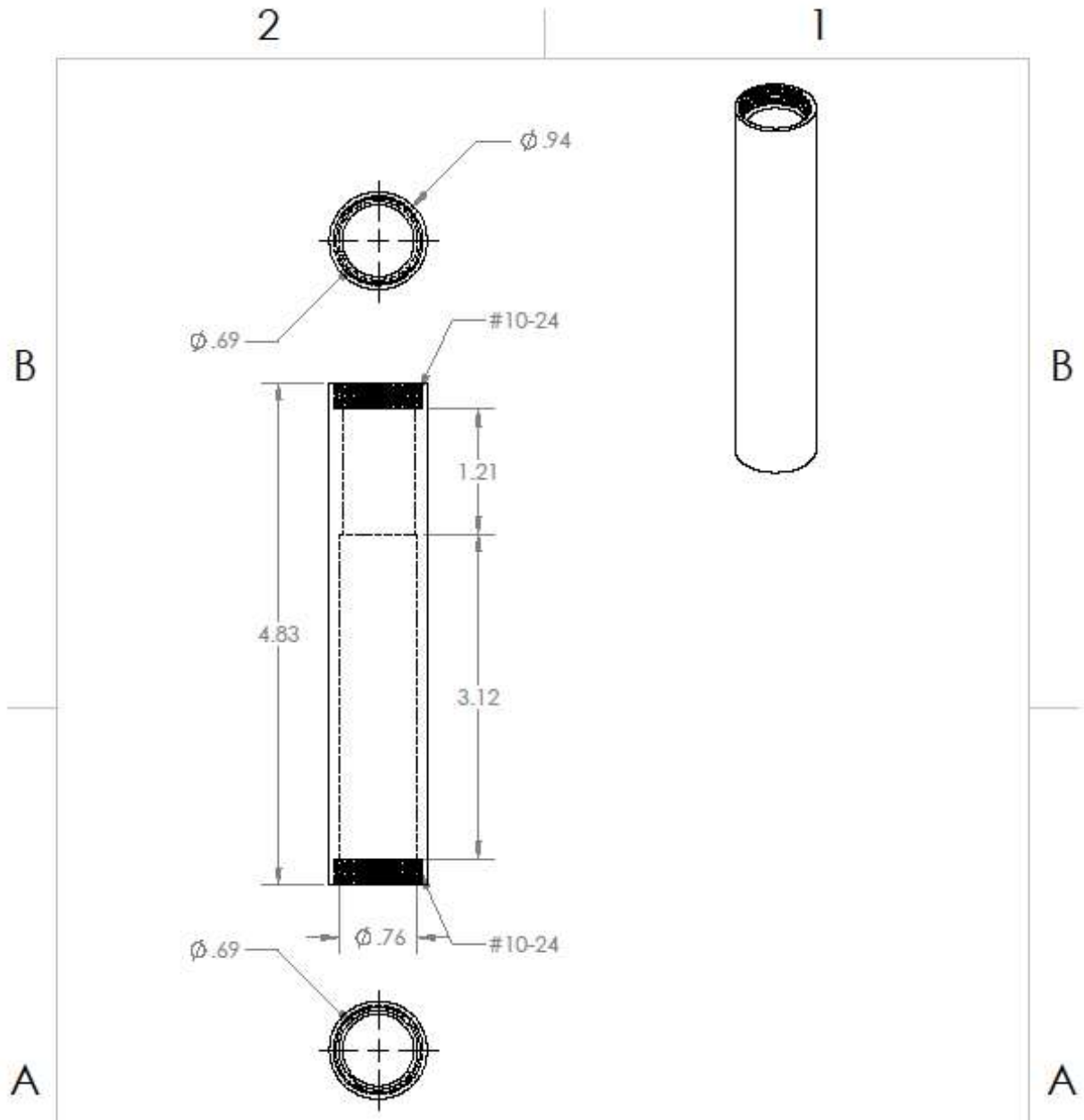

		DIMENSIONS ARE IN INCHES		NAME	DATE
			DRAWN	AB	27/08/20
			CHECKED		
			ENG APPR.		
			MFG APPR.		
		MATERIAL: PLOYLACTIC ACID	Q.A.		
			COMMENTS:		
NEXT ASSY	USED ON	FINISH: 3D PRINTED			
APPLICATION		DO NOT SCALE DRAWING			

PROPRIETARY AND CONFIDENTIAL

THE INFORMATION CONTAINED IN THIS DRAWING IS THE SOLE PROPERTY OF THE MPM LAB. ANY REPRODUCTION IN PART OR AS A WHOLE WITHOUT THE WRITTEN PERMISSION OF THE MPM LAB IS PROHIBITED.

MAIN CASING BODY

SIZE	DWG. NO.	REV.
A	1000	1

SCALE:1:1.25 | WEIGHT: | SHEET 1 OF 1

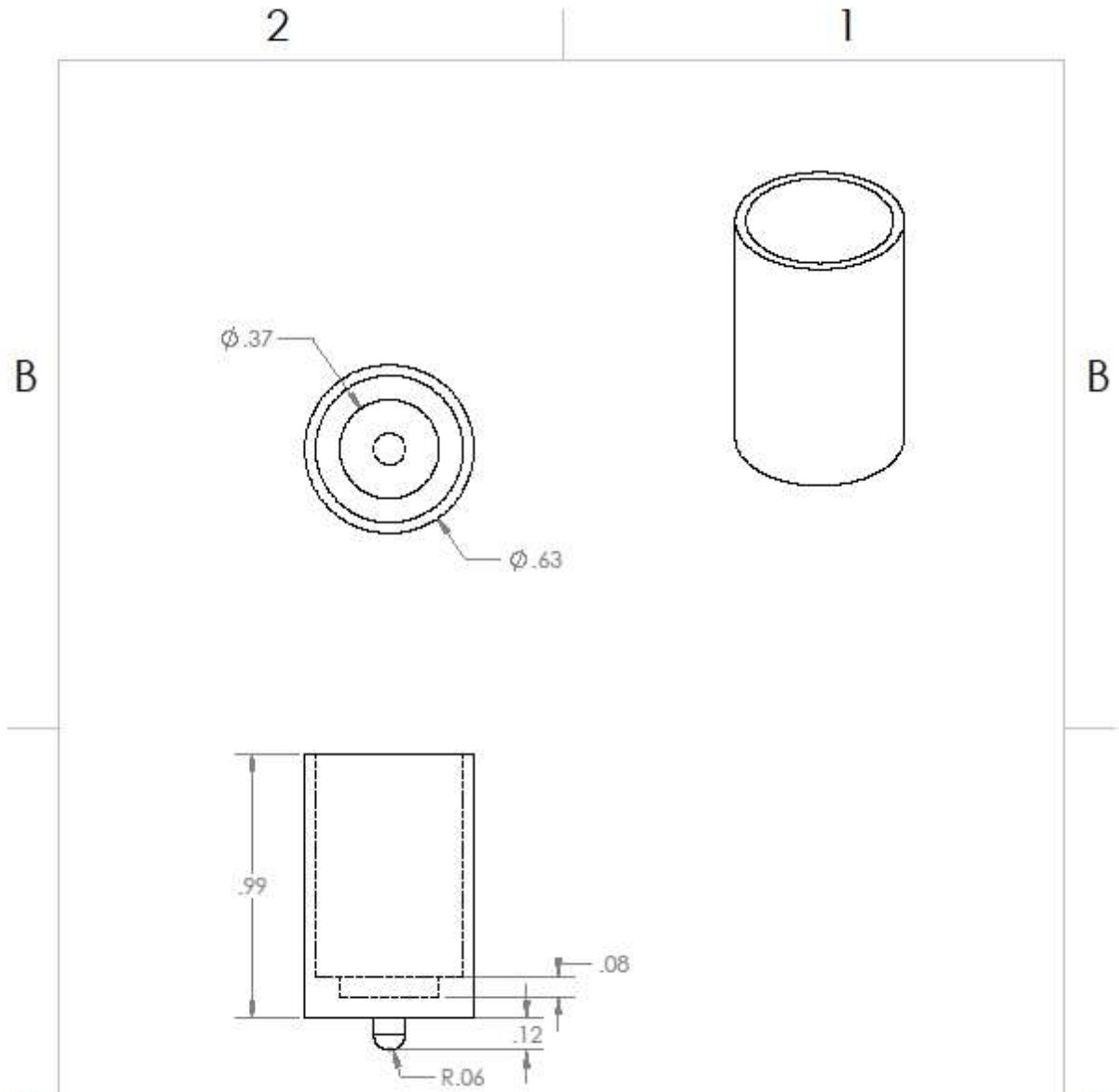

		DIMENSIONS ARE IN INCHES		NAME	DATE
			DRAWN	LM	27/01/22
			CHECKED		
			ENG APPR.		
			MFG APPR.		
		MATERIAL: POLYLACTIC ACID	Q.A.		
			COMMENTS:		
NEXT ASSY	USED ON	FINISH: 3D PRINTED			
APPLICATION		DO NOT SCALE DRAWING			

PROPRIETARY AND CONFIDENTIAL

THE INFORMATION CONTAINED IN THIS DRAWING IS THE SOLE PROPERTY OF THE MPM LAB. ANY REPRODUCTION IN PART OR AS A WHOLE WITHOUT THE WRITTEN PERMISSION OF THE MPM LAB IS PROHIBITED.

FORCE TRANSFER PLATE WITH OVERLOAD PROTECTION

SIZE	DWG. NO.	REV.
A	1000	1
SCALE:1:1	WEIGHT:	SHEET 1 OF 1

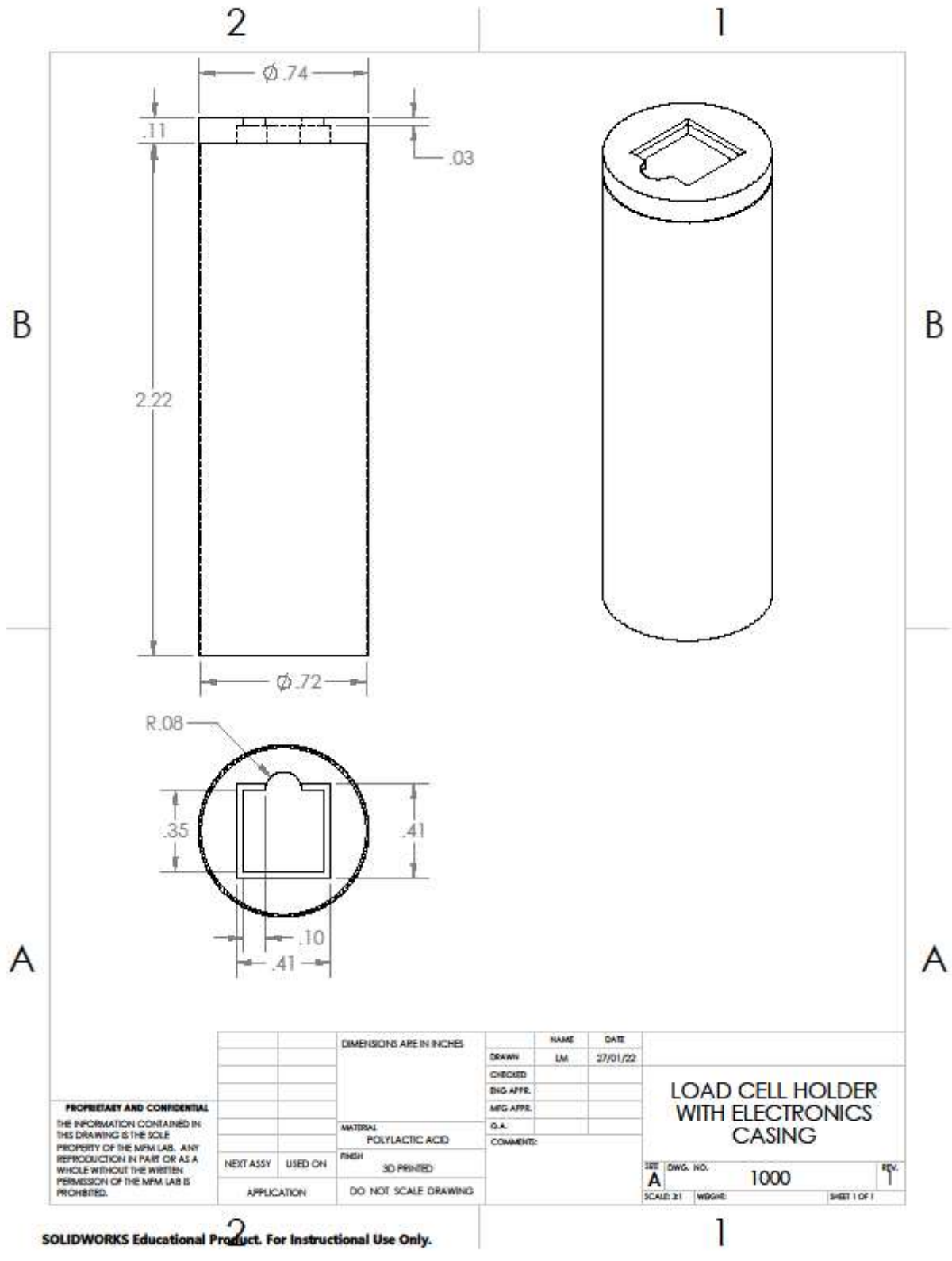
2
1
B
A
Ø.74
.11
.03
2.22
Ø.72
R.08
.35
.41
.10
.41
PROPRIETARY AND CONFIDENTIAL
THE INFORMATION CONTAINED IN THIS DRAWING IS THE SOLE PROPERTY OF THE MPM LAB. ANY REPRODUCTION IN PART OR AS A WHOLE WITHOUT THE WRITTEN PERMISSION OF THE MPM LAB IS PROHIBITED.
NEXT ASSY
USED ON
APPLICATION
DIMENSIONS ARE IN INCHES
MATERIAL
POLYLACTIC ACID
FINISH
3D PRINTED
DO NOT SCALE DRAWING
NAME
DATE
DRAWN
LM
27/01/22
CHECKED
ENG APPR.
MFG APPR.
Q.A.
COMMENTS:
LOAD CELL HOLDER WITH ELECTRONICS CASING
SIZE
A
DWG. NO.
1000
REV.
1
SCALE: 2:1
WEIGHT:
SHEET 1 OF 1
SOLIDWORKS Educational Product. For Instructional Use Only.

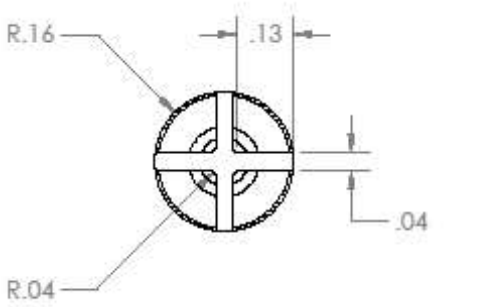

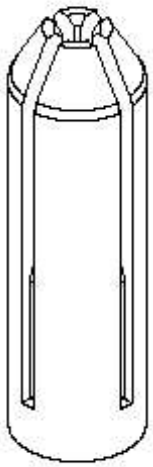

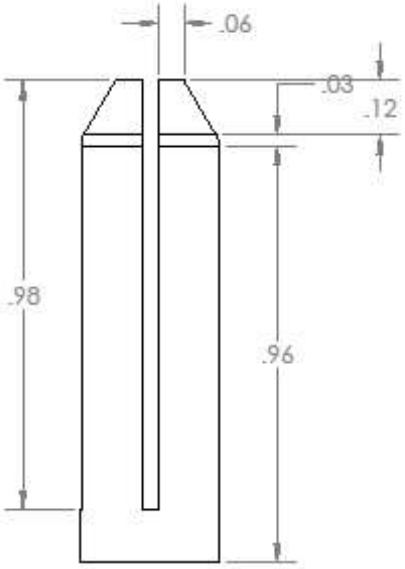

		DIMENSIONS ARE IN INCHES		NAME	DATE
			DRAWN	AB	27/08/20
			CHECKED		
			ENG APPR.		
			MFG APPR.		
		MATERIAL: POLYLACTIC ACID	Q.A.		
			COMMENTS:		
NEXT ASSY	USED ON	FINISH: 3D PRINTED			
APPLICATION		DO NOT SCALE DRAWING			

PROPRIETARY AND CONFIDENTIAL

THE INFORMATION CONTAINED IN THIS DRAWING IS THE SOLE PROPERTY OF THE MPM LAB. ANY REPRODUCTION IN PART OR AS A WHOLE WITHOUT THE WRITTEN PERMISSION OF THE MPM LAB IS PROHIBITED.

COLLET

SIZE A | DWG. NO. 1000 | REV. 1

SCALE: 2:1 | WEIGHT: | SHEET 1 OF 1

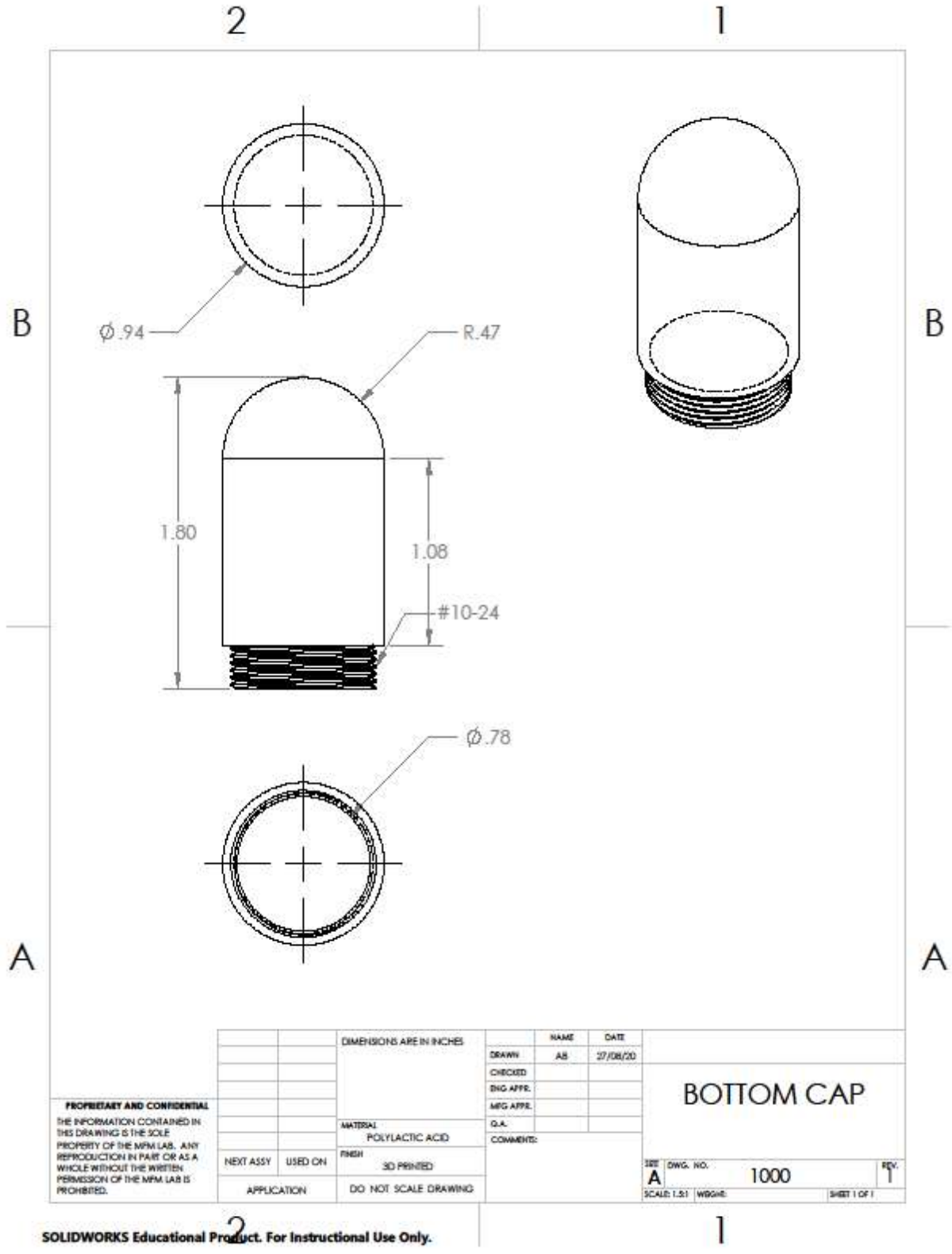
2
1
B
A
Ø.94
R.47
1.80
1.08
#10-24
Ø.78
DIMENSIONS ARE IN INCHES
DRAWN AB 27/08/20
CHECKED
ENG APPR.
MFG APPR.
Q.A.
COMMENTS:
MATERIAL
POLYLACTIC ACID
FINISH
3D PRINTED
NEXT ASSY
USED ON
APPLICATION
DO NOT SCALE DRAWING
PROPRIETARY AND CONFIDENTIAL
THE INFORMATION CONTAINED IN THIS DRAWING IS THE SOLE PROPERTY OF THE MPM LAB. ANY REPRODUCTION IN PART OR AS A WHOLE WITHOUT THE WRITTEN PERMISSION OF THE MPM LAB IS PROHIBITED.
BOTTOM CAP
SIZE A
DWG. NO. 1000
REV. 1
SCALE: 1.5:1
WEIGHT:
SHEET 1 OF 1
SOLIDWORKS Educational Product. For Instructional Use Only.

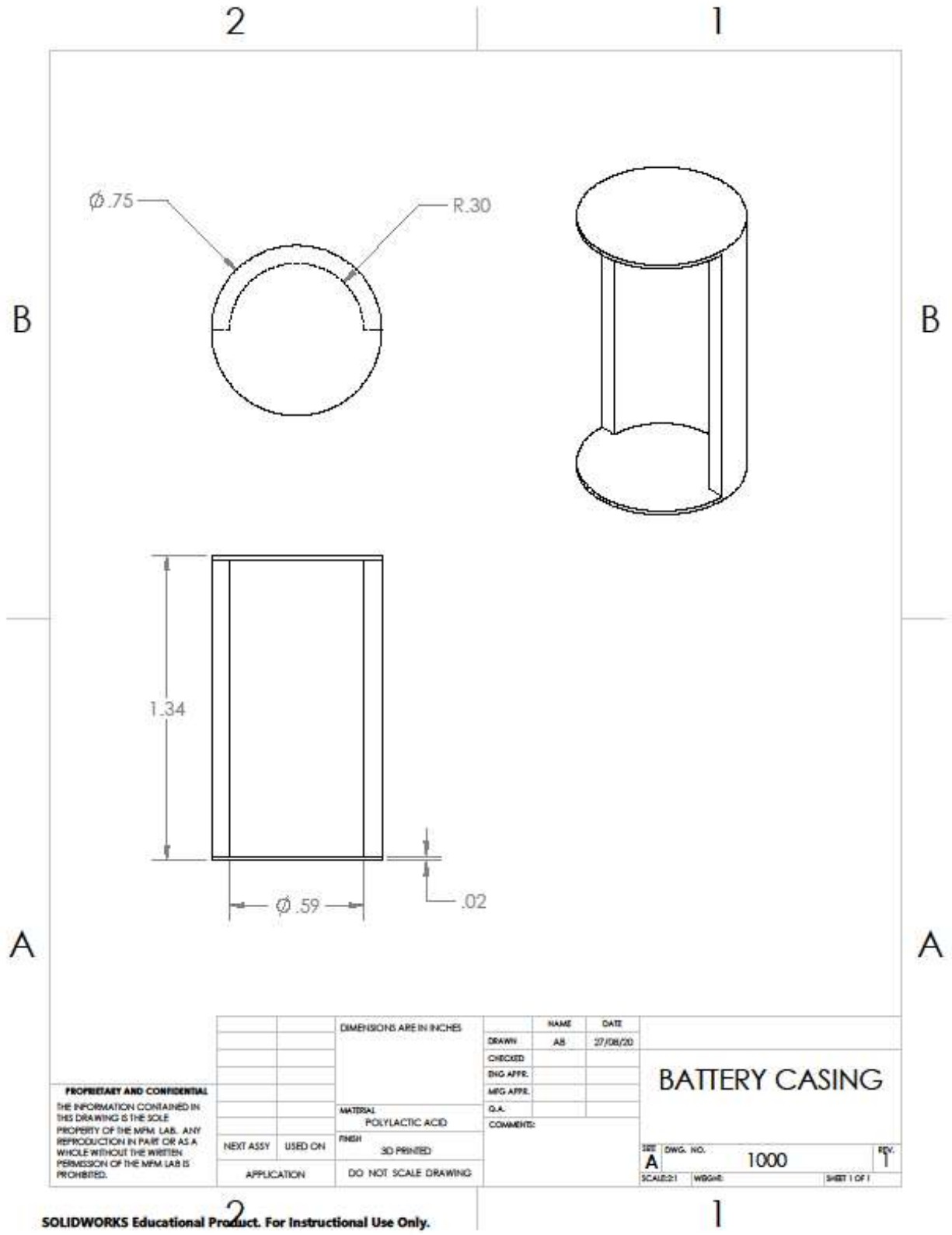
2
1
B
B
Ø.75
R.30
1.34
Ø.59
.02
A
A
DIMENSIONS ARE IN INCHES
NAME
DATE
DRAWN
AB
27/08/20
CHECKED
ENG APPR.
MFG APPR.
Q.A.
COMMENTS:
BATTERY CASING
MATERIAL
POLYLACTIC ACID
FINISH
3D PRINTED
NEXT ASSY
USED ON
APPLICATION
DO NOT SCALE DRAWING
SIZE
A
DWG. NO.
1000
REV.
1
SCALE:2:1
WEIGHT:
SHEET 1 OF 1
PROPRIETARY AND CONFIDENTIAL
THE INFORMATION CONTAINED IN THIS DRAWING IS THE SOLE PROPERTY OF THE MPM LAB. ANY REPRODUCTION IN PART OR AS A WHOLE WITHOUT THE WRITTEN PERMISSION OF THE MPM LAB IS PROHIBITED.
2
1
SOLIDWORKS Educational Product. For Instructional Use Only.

A.2 SMD S410 Miniature Low-Profile Button Load Cell

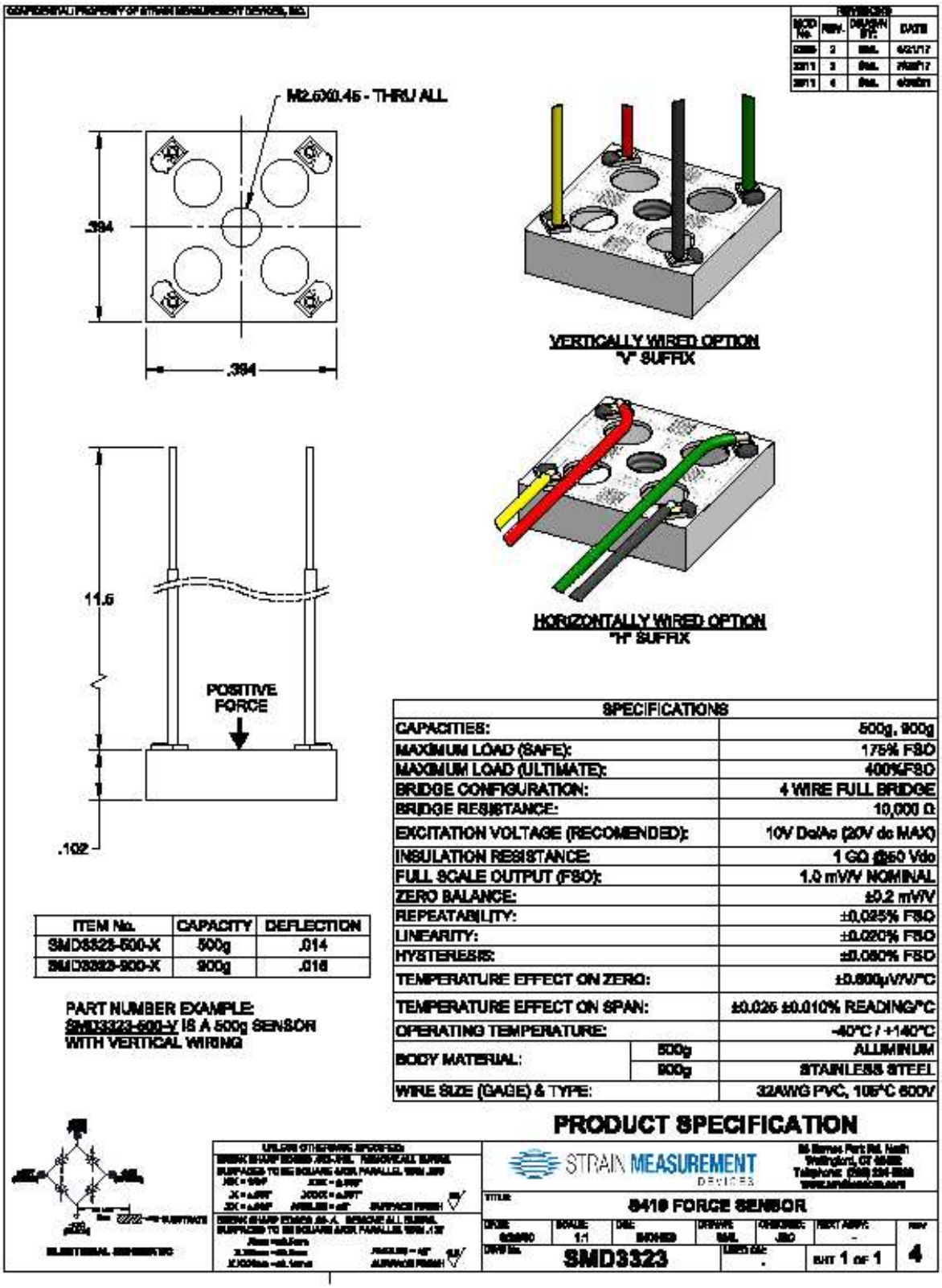

ITEM No.	CAPACITY	DEFLECTION
SMD3323-500-X	500g	.014
SMD3323-900-X	900g	.016

PART NUMBER EXAMPLE:
SMD3323-500-V IS A 500g SENSOR
WITH VERTICAL WIRING

SPECIFICATIONS		
CAPACITIES:		500g, 900g
MAXIMUM LOAD (SAFE):		175% FSO
MAXIMUM LOAD (ULTIMATE):		400%FSO
BRIDGE CONFIGURATION:		4 WIRE FULL BRIDGE
BRIDGE RESISTANCE:		10,000 Ω
EXCITATION VOLTAGE (RECOMENDED):		10V Dc/Ac (20V dc MAX)
INSULATION RESISTANCE:		1 GΩ @50 Vdc
FULL SCALE OUTPUT (FSO):		1.0 mV/V NOMINAL
ZERO BALANCE:		±0.2 mV/V
REPEATABILITY:		±0.025% FSO
LINEARITY:		±0.020% FSO
HYSTERESIS:		±0.050% FSO
TEMPERATURE EFFECT ON ZERO:		±0.600μV/V/°C
TEMPERATURE EFFECT ON SPAN:		±0.025 ±0.010% READING/°C
OPERATING TEMPERATURE:		-40°C / +140°C
BODY MATERIAL:	500g	ALUMINUM
	900g	STAINLESS STEEL
WIRE SIZE (GAGE) & TYPE:		32AWG PVC, 105°C 600V

A.3 ZSC31014 Signal Conditioner

RENESAS

RBic$_{ilite}$™ Digital Output Sensor Signal Conditioner

ZSC31014 Datasheet

Brief Description

The ZSC31014 is a CMOS integrated circuit for highly accurate amplification and analog-to-digital conversion of differential and half-bridge input signals. The ZSC31014 can compensate the measured signal for offset, 1st and 2nd order span, and 1st and 2nd order temperature (Tco and Tcg). It is well suited for sensor-specific correction of bridge sensors. Digital compensation of signal offset, sensitivity, temperature drift, and non-linearity is accomplished via an internal digital signal processor running a correction algorithm with calibration coefficients stored in a non-volatile EEPROM.

The ZSC31014 is adjustable to nearly all piezo-resistive bridge sensors. Measured and corrected bridge values are provided at digital output pins, which can be configured as I^{2}C™* or SPI. The digital I^{2}C™ interface can be used for a simple PC-controlled calibration procedure to program calibration coefficients into an on-chip EEPROM. The calibrated ZSC31014 and a specific sensor are mated digitally: fast, precise, and without the cost overhead associated with trimming by external devices or laser trimming.

The ZSC31014's integrated diagnostics functions are well suited for safety-critical applications.

Features

- High accuracy (±0.1% FSO @ -25 to +85°C; ±0.25% FSO @ -40 to +125°C)
- 2nd order charge-balancing analog-to-digital converter provides low noise, 14-bit data at sample rates exceeding 2kHz
- Fast power-up to data output response: 3ms at 4MHz
- Digital compensation of sensor offset, sensitivity, temperature drift, and non-linearity
- Eight programmable analog gain settings combine with a digital gain term; accommodates bridges with spans <1mV/V and high offset
- Internal temperature compensation for sensor correction and for corrected temperature output
- 48-bit customer ID field for module traceability

* I^{2}C™ is a trademark of NXP.

Benefits

- Simple PC-controlled configuration and single-pass digital calibration via I^{2}C™ interface – quick and precise; SPI option for measurement mode
- Eliminates need for external trimming components
- On-chip diagnostic features add safety to the application (e.g., EEPROM signature, bridge connection checks, bridge short detection).
- Low-power Sleep Mode lengthens battery life
- Enables multiple sensor networks

Available Support

- Evaluation Kit
- Application Notes
- Mass Calibration Solution

Physical Characteristics

- Wide supply voltage capability: 2.7V to 5.5V
- Current consumption as low as 70µA depending on programmed sample rate
- Low-power Sleep Mode (<2µA @ 25°C)
- Operation temperature: -40°C to +125°C
- Small SOP8 package

ZSC31014 Application: I^{2}C™ Interface, Low-Power Bsink Option, Internal Temperature Correction

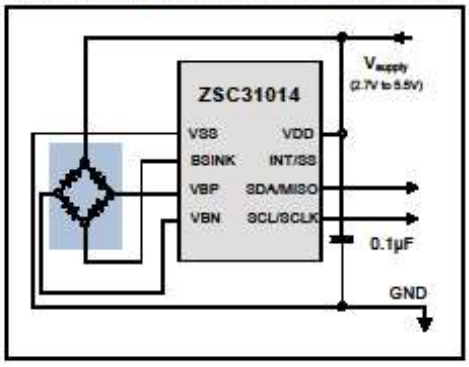

ZSC31014 Block Diagram

Applications:

Industrial: building automation, data loggers, pressure meters, leak detection monitoring

Medical: infusion pumps, blood pressure meters, air mattresses, apnea monitors

White Goods / Appliances: fluid level, refrigerant

Consumer: body monitors, portable monitors, desktop weather stations, bathroom scales, toys/games

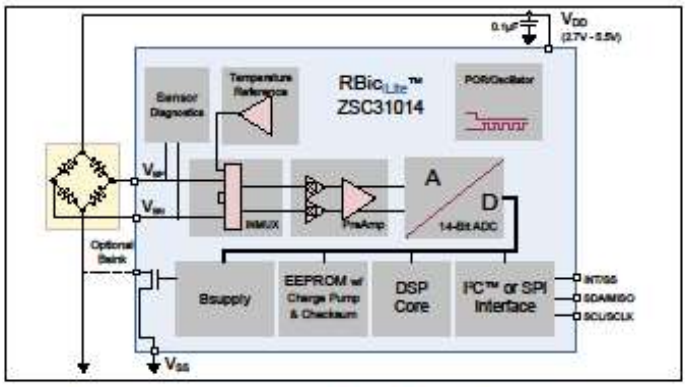

Application: *Half-Bridge Voltage Measurement*

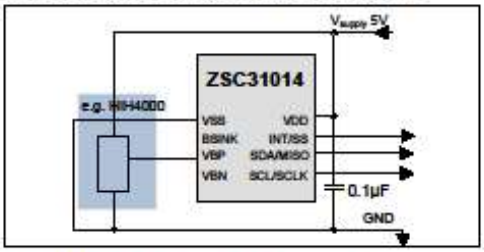

Application: *Generic Differential A2D Converter*

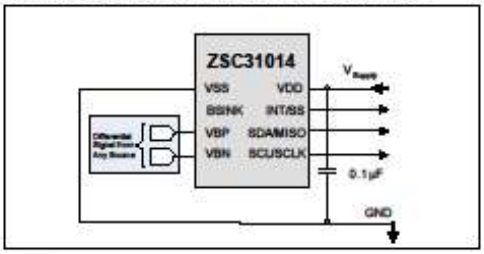

Ordering Examples *(Refer to section 10 in the data sheet for additional options.)*

Sales Code	Description	Package
ZSC31014EAB	ZSC31014 Die — Temperature range: -40°C to +125°C	Unsawn on Wafer
ZSC31014EAC	ZSC31014 Die — Temperature range: -40°C to +125°C	Sawn on Wafer Frame
ZSC31014EAG1	ZSC31014 SOP8 (150 mil) — Temperature range: -40° to +125°C	Tube: add "-T" to sales code / Reel: add "-R"
ZSC31014KIT	ZSC31014 SSC Evaluation Kit: Communication Board, SSC Board, Sensor Replacement Board, USB Cable, 5 IC Samples (software can downloaded on www.IDT.com/ZSC31014)	

A.4 v-QueST Custom Test Rig Technical Drawings

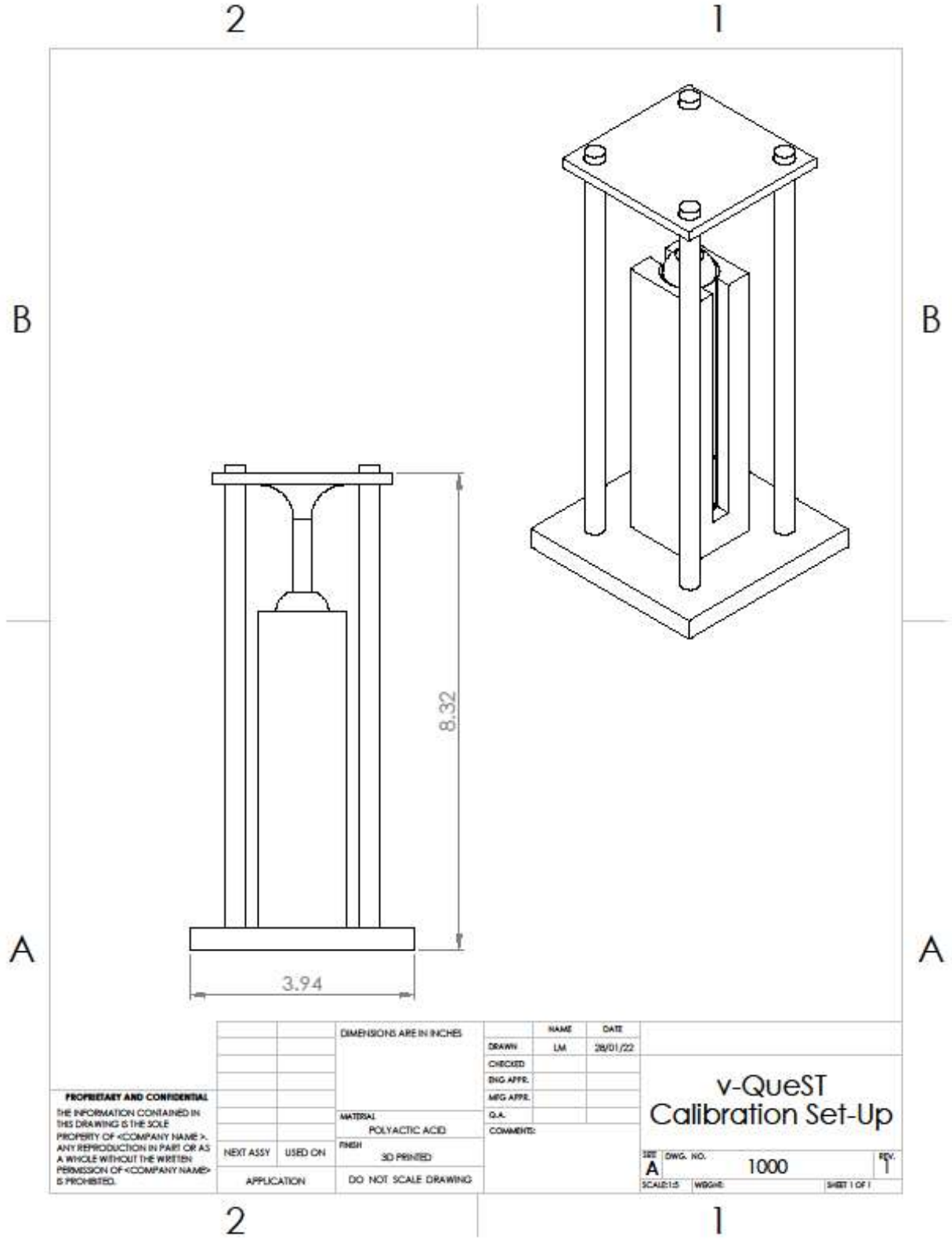

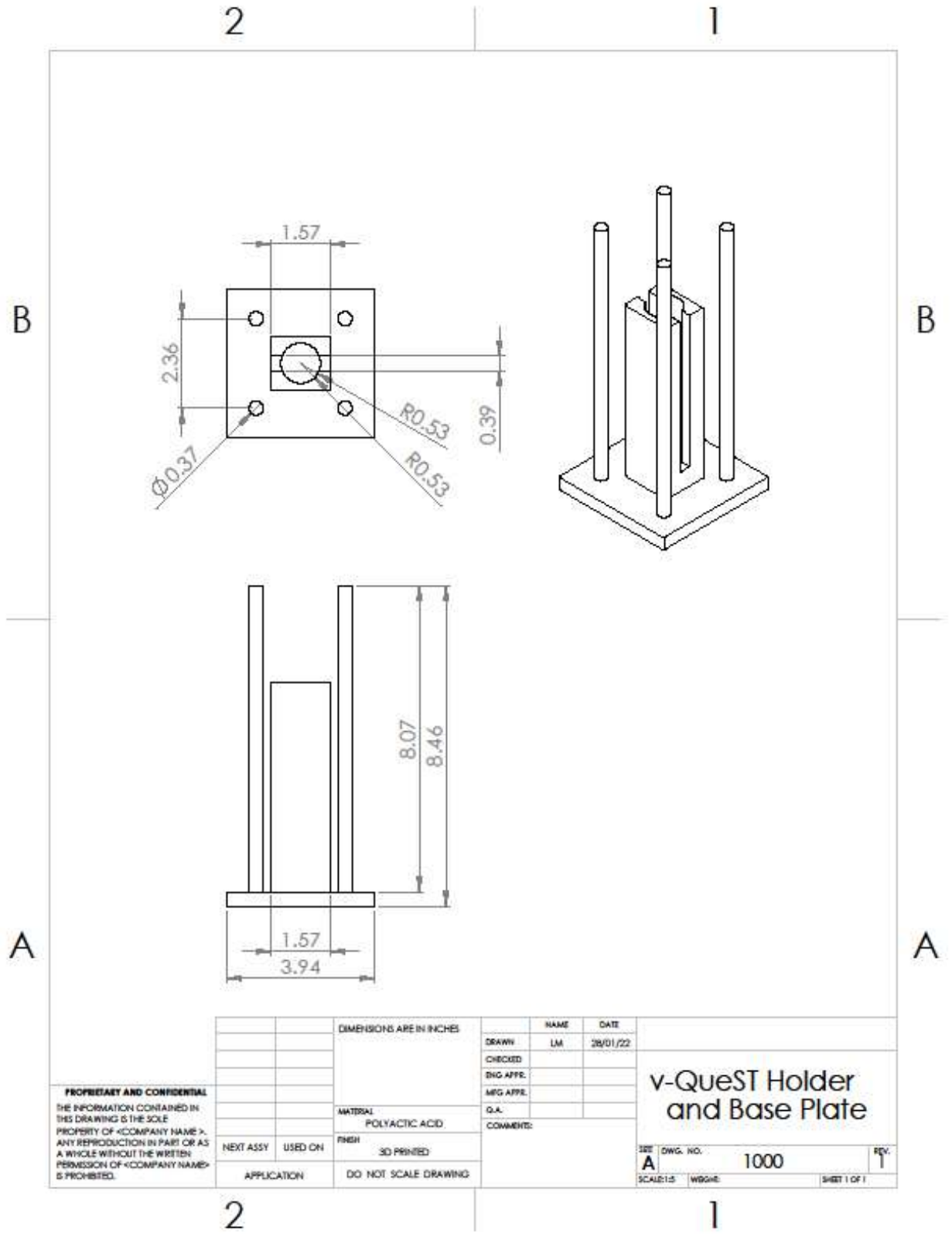
2
1
B
A
1.57
2.36
R0.53
0.39
Ø0.37
R0.53
8.07
8.46
1.57
3.94
DIMENSIONS ARE IN INCHES
NAME
DATE
DRAWN
LM
28/01/22
CHECKED
ENG APPR.
MFG APPR.
Q.A.
COMMENTS:
MATERIAL
POLYACTIC ACID
FINISH
3D PRINTED
NEXT ASSY
USED ON
APPLICATION
DO NOT SCALE DRAWING
PROPRIETARY AND CONFIDENTIAL
THE INFORMATION CONTAINED IN THIS DRAWING IS THE SOLE PROPERTY OF <COMPANY NAME >. ANY REPRODUCTION IN PART OR AS A WHOLE WITHOUT THE WRITTEN PERMISSION OF <COMPANY NAME> IS PROHIBITED.
v-QueST Holder and Base Plate
SIZE
A
DWG. NO.
1000
REV.
1
SCALE:1:5
WEIGHT:
SHEET 1 OF 1

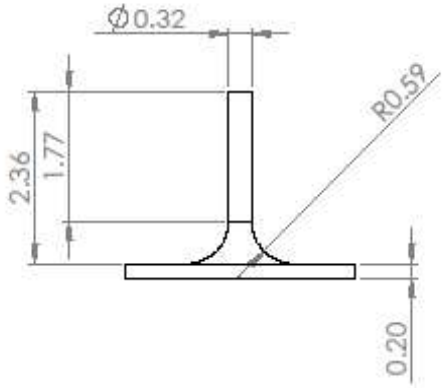

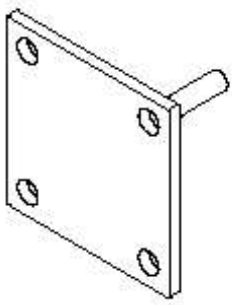

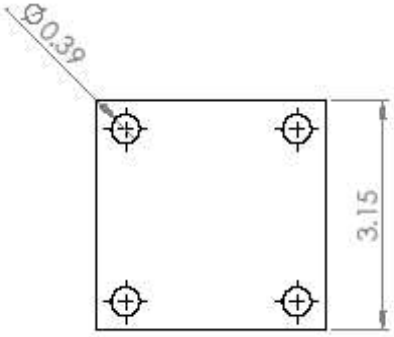

				NAME	DATE	
		DIMENSIONS ARE IN INCHES	DRAWN	LM	28/01/22	
			CHECKED			
			ENG APPR.			
			MFG APPR.			Extension Plate
		MATERIAL: POLYACTIC ACID	Q.A.			
NEXT ASSY	USED ON	FINISH: 3D PRINTED	COMMENTS:			SIZE A DWG. NO. 1000 REV. 1
APPLICATION		DO NOT SCALE DRAWING				SCALE:1:2 WEIGHT: SHEET 1 OF 1

Appendix B: Arduino Scripts

B.1 Initial Bluetooth Setup

```
//Setting up Bluetooth HC-06 --> open serial monitor and use the commands,
set up the bluetooth as instructed in the powerpoint
//If setting up BT for VGM --> Set name to be VGMBT, password 4102, and
baudrate 115200

//Command       Reply      Comment
//AT          OK      Communications test
//AT+VERSION     OKlinvorV1.8  Firmware version.
//AT+NAMEmyBTmodule  OKsetname    Sets the modules name to "myBTmodule"
//AT+PIN6789      OKsetPIN    Set the PIN to 6789
//AT+BAUD1       OK1200    Sets the baud rate to 1200
//AT+BAUD2       OK2400    Sets the baud rate to 2400
//AT+BAUD3       OK4800    Sets the baud rate to 4800
//AT+BAUD4       OK9600    Sets the baud rate to 9600
//AT+BAUD5       OK19200    Sets the baud rate to 19200
//AT+BAUD6       OK38400    Sets the baud rate to 38400
//AT+BAUD7       OK57600    Sets the baud rate to 57600
//AT+BAUD8       OK115200   Sets the baud rate to 115200
//AT+BAUD9       OK230400   Sets the baud rate to 230400
//AT+BAUDA       OK460800   Sets the baud rate to 460800
//AT+BAUDB       OK921600   Sets the baud rate to 921600
//AT+BAUDC       OK1382400   Sets the baud rate to 1382400

#include <SoftwareSerial.h>
SoftwareSerial mySerial(8, 9);

void setup()
{
 Serial.begin(9600);
 Serial.println("Enter AT commands:");
 //Serial.println("AT+BAUD4");

 // HC-06 default serial speed is 9600
 mySerial.begin(9600);
}

void loop()
{

 // Keep reading from HC-06 and send to Arduino Serial Monitor
 if (mySerial.available())
 {
  Serial.write(mySerial.read());
 }

 // Keep reading from Arduino Serial Monitor and send to HC-06
 if (Serial.available())
 {
  //delay(10);
  mySerial.write(Serial.read());
 }
}
```

B.2 Wireless v-QueST

```
//Reads input from load cell signal conditioner, converts data to grams and
writes the load cell reading in the bluetooth and Arduino serial monitor
//Bluetooth in slave configuration
//Sends VGM data to Android
unsigned long startMicros;
unsigned long currentMicros;
unsigned long number;
const unsigned long period = 1500; //the value is a number of microseconds
between sensor reading

#include <SoftwareSerial.h>
SoftwareSerial mySerial (8, 9); //Arduino D8 (RX) & D9(TX)

#include <Wire.h>

//--- Accelerometer Register Addresses

int ADXAddress = 0x28; //Device address in which is also included the 8th bit
for selecting the mode, read in this case.

byte byteone;
byte bytetwo;
byte mask = 63;
uint16_t fulldata;
float output;
char flag = ' ';
byte VGM;
int PPT = 5000;

void setup() {

 Wire.begin(); // Initiate the Wire library

 // open serial communication for communication from Arduino to computer
 Serial.begin(115200);

 //Open serial communication with Bluetooth and Arduino
 mySerial.begin(115200);

 startMicros = micros();

}

void loop() {

 // read from arduino and send to Bluetooth module
 // X-axis
 Wire.beginTransmission(ADXAddress); // Begin transmission to the Sensor
 Wire.write(0);
 Wire.requestFrom(ADXAddress, 2); // Request the transmitted two bytes from
the two registers
 byteone = Wire.read(); // Read the first byte from the register
 bytetwo = Wire.read(); // Read the second byte from the register
 //Apply bitmask to data, removes first two bits which are sensor status
```

```
 byteone = byteone & mask;
 bytetwo = bytetwo & mask;
 //Concatenate two bytes for full data
 fulldata = word(byteone, bytetwo);
 //convert data to float for output in serial monitor
 output = (float)fulldata;
 //convert data to grams (*900 is full range of sensor, 16323 is the maximum
possible I2C output)
 output = 900 * (output / 16323);


 currentMicros = micros();


 if (currentMicros - startMicros >= period) { //test whether the period has
elapsed

  // flag = mySerial.read();

  if (mySerial.available() > 0) {


   output = output + PPT;
   number = currentMicros - startMicros;
   mySerial.print(number);
   mySerial.print("|");
   mySerial.print(output); //print values from VGM to the app
   mySerial.print("|");
//   Serial.println(number);
//   Serial.println(output);
//
   mySerial.read();


  }

  number = currentMicros - startMicros;

  mySerial.print(number);
  mySerial.print("|");
  mySerial.print(output); //print values from VGM to the app
  mySerial.print("|");

//  Serial.println(number);
//  Serial.println(output);



  startMicros = currentMicros;
 }


}
```

B.3 Sampling Frequency Testing

```
//Reads input from load cell signal conditioner, converts data to grams and
writes 50 load cell readings in the bluetooth and Arduino serial monitor
every 5 minutes.
// Bluetooth in slave configuration
// Sends VGM data to Android
unsigned long startMicros;
unsigned long currentMicros;
unsigned long number;
unsigned long i=0;
const unsigned long period = 1500; //the value is a number of microseconds
between sensor reading

#include <SoftwareSerial.h>
SoftwareSerial mySerial (8, 9); //Arduino D8 (RX) & D9(TX)

#include <Wire.h>

//--- Accelerometer Register Addresses

int ADXAddress = 0x28; //Device address in which is also included the 8th bit
for selecting the mode, read in this case.

byte byteone;
byte bytetwo;
byte mask = 63;
uint16_t fulldata;
float output;
char flag = ' ';
byte VGM;
int j = 0;
int PPT = 5000;


void setup() {

 Wire.begin(); // Initiate the Wire library

 // open serial communication for communication from Arduino to computer
 Serial.begin(115200);

 //Open serial communication with Bluetooth and android
 mySerial.begin(115200);

 startMicros = micros();


}

void loop() {

 // read from arduino and send to Bluetooth module
 // X-axis
 Wire.beginTransmission(ADXAddress); // Begin transmission to the Sensor
 Wire.write(0);
```

```
 Wire.requestFrom(ADXAddress, 2); // Request the transmitted two bytes from
the two registers
 byteone = Wire.read(); // Read the first byte from the register
 bytetwo = Wire.read(); // Read the second byte from the register
 //Apply bitmask to data, removes first two bits which are sensor status
 byteone = byteone & mask;
 bytetwo = bytetwo & mask;
 //Concatenate two bytes for full data
 fulldata = word(byteone, bytetwo);
 //convert data to float for output in serial monitor
 output = (float)fulldata;
 //convert data to grams (*900 is full range of sensor, 16323 is the maximum
possible I2C output)
 output = 900 * (output / 16323);

 currentMicros = micros();

 if ((currentMicros - startMicros) >= period) { //test whether the period has
elapsed


  number = currentMicros - startMicros;
//  Serial.println(i);
//  Serial.println(j);

  if ((i > 300000000) && (j < 51)) {

   mySerial.print(number);
   mySerial.print("|");
   mySerial.print(output); //print values from VGM to the app
   mySerial.print("|");
 // Serial.println(number);
  //  Serial.println(output);


   //flag = mySerial.read();

   if (mySerial.available() > 0) {

    output = output + PPT;
    mySerial.print(number);
    mySerial.print("|");
    mySerial.print(output); //print values from VGM to the app
    mySerial.print("|");
//    Serial.println(number);
//    Serial.println(output);
    //
    //VGMarray[i] = output; //CHECK THIS OUT FIRST
    mySerial.read();

    //}
   }

   if (j<50){
    j=j+1;
   }
```

```
   if (j == 50) {
    i = 0;
    j = 0;
   }

  }

 }

 i = i + number;


 startMicros = currentMicros;
}
```

B.4 Trigger Button Activation Testing

```
//Analyzes how long an application button takes to be read by wireless
interface
unsigned long startMicros;
unsigned long currentMicros;
unsigned long number;
int reset = 13904372889235783;

#include <SoftwareSerial.h>
SoftwareSerial mySerial (8, 9); //Arduino D8 (RX) & D9 (TX)

void setup() {
 Serial.begin(115200);

 // open serial communication between bluetooth and android
 mySerial.begin(115200);

 startMicros = micros();


}

void loop() {
 currentMicros = micros();
 number = currentMicros - startMicros;
 Serial.println(number);
 if (mySerial.available() > 0) {
  currentMicros = micros();
  number = currentMicros - startMicros;
  Serial.println("now pressed");
  Serial.println(number);
  mySerial.read();
 }

 startMicros = currentMicros;

}
```

Appendix C: MIT AI2 Code

C.1 Wireless v-QueST

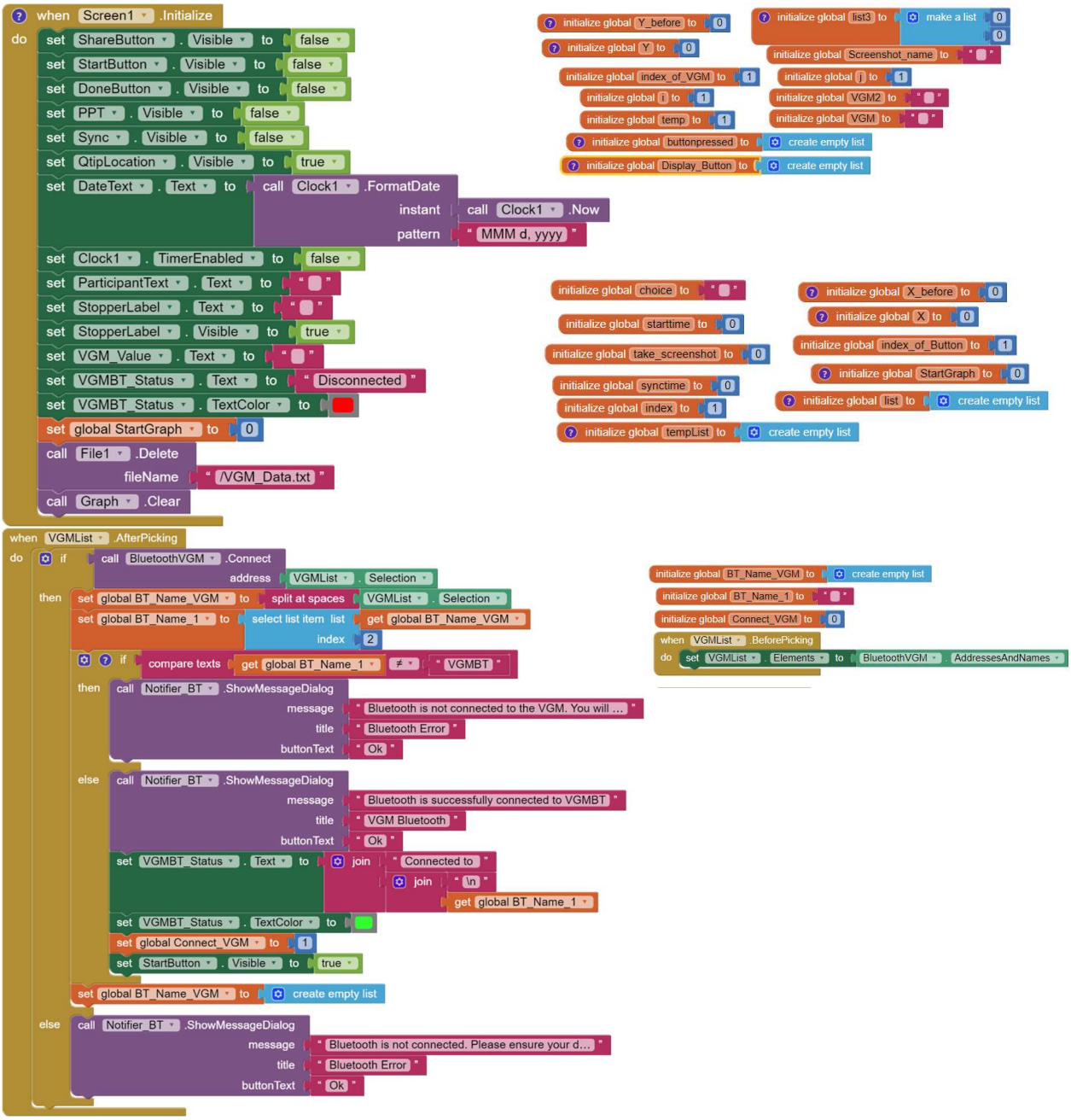


when Clock1 .Timer
do if BluetoothVGM . IsConnected = true and compare texts get global BT_Name_1 = " VGMBT "
then if get global StartGraph = 1
then if call BluetoothVGM .BytesAvailableToReceive > 0
then set global VGM to call BluetoothVGM .ReceiveText numberOfBytes call BluetoothVGM .BytesAvailableToReceive
set global list to split text get global VGM at " | "
set global index to length of list list get global list
if get global index ≥ 1 and is a list? thing get global list
then if get global index > 1
then set global index to get global index - 1
set global VGM to select list item list get global list index get global index
if get global VGM > 1500 and get global VGM < 4800
then set global VGM to select list item list get global list index get global index - 1
if get global VGM > 4800
then set global VGM to get global VGM - 5000
set VGM_Value . Text to join get global VGM " g "
call plot_on_graph
append to list list1 get global list3 list2 get global list
set global StartGraph to 1
set global list to create empty list
set global index to 1
set global VGM to " "
else set VGM_Value . Text to " Error "
else set global StartGraph to 0
to plot_on_graph
do set global X_before to get global X
set global Y_before to get global Y
set global X to get global X + 5
set global Y to get global VGM
call Graph .DrawLine x1 get global X_before y1 Graph . Height - get global Y_before × 0.3 x2 get global X y2 Graph . Height - get global Y × 0.3
if get global X ≥ Graph . Width
then call Graph .Clear
set global X to 0
set global X_before to 0
if get global take_screenshot = 1
then set global Screenshot_name to join call Clock1 .FormatDateTime instant call Clock1 .Now pattern " MM-dd-yyyy-hh-mm-ss " " .jpg "
set TaifunScreenshot1 . FileName to get global Screenshot_name
call TaifunScreenshot1 .TakeScreenshot
evaluate but ignore result call TaifunTools1 .GalleryRefresh fileName join " /storage/emulated/0/ " get global Screenshot_name
set global take_screenshot to 0
when Clock2 .Timer
do if not BluetoothVGM . IsConnected = true and not compare texts get global BT_Name_1 = " VGMBT " and get global Connect_VGM = 1
then set VGMBT_Status . TextColor to
call Notifier_BT .ShowMessageDialog message " Bluetooth is no longer connected. " title " Bluetooth Error " buttonText " Ok "
set VGMBT_Status . Text to " Disconnected "
set global Connect_VGM to 0

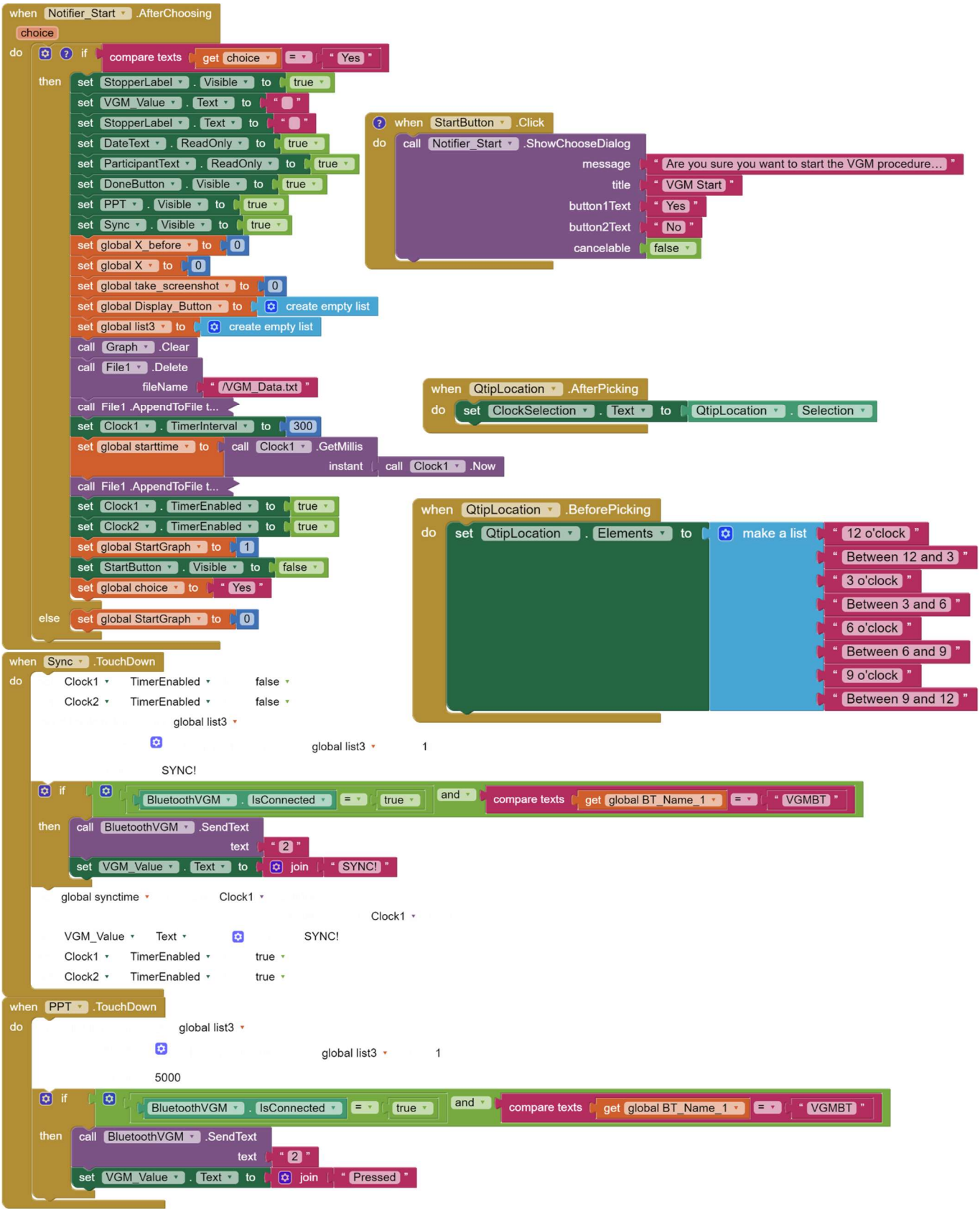
when Notifier_Start .AfterChoosing
choice
do if compare texts get choice = " Yes "
then set StopperLabel . Visible to true
set VGM_Value . Text to " "
set StopperLabel . Text to " "
set DateText . ReadOnly to true
set ParticipantText . ReadOnly to true
set DoneButton . Visible to true
set PPT . Visible to true
set Sync . Visible to true
set global X_before to 0
set global X to 0
set global take_screenshot to 0
set global Display_Button to create empty list
set global list3 to create empty list
call Graph .Clear
call File1 .Delete
fileName " /VGM_Data.txt "
call File1 .AppendToFile t...
set Clock1 . TimerInterval to 300
set global starttime to call Clock1 .GetMillis
instant call Clock1 .Now
call File1 .AppendToFile t...
set Clock1 . TimerEnabled to true
set Clock2 . TimerEnabled to true
set global StartGraph to 1
set StartButton . Visible to false
set global choice to " Yes "
else set global StartGraph to 0
when StartButton .Click
do call Notifier_Start .ShowChooseDialog
message " Are you sure you want to start the VGM procedure... "
title " VGM Start "
button1Text " Yes "
button2Text " No "
cancelable false
when QtipLocation .AfterPicking
do set ClockSelection . Text to QtipLocation . Selection
when QtipLocation .BeforePicking
do set QtipLocation . Elements to make a list
" 12 o'clock "
" Between 12 and 3 "
" 3 o'clock "
" Between 3 and 6 "
" 6 o'clock "
" Between 6 and 9 "
" 9 o'clock "
" Between 9 and 12 "
when Sync .TouchDown
do Clock1 TimerEnabled false
Clock2 TimerEnabled false
global list3
global list3 1
SYNC!
if BluetoothVGM . IsConnected = true and compare texts get global BT_Name_1 = " VGMBT "
then call BluetoothVGM .SendText
text " 2 "
set VGM_Value . Text to join " SYNC! "
global synctime Clock1
Clock1
VGM_Value Text SYNC!
Clock1 TimerEnabled true
Clock2 TimerEnabled true
when PPT .TouchDown
do global list3
global list3 1
5000
if BluetoothVGM . IsConnected = true and compare texts get global BT_Name_1 = " VGMBT "
then call BluetoothVGM .SendText
text " 2 "
set VGM_Value . Text to join " Pressed "

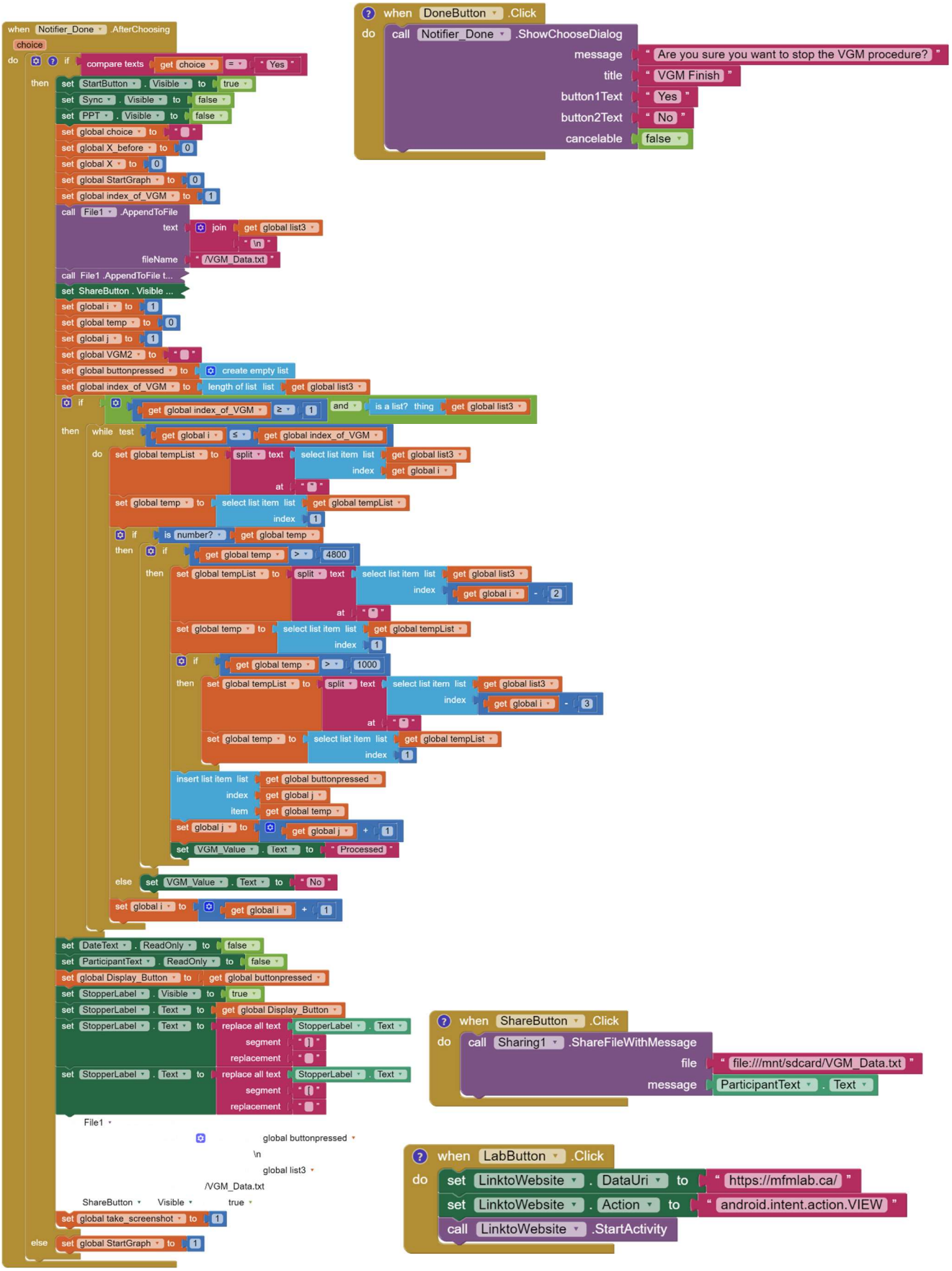
when Notifier_Done .AfterChoosing
choice
do if compare texts get choice = " Yes "
then set StartButton . Visible to true
set Sync . Visible to false
set PPT . Visible to false
set global choice to " "
set global X_before to 0
set global X to 0
set global StartGraph to 0
set global index_of_VGM to 1
call File1 .AppendToFile
text join get global list3 " \n "
fileName " /VGM_Data.txt "
call File1 .AppendToFile t...
set ShareButton . Visible ...
set global i to 1
set global temp to 0
set global j to 1
set global VGM2 to " "
set global buttonpressed to create empty list
set global index_of_VGM to length of list list get global list3
if get global index_of_VGM ≥ 1 and is a list? thing get global list3
then while test get global i ≤ get global index_of_VGM
do set global tempList to split text select list item list get global list3 index get global i at " "
set global temp to select list item list get global tempList index 1
if is number? get global temp
then if get global temp > 4800
then set global tempList to split text select list item list get global list3 index get global i - 2 at " "
set global temp to select list item list get global tempList index 1
if get global temp > 1000
then set global tempList to split text select list item list get global list3 index get global i - 3 at " "
set global temp to select list item list get global tempList index 1
insert list item list get global buttonpressed index get global j item get global temp
set global j to get global j + 1
set VGM_Value . Text to " Processed "
else set VGM_Value . Text to " No "
set global i to get global i + 1
set DateText . ReadOnly to false
set ParticipantText . ReadOnly to false
set global Display_Button to get global buttonpressed
set StopperLabel . Visible to true
set StopperLabel . Text to get global Display_Button
set StopperLabel . Text to replace all text StopperLabel . Text segment " [] " replacement " , "
set StopperLabel . Text to replace all text StopperLabel . Text segment " [" replacement " , "
File1
global buttonpressed
\n
global list3
/VGM_Data.txt
ShareButton Visible true
set global take_screenshot to 1
else set global StartGraph to 1
when DoneButton .Click
do call Notifier_Done .ShowChooseDialog
message " Are you sure you want to stop the VGM procedure? "
title " VGM Finish "
button1Text " Yes "
button2Text " No "
cancelable false
when ShareButton .Click
do call Sharing1 .ShareFileWithMessage
file " file:///mnt/sdcard/VGM_Data.txt "
message ParticipantText . Text
when LabButton .Click
do set LinktoWebsite . DataUri to " https://mfmlab.ca/ "
set LinktoWebsite . Action to " android.intent.action.VIEW "
call LinktoWebsite .StartActivity

C.2 Trigger Button Activation Testing

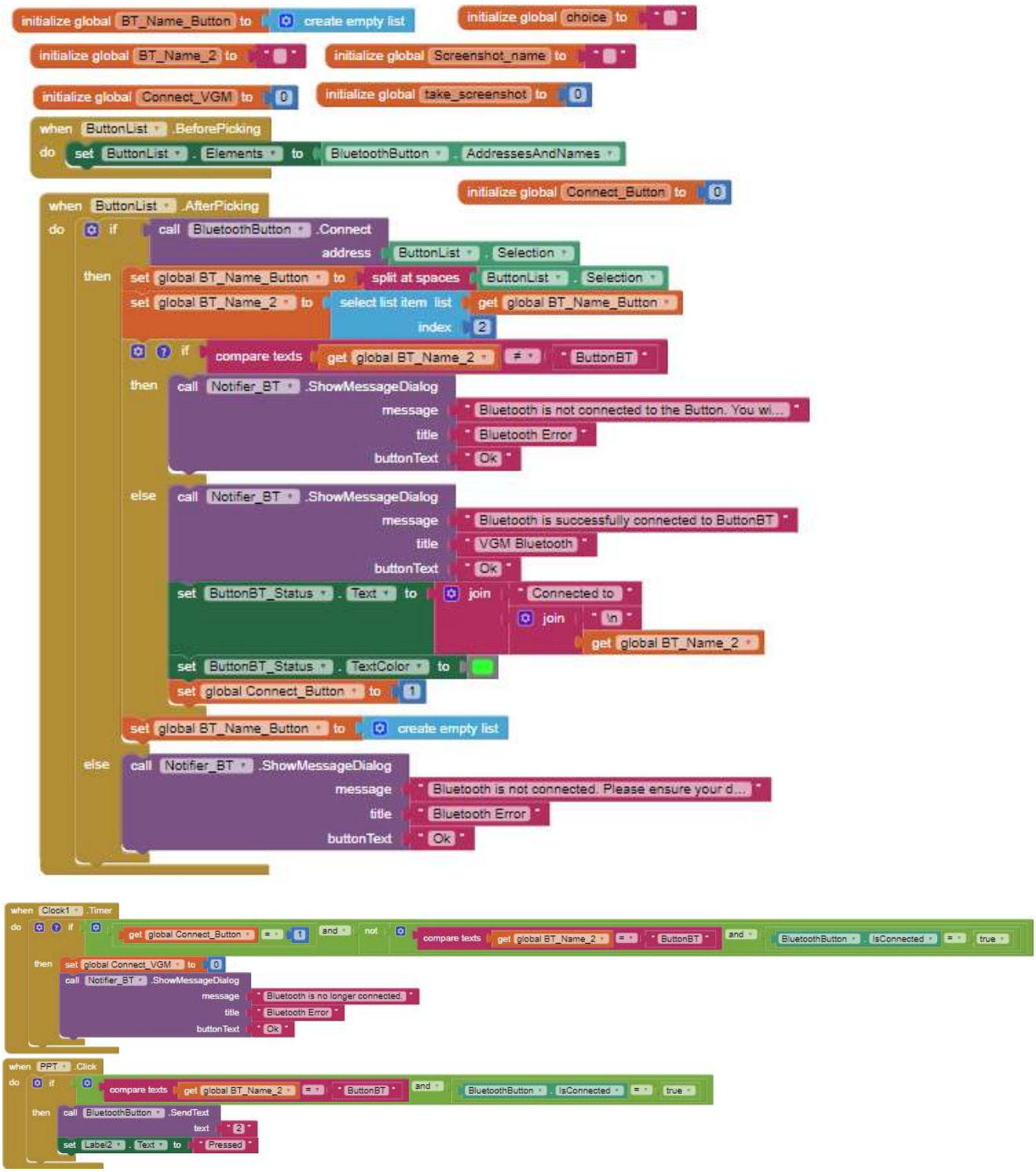

Appendix D: MATLAB R2021b Code

D.1 v-QueST Parse

```
close all
clear all
clc
%Prep the command-window and work space

Lines=[];
values = '';
cleaned_values='';
values_array=[];
final_array=[];
i=1;
j=1;
time=[];
final_time=[];
pressure=[];
P=[];
T=[];

addpath('C:\\Users\\layla\\OneDrive\\Documents\\Masters\\Thesis\\TrialRuns'); %add
path of where functions are
DIR=uigetdir; % select directory
cd(DIR); %change the current folder to where the data is
txt_file = [DIR, 'VGM_Data.txt']; %accessing specific file in selected path

fid=fopen(txt_file, 'r'); %open vgm file but only read
Lines=readlines("VGM_Data.txt");
values=Lines(5);
start_time=str2double(Lines(4));
sync_time=str2double(Lines(6));
difference=sync_time-start_time;

%parsing out specific characters and separating csv
cleaned_values=regexprep(values,'"','');
cleaned_values=regexprep(cleaned_values,'[','');
cleaned_values=regexprep(cleaned_values,']','');
values_array=strsplit(cleaned_values,',');
length_array=length(values_array);

%removing the blank spaces
while i<=length_array
  if values_array(i)~= " "
    if values_array(i)==" SYNC!"
      final_array(j)=100000;%str2double((values_array(i));
      j=j+1;
    elseif values_array(i)==""
      j=j;
    else
      final_array(j)=str2double(values_array(i));
      j=j+1;
    end
```

```
  end

  i=i+1;
end
i=1;
j=1;
k=1;
length_array=length(final_array);
while i<=length_array
  if mod(i,2)==0
    pressure(j)=final_array(i);
    j=j+1;
  else
    time(k)=final_array(i);
    k=k+1;
  end
  i=i+1;
end

% i=1;
% j=2;
% final_time(1)=0;
%
% while i<length(time)
%   final_time(j)=((final_time(j-1))+time(i));
%   i=i+1;
%   j=j+1;
% end
%
%
% final_time=final_time/1000;
%%


i=1;
j=1;
l=length(pressure);

while i<=l
  if pressure(i)>1000 && pressure(i)<4800
    pressure_index(j)=i;
    j=j+1;
  end
  i=i+1;
end

i=1;
j=1;
l=length(time);

while i<=l
  if time(i)<1500
    time_index(j)=i;
    j=j+1;
  end
```

```
  i=i+1;
end

%%
j=1;
i=1;
k=1;
len=1;
l=length(time_index);
l_2=length(pressure_index);
new_pressure=[];
new_time=[];

if l>l_2
  len=l_2;
else
  len=l;
end

while j<=len

  if pressure_index(j)==time_index(j) && (pressure_index(j)) <= length(pressure) &&
time_index(j) <= length(time)
    k=pressure(pressure_index(j));
    pressure(pressure_index(j))=time(time_index(j));
    time(time_index(j))=k;
  elseif pressure_index(j)~= time_index(j) && (pressure_index(j)) <= length(pressure)
&& time_index(j) <= length(time)
    while i<=len
      if pressure_index(j)==time_index(i)
        k=pressure(pressure_index(j));
        pressure(pressure_index(j))=time(time_index(i));
        time(time_index(i))=k;
      end
      i=i+1;

    end

  end
  j=j+1;
  i=1;

end


i=1;
j=1;
l=length(pressure);

while i<=l
  if pressure(i)>1000 && pressure(i)<4800
    pressure_index_new(j)=i;
    j=j+1;
  end
  i=i+1;
```

```
end

i=1;
j=1;
l=length(time);

while i<=l
  if time(i)<1500
    time_index_new(j)=i;
    j=j+1;
  end
  i=i+1;
end
```

D.2 Time Delay Analysis

```
close all
clear all
clc

%Prep the command-window and work space

addpath('C:\Users\layla\OneDrive\Documents\Masters\Thesis\TrialRuns');
%Ask a series of questions to determine appropriate filename
DIR = uigetdir;
cd(DIR); %change the current folder to where the data is
DIR = [DIR,'\'];


%% Parse

Trial='Trial';
filename = strcat(DIR,Trial,'.mat');

load ([filename]);
len = dataend(2,1);

for i= 1:7 %3 is the number of channels
  chnl=titles(i,:);
  chnll = deblank(chnl);
  channel=regexprep(chnll,'\s','');%remeoves spaces from channel name

  idx1=datastart(i,1);
  idx2=dataend(i,1);

  if idx1~=-1 && idx2 ~=-1
    load=data(idx1:idx2);
    New.(channel)=load;
  end


end
close all



%% Find trigger or sync
% New.ButtonTrigger=resample(New.ButtonTrigger, 482, 1000);
% len2=length(New.ButtonTrigger);
i=1;
for k = 1:len
  holderr = New.ButtonTrigger(1,k);

    if holderr > 1.0
      triggerat = k;
      i=i+1;
      %break
```

```
%       if holderr>1.0 && (k-i)>0
%         triggerat=k;
%         break
%       end
 %    break

    end

end
i=1;
time = 0:1/(tickrate):((len-1)/tickrate);

%% Calibration equation for loadcell
len2=length(New.LoadCell2);
for k=1:len2
  if New.LoadCell2(k) <= 0.579041977327009
    New.LoadCell2(k)= (-13.4266*((New.LoadCell2(k))^2))+(14.0361*New.LoadCell2(k))-
2.1510;
  else
    New.LoadCell2(k)=(1.1911*(New.LoadCell2(k)))+1.0503;
  end
end
%% Filter data
Fc = 10;%change this too
ftype= 'low';
Fs = 1000;%change this
Unfilter=New.LoadCell2;
Force=New.LoadCell2;
New.LoadCell2 = butter_filterMfm(Force,Fc,Fs,ftype);

%plot(time, Unfilter, time, New.LoadCell2);

%% Read data from excel and calibration add equation
Time_App= xlsread( 'Trial', 'Final', 'B1:B1048576' );
Load_App= xlsread( 'Trial', 'Final', 'E1:E1048576' );

for k=1:(length(Load_App))
  Load_App_New(k)=(((Load_App(k)/101.97162)*1.0232)+0.1462);

end

Time_App_New(1)=0;
for k=2:(length(Time_App))
  Time_App_New(k)=Time_App_New(k-1)+(Time_App(k)/1000000);
end

Time_App_New=transpose(Time_App_New);
Load_App_New=transpose(Load_App_New);


%% Only Plot where trigger is at
New_Time= [];
New_Time(1)=0;
j=2;
len2=length(time);
```

```
for i = triggerat:len2
  if i<len2
    diff=time(i+1)-time(i);
    New_Time(j)=New_Time(j-1)+diff;
    j=j+1;
    i=i+1;
  else
    break
  end

end

j=1;
for i = triggerat:len2
  NewLoadCell2(j)=New.LoadCell2(i);
  j=j+1;
end

%% Interpolating VGM signal

Load_App_New=interp(Load_App_New,2);
Time_App_New=interp(Time_App_New,2);

if length(Time_App_New)>length(Load_App_New)
  len_App = length(Load_App_New);
else
  len_App = length(Time_App_New);
end

%% Remove gravity correction factor on dyno
if length(New_Time)>length(NewLoadCell2)
  len2 = length(NewLoadCell2);
else
  len2 = length(New_Time);
end

plot(New_Time(1:len2),NewLoadCell2(1:len2))
hold on
plot(Time_App_New(1:len_App), Load_App_New(1:len_App))
set(gca,'XLim',[Time_App_New(1) 10])
set(gca,'XTick',(Time_App_New(1):0.5:10))
set(gca,'YLim',[-1 10])
set(gca,'YTick',(-1:1:10))

hold on
legend('PowerLab','v-QueST')
xlabel('Time(s)')
ylabel('Force(N)')

[x1,y1] = ginput(4);

plot(x1(1),y1(1),'r*');
plot(x1(2),y1(2),'r*');
plot(x1(3),y1(3),'r*');
plot(x1(4),y1(4),'r*');
```

```
hold off

index_VT1=find(Time_App_New>x1(1));
if ((abs(Time_App_New(index_VT1(1))-x1(1)))<(abs(Time_App_New((index_VT1(1)-1))-
x1(1))))
  Index_VT1=index_VT1(1);
else
  Index_VT1=index_VT1(1)-1;
end

index_VT2=find(Time_App_New>x1(2));
if ((abs(Time_App_New(index_VT2(1))-x1(1)))<(abs(Time_App_New((index_VT2(1)-1))-
x1(1))))
  Index_VT2=index_VT2(1);
else
  Index_VT2=index_VT2(1)-1;
end

index_PT1=find(New_Time>x1(3));
if ((abs(New_Time(index_PT1(1))-x1(1)))<(abs(New_Time((index_PT1(1)-1))-x1(1))))
  Index_PT1=index_PT1(1);
else
  Index_PT1=index_PT1(1)-1;
end

index_PT2=find(New_Time>x1(4));
if ((abs(New_Time(index_PT2(1))-x1(1)))<(abs(New_Time((index_PT2(1)-1))-x1(1))))
  Index_PT2=index_PT2(1);
else
  Index_PT2=index_PT2(1)-1;
end

MeanVGM_baseline=mean(Load_App_New(Index_VT1:Index_VT2));
MeanPL_baseline=mean(NewLoadCell2(Index_PT1:Index_PT2));

Load_App_New=Load_App_New-(abs(MeanVGM_baseline-MeanPL_baseline));

%% Plot with 4, 5, 6 N
clf

for i=1:len2
  if NewLoadCell2(i)>4 || NewLoadCell2(i)==4
    if (abs(NewLoadCell2(i)-4)<abs((NewLoadCell2(i-1))-4))
      y2=NewLoadCell2(i);
      x2=New_Time(i);
    else
      y2=NewLoadCell2(i-1);
      x2=New_Time(i-1);
    end
    break
  end
end

for i=1:len_App
```

```
  if Load_App_New(i)>4 || Load_App_New(i)==4
    if (abs(Load_App_New(i)-4)<abs((Load_App_New(i-1))-4))
      y3=Load_App_New(i);
      x3=Time_App_New(i);
    else
      y3=Load_App_New(i-1);
      x3=Time_App_New(i-1);
    end
    indexdelay(1)=i;
    break
  end
end

for i=1:len2
  if NewLoadCell2(i)>5 || NewLoadCell2(i)==5
    if (abs(NewLoadCell2(i)-5)<abs((NewLoadCell2(i-1))-5))
      y4=NewLoadCell2(i);
      x4=New_Time(i);
    else
      y4=NewLoadCell2(i-1);
      x4=New_Time(i-1);
    end
    break
  end
end

for i=1:len_App
  if Load_App_New(i)>5 || Load_App_New(i)==5
    if (abs(Load_App_New(i)-5)<abs((Load_App_New(i-1))-5))
      y5=Load_App_New(i);
      x5=Time_App_New(i);
    else
      y5=Load_App_New(i-1);
      x5=Time_App_New(i-1);
    end
    indexdelay(2)=i;
    break
  end
end

for i=1:len2
  if NewLoadCell2(i)>6|| NewLoadCell2(i)==6
    if (abs(NewLoadCell2(i)-6)<abs((NewLoadCell2(i-1))-6))
      y6=NewLoadCell2(i);
      x6=New_Time(i);
    else
      y6=NewLoadCell2(i-1);
      x6=New_Time(i-1);
    end
    break
  end
end

for i=1:len_App
  if Load_App_New(i)>6 || Load_App_New(i)==6
```

```
    if (abs(Load_App_New(i)-6)<abs((Load_App_New(i-1))-6))
      y7=Load_App_New(i);
      x7=Time_App_New(i);
    else
      y7=Load_App_New(i-1);
      x7=Time_App_New(i-1);
    end
    indexdelay(3)=i;
    break
  end
end


if length(New_Time)>length(NewLoadCell2)
  len2 = length(NewLoadCell2);
else
  len2 = length(New_Time);
end

% subplot(3,3, [4:5 7:8])
PL= plot(New_Time(1:len2),NewLoadCell2(1:len2));
hold on
VGM= plot(Time_App_New(1:len_App), Load_App_New(1:len_App));
set(gca,'XLim',[Time_App_New(1) 10])
set(gca,'XTick',(Time_App_New(1):0.5:10))
set(gca,'YLim',[-1 10])
set(gca,'YTick',(-1:1:10))

hold on

if exist ('x2','var')==1
  Four=plot(x2,y2,'r*');
end

hold on

if exist ('x3','var')==1
  plot(x3,y3,'r*');
end

hold on

if exist ('x4','var')==1
  Five=plot(x4,y4,'g*');
end

hold on

if exist ('x5','var')==1
  plot(x5,y5,'g*');
end

hold on

if exist ('x6','var')==1
```

```
  Six=plot(x6,y6,'m*');
end

hold on

if exist ('x7','var')==1
  plot(x7,y7,'m*');
end


hold on

legend([PL VGM Four Five Six],'PowerLab','v-QueST', '4N', '5N', '6N')
xlabel('Time(s)')
ylabel('Force(N)')

hold on

% subplot(3,3,[2:3])
% plot(New_Time(2141:4801),NewLoadCell2(2141:4801),Time_App_New(2060:4623),
Load_App_New(2060:4623)...
%   ,x2,y2,'r*',x3,y3,'r*',x4,y4,'g*',x5,y5,'g*',x6,y6,'m*',x7,y7,'m*')
%
% set(gca,'XLim',[2.14 4.8])
% set(gca,'XTick',(2.14:0.25:4.8))
% set(gca,'YLim',[3.7 6.3])
% set(gca,'YTick',(3.7:0.5:6.3))
% title('Zoomed In')

hold off
if exist ('x2','var')==1 && exist ('x3','var')==1
  diff4=x3-x2;
end

if exist ('x4','var')==1 && exist ('x5','var')==1
  diff5=x5-x4;
end

if exist ('x6','var')==1 && exist ('x7','var')==1
  diff6=x7-x6;
end

diff_select=abs(MeanVGM_baseline-MeanPL_baseline);

fprintf('%0.4f\t%0.4f\t%0.4f\t%0.4f\t%0.4f\t%0.4f\t%0.4f\t%0.4f\t%0.4f',...
  diff4,x2,x3,diff5,x4,x5,diff6,x6,x7,diff_select)

function y = butter_filterMfm(x, Fc, Fs,ftype)

% This function designs a butterworth filter and then runs the filter
% y = filtered signal
% x = input data
% Fc = frequency cutoff (single value for lowpass and highpass, range for
% stop (notch filter)
% Fs= sampling frequency
```

```
% fype= filter type: lowpass, highpass, or bandstop (stop) used for notch filter


%% Setting up filter
clear Wn
tf=strcmp('stop',ftype); %if 'bandpass' were to be used rather than high then low
pass, then this would also need to be true
if tf==1
  n=3; %bandstop filter designs are of order 2n (so 3*2n is a 6th order butterworth
filter)

else n=6; %low or high pass filters are of order n: 6th order

end

Wn =(Fc/(Fs/2)); %Wn = cut off frequency between 0<wn<1.0 with 1.0 = half sampling
rate
[b, a] = butter(n, Wn,ftype); %setting up butterworth where n= order, Wn = cut off
frequency between 0<wn<1.0 with 1.0 = half sampling rate


%% Filtering data
y=filtfilt(b, a, x); %zero-phase lag filtering by processing data in forward and
reverse directions
end
```